National Library
of Canada

Acquisitions and
Bibliographic Services Branch

395 Wellington Street
Ottawa, Ontario
K1A 0N4

Bibliothèque nationale
du Canada

Direction des acquisitions et
des services bibliographiques

395, rue Wellington
Ottawa (Ontario)
K1A 0N4

Your file Votre référence

Our file Notre référence

NOTICE

The quality of this microform is heavily dependent upon the quality of the original thesis submitted for microfilming. Every effort has been made to ensure the highest quality of reproduction possible.

If pages are missing, contact the university which granted the degree.

Some pages may have indistinct print especially if the original pages were typed with a poor typewriter ribbon or if the university sent us an inferior photocopy.

Reproduction in full or in part of this microform is governed by the Canadian Copyright Act, R.S.C. 1970, c. C-30, and subsequent amendments.

AVIS

La qualité de cette microforme dépend grandement de la qualité de la thèse soumise au microfilmage. Nous avons tout fait pour assurer une qualité supérieure de reproduction.

S'il manque des pages, veuillez communiquer avec l'université qui a conféré le grade.

La qualité d'impression de certaines pages peut laisser à désirer, surtout si les pages originales ont été dactylographiées à l'aide d'un ruban usé ou si l'université nous a fait parvenir une photocopie de qualité inférieure.

La reproduction, même partielle, de cette microforme est soumise à la Loi canadienne sur le droit d'auteur, SRC 1970, c. C-30, et ses amendements subséquents.

Canada

University of Alberta

AN EFFICIENT ANALYTICAL APPROACH FOR GENERATING DIGITAL ELEVATION MODELS

BY

DANIEL HEMENWAY ©

A Thesis
Submitted to the Faculty of Graduate Studies and Research
in partial fulfillment of the requirements
for the degree of
MASTER OF SCIENCE

DEPARTMENT OF GEOGRAPHY

EDMONTON, ALBERTA
FALL 1995

National Library
of Canada

Acquisitions and
Bibliographic Services Branch

395 Wellington Street
Ottawa, Ontario
K1A 0N4

Bibliothèque nationale
du Canada

Direction des acquisitions et
des services bibliographiques

395, rue Wellington
Ottawa (Ontario)
K1A 0N4

Your file Votre référence

Our file Notre référence

THE AUTHOR HAS GRANTED AN IRREVOCABLE NON-EXCLUSIVE LICENCE ALLOWING THE NATIONAL LIBRARY OF CANADA TO REPRODUCE, LOAN, DISTRIBUTE OR SELL COPIES OF HIS/HER THESIS BY ANY MEANS AND IN ANY FORM OR FORMAT, MAKING THIS THESIS AVAILABLE TO INTERESTED PERSONS.

L'AUTEUR A ACCORDE UNE LICENCE IRREVOCABLE ET NON EXCLUSIVE PERMETTANT A LA BIBLIOTHEQUE NATIONALE DU CANADA DE REPRODUIRE, PRETER, DISTRIBUER OU VENDRE DES COPIES DE SA THESE DE QUELQUE MANIERE ET SOUS QUELQUE FORME QUE CE SOIT POUR METTRE DES EXEMPLAIRES DE CETTE THESE A LA DISPOSITION DES PERSONNE INTERESSEES.

THE AUTHOR RETAINS OWNERSHIP OF THE COPYRIGHT IN HIS/HER THESIS. NEITHER THE THESIS NOR SUBSTANTIAL EXTRACTS FROM IT MAY BE PRINTED OR OTHERWISE REPRODUCED WITHOUT HIS/HER PERMISSION.

L'AUTEUR CONSERVE LA PROPRIETE DU DROIT D'AUTEUR QUI PROTEGE SA THESE. NI LA THESE NI DES EXTRAITS SUBSTANTIELS DE CELLE-CI NE DOIVENT ETRE IMPRIMES OU AUTREMENT REPRODUITS SANS SON AUTORISATION.

ISBN 0-612-06481-6

Canada

University of Alberta

Library Release Form

NAME OF AUTHOR: **Daniel David Hemenway**

TITLE OF THESIS: **An Efficient Analytical Approach for Generating Digital Elevation Models**

DEGREE: **Master of Science**

YEAR THIS DEGREE GRANTED: **1995**

Permission is hereby granted to the University of Alberta Library to reproduce single copies of this thesis and to lend or sell such copies for private, scholarly, or scientific research purposes only.

The author reserves all other publication and other rights in association with the copyright in the thesis, and except as hereinbefore provided, neither the thesis nor any substantial portion thereof may be printed or otherwise reproduced in any material form whatever without the author's prior written permission.

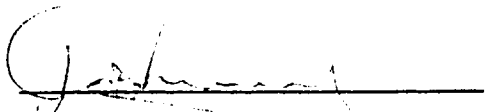

12615- 42 Ave.
Edmonton, Alberta, Canada
T6J 0X3

August 1, 1995

University of Alberta

Faculty of Graduate Studies and Research

The undersigned certify that they have read, and recommend to the Faculty of Graduate Studies and Research for acceptance, a thesis entitled AN EFFICIENT ANALYTICAL APPROACH FOR GENERATING DIGITAL ELEVATION MODELS submitted by DANIEL DAVID HEMENWAY in partial fulfillment of the requirements for the degree of MASTER OF SCIENCE.

Dr. J. Ronald Eyton

Dr. Ian Campbell

Dr. Peter Crown

July 27, 1995

Dedicated to
Toga, Trinket, Mist,
the pups
and most importantly
Allana
-for always being there-

Abstract

Digital elevation models (DEMs) have become vital data for nearly every profession which deals directly or indirectly with studying, planning, or developing land. Generating DEMs necessary for many of these applications can be an expensive and time consuming endeavor Developing a computerized image processing approach to perform the task of digitizing map contours provided a means for even inexperienced users to acquire digital topographic information in an accurate and affordable manner. Analytical surfacing methodologies based on multiquadric equations produce DEMs that are exact fitting and free of artifact irregularities associated with currently popular numerical approaches. Multiquadric equations generate global surfacing solutions involving all initial points. Limitations in computer memory and processing power prevent the use of multiquadric equations for large topographic data sets. An adaptive global tiling approach was developed which overcomes these impediments by strategically partitioning data points into manageable subsets, allowing implementation of multiquadric interpolation techniques on any computer system.

Acknowledgements

I would like to acknowledge and thank my supervisor, Dr. Ron Eyton, for his many years of support while this project evolved. I would also like to thank Dr. Ian Campbell and Dr. Peter Crown for their input and contributions to the final thesis. Stu Cruikshank, Kent Holden, Darren Sjogren, Craig Coburn and many others over the years must be thanked for patiently testing and re-testing the different pieces of software developed in this project. I would like to acknowledge and thank the entire Department of Geography for the many years of employment and support and especially Joan MacLeod for keeping the red tape to a minimum. Finally, I would like to thank Allana Hemenway for the years of patient support and direction. Her presence provided the focus, stability, and environment for making this dream come true.

Table of Contents

Chapter 1 Introduction 1

The Need for an Efficient Methodology for Generating DEMs 2
Research Objectives 3

Chapter 2 A Brief Review of Surfacing Methodology 4

Data Sources 4
Acquisition of Secondary Data 5
Surface Generation 6

Chapter 3 Methodology Overview 8

Test Data 8
Image Processing for Digital Data Capture 8
Data Management for Small Computers 10
An Analytical Tiling Approach to Surfacing 11

Chapter 4 Image Processing for Digital Data Capture 13

Scanning Topographic Maps 13
Image Processing 15
Elevation Encoding 15
Image Data Reduction 18
Extracting Elevation Information from a Raster Image 21

Chapter 5 Data Management for Small Computers 22

Range Searching 22
Two Dimensional Binary Search Trees 23

Chapter 6 An Analytical Tiling Approach to Surfacing 26

Multiquadric Equations 27
Tiling 29

Tile Boundary Effects 30
Adaptive Tiling 30
Directional Point Selection 31

Post-Processing 31
Qsurf 34

Chapter 7 Comparison with the Alberta 1:20,000 DEM 39

Edge Contours 39
Lambertian Light Model 41
Slope Magnitude 41
Across Slope Curvature 41
Down Slope Curvature 45
Statistical and Numerical Comparisons 47

Chapter 8 Summary 51

References 53

List of Tables

Table 7.1 Residual Surface Cumulative Frequency Distribution **50**

List of Figures

Figure 3.1 Three dimensional view of the topography in map sheet 83C/01NW. View azimuth is 210° at an elevation of 28°. Solar illumination is from an azimuth of 140° at an elevation of 30°. Vertical exaggeration is 1X. **9**

Figure 4.1 Sample scans at: a. coarse; b. medium; c. fine resolutions. **14**

Figure 4.2 Rotation of scanned map segments for rectangular alignment of UTM registration marks **16**

Figure 4.3 Contour lines are isolated by erasing connecting pixels along the contour borders. **17**

Figure 4.4 A contour mask is created by thresholding a copy of the scanned image. The mask is pasted over the final encoded image to thin the contours to their centers. **20**

Figure 5.1 Sample two dimensional binary search tree with 11 nodes containing XYZ coordinate information. **24**

Figure 6.1 Example summary for evaluating a multiquadric solution.
Source: Eyton, 1974 **28**

Figure 6.2 Point density variations over the area of a uniform tile may cause surface discontinuities with adjacent tiles. **32**

Figure 6.3 For adaptive directional tiling, similar numbers of points are selected from eight sectors radiating around the tile center. Sector sizes adapt to local density variations in data point distributions. **33**

Figure 6.4 Even with adaptive directional tiling, specific patterns in data point distributions can cause surface discontinuities at tile boundaries. **35**

Figure 6.5 Performance chart indicating the relationship between total surfacing time and average number of points selected from each sector of a tile partition. **37**

Figure 7.1 Edge contour images. Base reference elevation is 1300m. Contour interval is 50m. **40**

Figure 7.2 Relative radiance images using a Lambertian Light model. Solar illumination is from 300° at an elevation of 30°. **42**

Figure 7.3 Slope magnitude images. Maximum magnitudes were clipped at 48° of slope to enhance low-magnitude slope details. **43**

Figure 7.4 Across slope curvature scaled between -80° and 80° of change in slope per 100m. **44**

Figure 7.5 Down slope curvature scaled between -80° and 80° of change in slope per 100m. **46**

Figure 7.6 Residual difference image produced by subtracting the Qsurf DEM from the SCOP DEM. Differences are scaled between -10m (black) and +10m (white). **48**

Chapter 1
Introduction

For centuries topographic and elevation information was vaguely represented in two dimensions by lines, symbols, and shades on map-like products. As technology evolved and methods of measuring changes in elevation became more precise, cartographic representation of elevations evolved from these loosely defined artistic impressions to accurately located contour lines connecting locations of equal topographic value. Elevation data presented in the format of accurate map contours permitted useful numerical information to be extracted through simple, though tedious calculations. Today, the high degree of accuracy obtainable for measuring, storing, and displaying the surface of the earth has increased demand for new methods of extracting information from positional measurements. Nearly every profession which deals directly or indirectly with studying, locating, or developing land now requires accurate calculations based on detailed topographic information. The advent of the computer has provided both the ability and the drive to extract large quantities of meaningful information from terrain data at high precision. As the processing power of computers has increased, combined with a steady decrease in computer costs, more applications than ever require topographic data collected and stored in digital format.

Digital representation of topographic information has evolved into two dominant formats over the past twenty years. The two formats are closely tied to the traditional raster and vector methods of displaying or representing items of information at discrete locations. The two methods of representing topographic information are the Digital Elevation Model (DEM) and the Triangulated Irregular Network (TIN) model.

The DEM format consists of elevation values stored in a matrix or raster arrangement where exact spatial locations are implied by row and column location. A value stored at a given matrix location is assumed to represent the characteristics of the entire area covered by the grid cell. Spatial coverage of a region by a DEM is complete since all grid cells in a matrix must exist for the matrix structure to be valid. A cell in the matrix may have an undefined value which does not reflect characteristics of the true land surface, however, the location of the cell and the surface area

represented by the cell are "guaranteed" by the rigid raster structure of the DEM.

The TIN format for storing topographic information follows the traditional vector approach. Elevation values stored in a TIN format are described by a complete set of three dimensional coordinates. The exact location of points in a TIN format dictates that there is no point-to-area generalization of the type inherent in the DEM format. Consequently, non-represented locations in the TIN format are not spatially identifiable without interpolation of the data.

The "guaranteed" coverage of the DEM format, combined with its simple data structure and modest storage requirements have increased the popularity of the DEM format and it is commonly used as a method for modelling and archiving the topography of the earth. A comprehensive evaluation of the accuracy and effectiveness of the DEM format as compared to the TIN format conducted by Kumler (1994) concluded that in all cases investigated, the DEM format was equal to or superior to the TIN format in storing, processing, and presenting topographic information.

The Need for an Efficient Methodology for Generating DEMs

Traditional DEM production has required the use of specialized and sophisticated combinations of hardware and software. These requirements demand large investments of capital resources and technical skill to collect topographic data and process the information into a useful product. Applications of topographic information in many disciplines has increased the need for DEMs to be accessible to individuals with limited equipment, capital, and training resources. Many small companies and individuals (e.g. geomorphologists involved in fieldwork) who would benefit from the use of DEMs in their work may not have the resources necessary to purchase or develop specialized DEMs generated by traditional methods. The need to produce accurate and effective DEMs in a timely and cost efficient manner can be expected to increase as the use and accessibility of Global Positioning System units rises over the next decade.

Research Objectives

The objectives of this research are:

1. To develop an accurate, effective, and affordable method of acquiring discretely located elevation data of sufficient quality and quantity as to be useful in generating a digital elevation model.

2. To develop a product by which irregularly distributed data values may be interpolated to produce an accurate representation of the surface topography limited only by the initial data capture.

The first objective contains several explicitly stated conditions that qualify the acceptability of any data acquisition method developed. The conditions that a method must be accurate, effective, and affordable dictate that the method must be spatially precise, simple to use without extensive training, and must utilize multi-purpose hardware or software to reduce allocation of resources to specialized tasks. A digitizing table is considered a specialized and single purpose piece of hardware which would not be available to many people and consequently would not be acceptable to the methodology restrictions given here. The second objective contains the restriction that the developed product generates an interpolated surface that exactly reproduces initial data values and reasonably represents the surface at all other locations. The program should be simple to use and should be executable in as many computing environments as possible.

Chapter 2
A Brief Review of Surfacing Methodology

Modelling continuous surfaces typically involves two distinct phases of operation. The initial phase involves sampling, correcting, and storing the discrete spatial values which represent the surface to be modelled. The second phase deals with organizing and interpreting sample data in order to calculate realistic values for unknown locations within the surface domain. The second phase also deals with the file format for storing and retrieving a generated surface model. The development of highly precise ortho-photo plotters, stereo-parallax satellite imagery, and laser profilers capable of sampling complete surface models directly has clouded the distinction between these two phases of operation; however, for general surfacing applications the two phases remain distinct from each other.

Data Sources

Sources of sample data representing geographic surfaces may be labelled as either primary or secondary. Primary sources provide the highest level of accuracy in measured topographic information. Common forms of primary data sources include ground surveys, aerial photographic stereo-pairs and ortho-photos, stereo-parallax satellite imagery, airborne laser profilers, and global positioning system measurements. Primary data sources provide topographic information by directly measuring a surface using physical sensing or photogrammetric techniques. The measurement process and precision requirements of primary data sources requires specialized equipment and training to collect and compile the data into useable form. The costs involved with acquiring data from primary sources prohibits the use of this type of data for many small scale and low budget applications.

Secondary topographic data sources are provided in a pre-processed format and yield generalized information about the characteristics of a surface. The most common and accessible source of secondary terrain information is the topographic map. Elevation information on a topographic map has been generalized into discrete categories delineated by contour lines. Elevation information within each category can only be estimated by

proximity to the bounding contours. With sufficiently small contour intervals the terrain information encoded in a topographic map may approach the accuracy of data provided from primary data sources. The cost of purchasing topographic maps is very small and maps at various scales are available for much of the earth's surface. Topographic data collected from secondary sources such as contour maps are commonly used for small scale terrain modelling applications.

Acquisition of Secondary Data

Converting analogue information from topographic maps into useable digital data typically requires the use of specialized hardware and the skill of a trained operator to digitize the elevation contours. Digitizing maps may occur in several different ways, however the underlying procedure of logging values at locations identified by a sensing device is a common characteristic. Differences in digitizing methods are generally attributed to the pattern and manner in which contours are selected for processing. *Line following* digitizing is the most common method and requires the use of a standard digitizing table. In line following digitizing, contours are traced by the operator using a location sensitive cursor or pen. Data values are recorded at regular intervals or at operator specified locations. Accuracy with line following digitizing is largely determined by the skill and steady coordination of the operator.

Contour crossing digitizing is an alternative to the line following method. The contour crossing pattern of digitizing requires moving a cursor in parallel scan lines across the face of a map sheet and recording a point whenever a contour line is encountered. While contour crossing digitizing can be performed on a standard digitizing table, this pattern of digitizing is usually performed on a specialized motor driven table where the spacing of parallel scan lines may be precisely set. Attempts have been made to automate both line following and contour crossing methods of digitizing through the use of sophisticated optical sensors and control programs. The resulting automated digitizing apparatus still requires operator intervention to differentiate ambiguous situations and to identify non-topographic symbology on the maps. A third method of converting map information to digital form is a process called *scan conversion*. With scan conversion, a map

is scanned as a raster image. Pattern recognition programs then try to identify and isolate the text, symbology, and contour information that is embedded in the image.

Surface Generation

The choice of methodologies available for generating topographic surfaces depends upon the type of elevation model in which the surface will be stored. When a triangulated irregular network model is used, data points are processed to determine an optimal triangular network from within the data. No further interpolation or addition of data points takes place. The two most often used methods for generating TIN models are the Delauney Triangulation and the Radial Sweep methods (Stefanovic, 1988). Both methods require intensive processing of the data points to construct networks of optimal triangles. When the digital elevation model is used to store a surface the number of surfacing methods available increases dramatically. For all DEM methods of generating surfaces, initial data points are interpreted to predict new values on a regular grid. The predicted grid values are then stored in the model and the initial irregularly distributed data points are discarded.

Techniques used to create modelling functions for DEMs depend in part upon the pattern followed in digitizing the map. When the contour crossing method of digitizing is used, modelling functions may be based on profiles fit through the data points along each scan line. When interpolation of scan lines occurs, two dimensional mathematical functions of linear, polynomial (splines) (Davis, 1973), and multiquadric (Eyton, 1987) profiles are generally used. Alternatively, data points obtained from contour crossing digitizing may be treated as any set of irregularly spaced points and the modelling function may be based on a three dimensional interpretation of the data.

Many numerical, statistical, and analytical modelling functions have been researched and developed for generating DEMs (Franke, 1979). The most often used functions in geographical applications are numerical in design. Numerical modelling functions work by assigning weights to data points nearest a location to be evaluated. A new elevation value is predicted based on the weights of these points. The inverse weighted distance method

of surfacing is the most common implementation of a numerical modelling function and can be found in virtually all commercial surfacing packages. A characteristic of numerical modelling functions is their sensitivity to anomalies and distribution patterns in the data. Most DEM surfaces generated using numerical modelling functions contain artifacts which are introduced by the functions and not by the data. The artifacts may be cleaned from the DEM using low-pass filters; however, the presence of artifacts signifies an underlying flaw inherent in numerical modelling functions. Numerical modelling functions are easy to comprehend and implement. These characteristics, combined with a low demand for computer resources, make numerical modelling functions attractive for surfacing applications even though flaws persist.

Statistical surfacing, also known as kriging, is similar to numerical surfacing with the exception that the weights assigned to initial data points are determined from semivariograms. The semivariogram gives a statistical measure of spatial continuity of regionalized data points (Davis, 1973). Points which are statistically significant are included in the modelling function while other points are not. Surfaces generated by kriging produce artifacts similar to the artifacts generated by numerical surfacing methods.

Analytical modelling functions work by fitting a continuous mathematical function through all initial data points. The mathematical surface is then evaluated at specific locations to predict new elevation values. Analytical surface modelling functions are not subject to the proximity induced artifact problems of numerical and kriging functions since the influence assigned to initial data points is not dependent on their locations relative to new values. All initial data points in an analytical modelling function contain equal significance in calculating new values. Although not utilized as frequently as the numerical and statistical modelling functions for geographic applications, analytical modelling functions provide the cleanest and most dependable surfaces for DEM production.

Chapter 3
Methodology Overview

Topographic data acquisition from secondary sources has traditionally been accomplished through manually digitizing contour maps. The process of digitizing requires significant investment in terms of operator training and capital expenditures involving specialized hardware and software. One of the objectives of this research was to develop a cost effective procedure for generating digital elevation models without the use of expensive and highly specialized hardware. An adaptation of digital image processing provided the methodology to fulfil this objective in a manner that was timely and accurate, yet required only the standard hardware and software used for image processing applications.

Test Data

The map sheet selected as a test case for techniques developed in this research was the 1:20,000 scale topographic map identified as 83C/01NW. The area was chosen for the variety of topographic features it contains (Figure 3.1). Within the 17 km by 14 km region covered by the map sheet there are steep mountain slopes, sharply defined ridges, deeply incised river valleys, shallow stream channels, low relief uplands, low relief flood plains, and several alluvial fans. The test area is also available from the Provincial Government of Alberta as a digital elevation model. The provincial DEM provided the basis for qualitative and quantitative comparisons between the results of this research and a commercially developed product.

Image Processing for Digital Data Capture

The premise behind using image processing techniques for digital data capture relies upon the highly precise spatial resolution of scanning devices, and on the generalized portrayal of elevations as contours on topographic maps. High precision in the spatial resolution of scanners enables assumptions to be made about relationships between the shapes and sizes of the pixels in a scanned raster image and the shapes and sizes of ground coverage the pixels represent. These assumptions allow for quick and

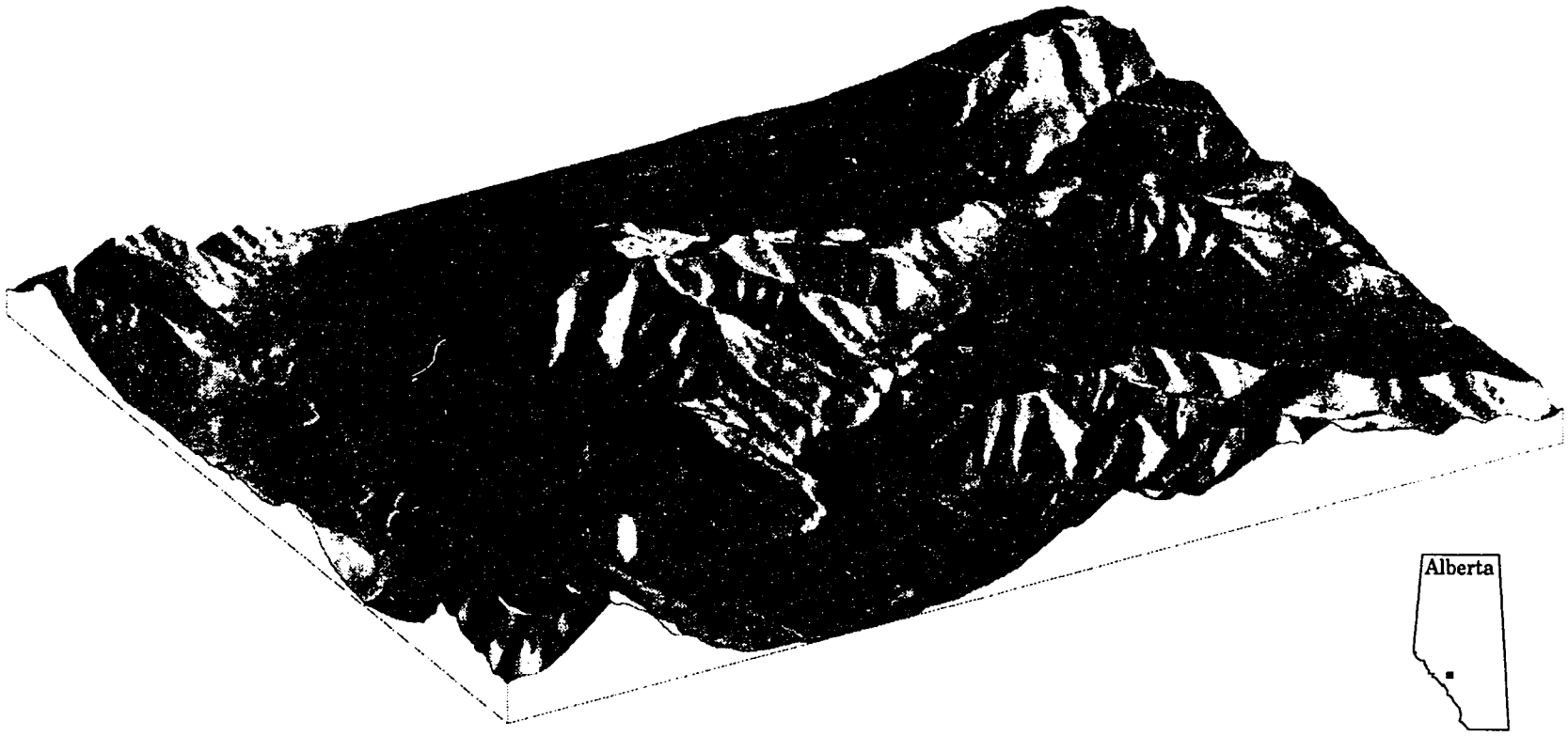

Figure 3.1. Three dimensional view of the topography in map sheet 83C/01NW. View azimuth is 210° at an elevation of 28°. Solar illumination is from an azimuth of 140° at an elevation of 30°. Vertical exaggeration is 1X.

accurate spatial location of features represented in an image limited only by the spatial resolution of the scan. Using image processing techniques, contour lines can be digitally encoded as grey tones or grey level values (GLVs). For an 8 bit grey scale image, there are 2^8 or 256 possible grey tones. A typical topographic map contains fewer than 100 unique contour levels which can easily be identified as GLVs in an 8 bit image.

Extraction of elevation information in the form of XYZ triplets from an encoded raster image is a straightforward exercise; knowing the world coordinates of a corner of a DEM grid and the size of an image pixel or grid cell are all that is necessary to calculate the two dimensional world coordinate values for every cell in the image. The elevation for a given point can be determined from the assigned grey tone using the encoding scheme to complete the XYZ triplet information. A simple program was written in C code to perform the extraction.

Accuracy concerns with applying image processing to digital data capture are related to the spatial location of captured elevation values. The spatial location of contours acquired using image processing is controlled by the spatial resolution of the scan used to capture the image. Current desktop scanners typically scan to a resolution of 0.00635 cm (158 dots per cm) which exceeds the accuracy contained in topographic maps where the pens used to plot contour lines may be 0.0127 cm or greater in thickness. The actual elevation values in a topographic map are generalized as contour lines. There is no interpolation of elevation during the data capture which ensures that elevation information is essentially at the same level of accuracy as that associated with the topographic map.

Data Management for Small Computers

Efficient management of data is important in all computer programming. When the amount of data is large and many items are manipulated repeatedly, efficient management is crucial to effective program design and execution. Research in computer science has produced many highly efficient methods for managing data in various computing environments (Aho et al., 1983; Claybrook, 1983). For situations where data are repeatedly searched and indexed, the most efficient techniques developed involve two distinct phases of implementation. The two phases are a pre-

processing phase designed to create an optimal data structure and a searching phase where the data structure is utilized. The definition of an optimal data structure depends heavily upon the nature of the data to be stored.

Spatially distributed elevation data captured for the purpose of generating DEMs can logically be visualized as records of elevation values stored at specific locations within a two dimensional plane. An efficient storage and retrieval algorithm for this data should take advantage of, or at least take into account, this multidimensional nature. Through the course of this research, multidimensional binary search trees were implemented as a highly efficient method for managing large amounts of data with a minimal amount of computer resources committed as overhead. The multidimensional tree algorithms were incorporated into several computer programs which were executed in both DOS and UNIX operating environments.

An Analytical Tiling Approach to Surfacing

Predicting unknown surface values from known sample coordinates is a complex task. Investigations into predicting surfaces has produced many techniques and methodologies with varied degrees of accuracy and success. The distinction is made between accuracy and success because the accuracy of a surface in representing topographic information is not always related to the successful use of the surface in an intended application. The targeted use of a generated surface can make a significant contribution in deciding how accurate the surface must be. Low order polynomial trend surfaces are a good example of low accuracy surfaces that are very successful at clearly presenting generalized information.

Multiquadric interpolation (Hardy, 1971) is a surfacing technique that has been proven highly accurate at predicting topographic surfaces (Franke, 1979; Hein, 1979: cited in Schiro and Williams, 1983; Schiro and Williams, 1984). Multiquadric interpolation is an exact-fitting analytical surfacing technique that provides neutral interpolation through areas of low sample point density while maintaining sharp control through areas of high density. Difficulties with implementing multiquadric interpolations occur with the large demand for computer resources required to develop a modelling function for a given set of data points. Using a "divide and conquer"

approach to reduce the surfacing area into adjacent surface tiles with associated sub-sets of data points removes the computer resource problems. If the surface and data points are reduced to small enough sub-sets then multiquadric interpolation techniques can be implemented even on small computer systems. The issue then becomes one of intelligently partitioning the data points into sub-sets in a manner that optimizes computational time while maintaining the characteristics of the surface being modelled.

The approach used to partition data points will have a significant impact on both the time needed to compute the surface and on the quality of the surface itself. An appropriate and efficient partitioning approach should make allowances for sudden and unpredictable variations in data point densities without artificially altering the topographic information contained within the patterns of point distributions. An adaptive surfacing approach that dynamically partitions data points and maintains the directional patterns within point distributions was developed. The adaptive tiling approach intelligently partitions data points before using multiquadric interpolation techniques to produce high quality surface segments which are combined to form a complete DEM. Adaptive tiling allows the surfacing routine to function adequately on any computer platform regardless of internal memory structure and memory limitations.

Chapter 4
Image Processing for Digital Data Capture

The image processing techniques required to capture elevation data from topographic maps are simple, generic, and are part of virtually all digital image processing systems. The hardware requirements are a flatbed scanner used to capture a grey scaled raster image of contour lines, and a computer with sufficient power and memory to process the image. Limitations in processing power and memory of the computer can be compensated for by segmenting the image into manageable sub-images during processing and recombining them to produce a final product. The image processing functions required are cropping, rotation, scaling, copying / pasting, thresholding, and painting. The image processing software utilized in this research was Adobe Photoshop version 3.0. Photoshop provides all the tools indicated above along with many others which, though useful, were not essential nor required in the completion of this work. Any image processing system which contains the basic operations stated above could have been used to achieve the same final results.

Scanning Topographic Maps

Conversion of elevation data from the paper map format to a digital file format occurred in five separate stages. Adobe Photoshop and associated image processing operations were central to the first four stages. The fifth stage involved converting the final processed raster image to XYZ point values and required a special program developed for that purpose.

The first stage was the actual capture or scanning of the topographic map. Scanning began with selection of a suitable spatial resolution which would cleanly differentiate most of the contour lines without providing excessive detail. Several small test scans were taken at various resolutions to identify a resolution which would capture contour lines at a width of 3 to 4 pixels (Figure 4.1). The reasons for selecting a resolution in this manner are twofold. First, the center of the contour lines can be identified by thresholding or clipping the grey level values. Placing elevation values at the center of the contour lines using a medium pixel resolution (Figure 4.1b) gives a higher level of accuracy than is possible with a coarse resolution

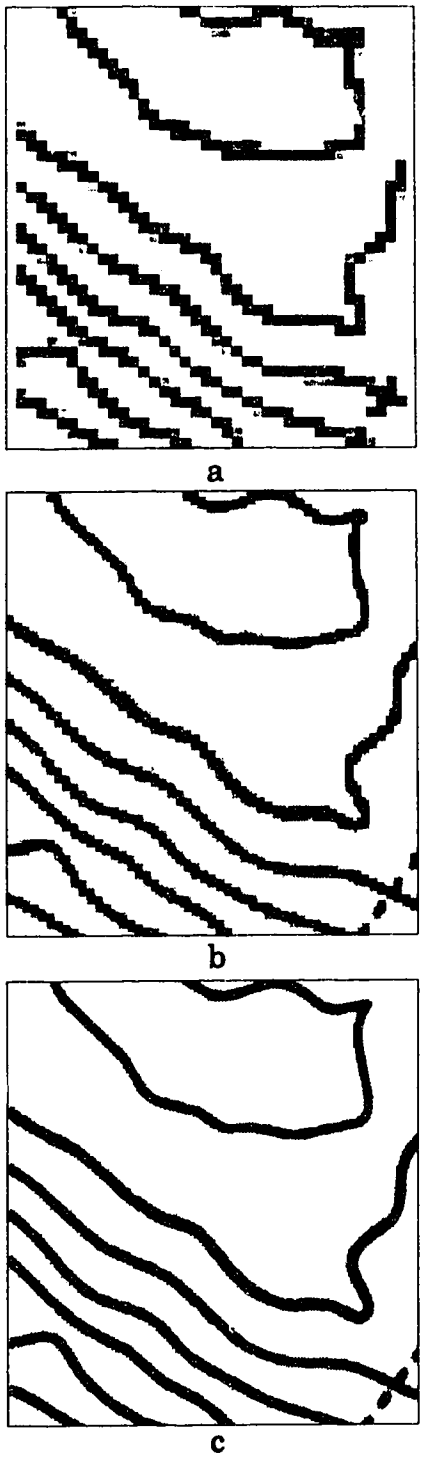

Figure 4.1. Sample scans at: a. coarse; b. medium; c. fine resolutions.

(Figure 4.1a). A very fine scan resolution (Figure 4.1c) would result in huge and unmanageable file sizes while incorrectly providing more location accuracy than the map actually contains. Second, the "magic wand" tool in Photoshop, a tool which can select contiguous areas of similar pixels, will only locate chains of pixels with contiguous edges as in Figure 4.1b and Figure 4.1c. Diagonal chains of single pixels (Figure 4.1a) can not be automatically selected with the wand tool. The wand tool is one of the previously mentioned useful, though not essential, functions which made encoding of the elevation data much more efficient.

Following determination of an appropriate resolution, the entire map sheet was scanned as 8 bit grey scaled image segments until complete coverage was achieved. Each of segment was geometrically corrected with the rotation operator until UTM registration marks were horizontally and vertically aligned (Figure 4.2). The segments were then combined to form a complete digital scan of the entire map sheet.

Image Processing

The second stage of data capture focused on cleaning and preparing the scanned image for data encoding. Cleaning the image involved using the digital eraser to remove pixels of text, symbols, and other markers which came in contact with the pixels of contour lines (Figure 4.3). If these "noise" pixels were not removed, the wand tool would include them as part of the contour lines when those specific contour lines were selected. Often several adjacent contours would be selected together when the "noise" bridged the spaces between them. A copy of the final cleaned image was then saved for use in the data reduction stage.

Elevation Encoding

The choice of which grey tones to assign to each contour level was determined by identifying the elevation extremes in the map through inspection. The range of elevations for map sheet 83C/01-NW proceeded from a low of 1316m at lake level to a high of 2820m with a contour interval of 20m. Therefore, there were (2820 - 1316) / 20 + 1 or 76 separate elevation levels to label. An elevation increase of 10m per grey tone would require a

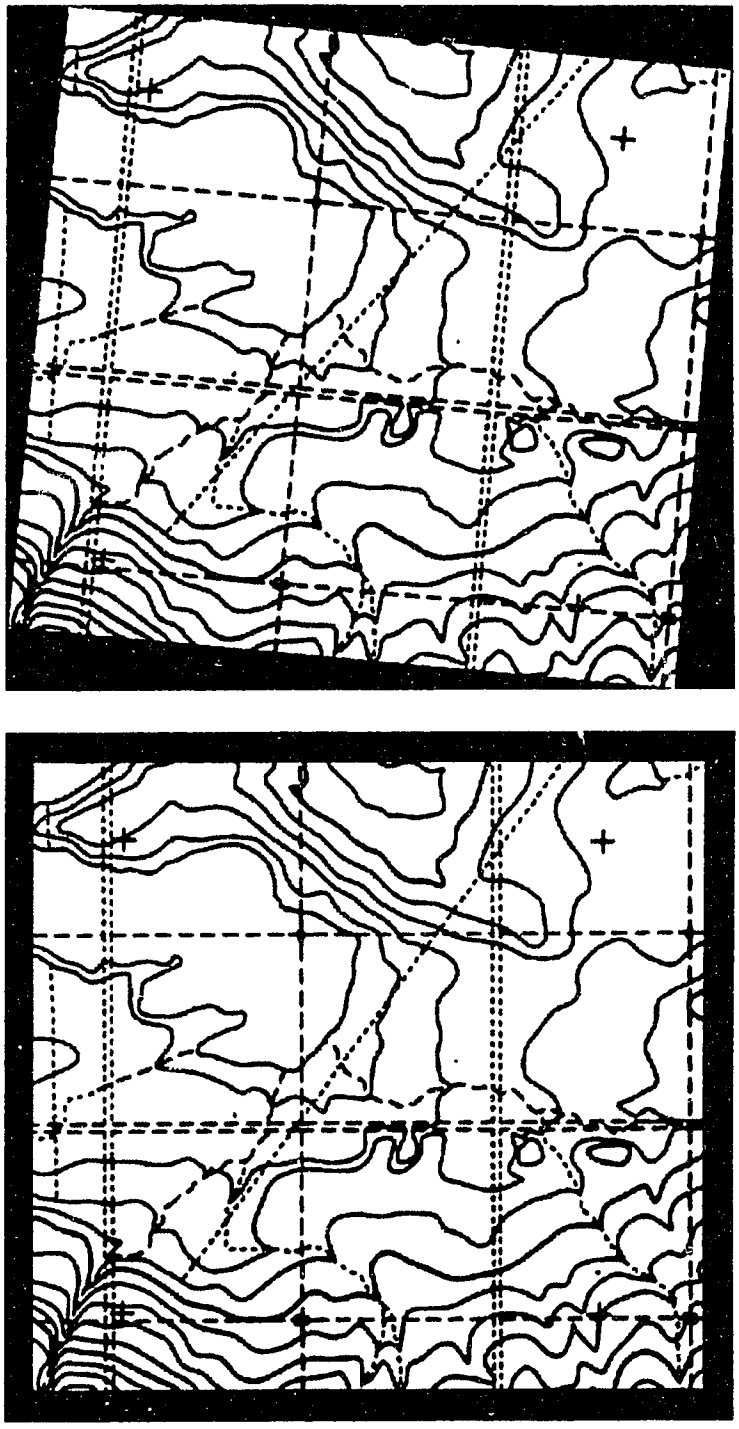

Figure 4.2. Rotation of scanned map segments for rectangular alignment of UTM registration marks.

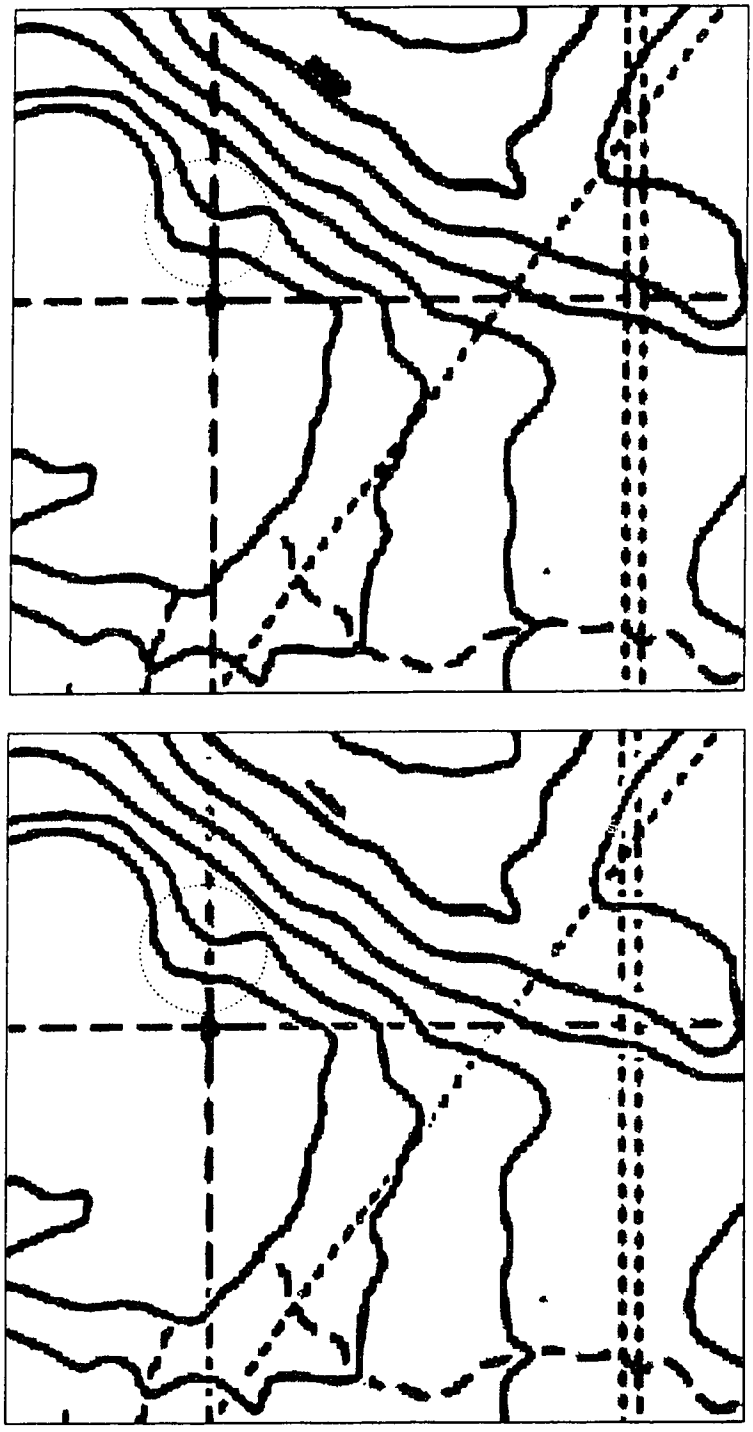

Figure 4.3. Contour lines are isolated by erasing connecting pixels along the contour borders.

sequence of 150 grey tones and would easily fit within the range of 256 tones available. An initial grey tone of 62 was chosen to represent elevation 1320m to enable easy visual differentiation between processed contours (dark grey to light grey) and unprocessed contours (black). Final selection of grey tones used to encode elevation data ranged from 62 to 212 and covered all contour elevations on the map.

Encoding elevation data was a simple repetitive cycle of manually selecting a contour then filling the selection with the appropriate grey tone value. The magic wand tool in Photoshop would select an entire contour line or continuous segment of a line permitting the entire set of pixels to be filled with a grey tone quickly and efficiently. The majority of contour lines in the test map were encoded using this select and fill cycle. Exceptions to the select and fill process occurred where steepness of the represented elevation changes caused the contour lines to merge. When contours merged the wand tool could not separate them for individual processing. The pencil tool was used to uniquely encode the separate pixels of merged contour lines.

Complete encoding of all contours in the test map was accomplished in several sittings and took approximately 28 hours including time spent cleaning the image in stage 2. For comparison purposes, a section of the map sheet was then encoded using traditional methods on a digitizing table. The time required to encode the entire map through digitizing was extrapolated from the sample and was determined to range between 35 and 40 hours depending on the care taken to digitize the center of contour lines. The time to encode the map using image processing techniques compares favorably with the traditional digitizing process. An additional benefit of the image processing approach is that locational accuracy is constant and consistent throughout the map and does not depend on the steady hand-eye coordination of the operator. Long periods of traditional map digitizing can lead to muscle fatigue and eye strain for the operator. Both of these physiological responses to protracted and repetitive digitizing motions can result in digitized points which do not coincide with the centers of contour lines.

Image Data Reduction

The fourth stage of encoding elevation data involved reducing the actual amount of encoded data while improving locational accuracy of the

retained information. The dual purpose procedure was achieved by thinning the encoded contour lines from their three to four pixel wide representations down to the single pixel centers of the lines (Figure 4.4). Thinning the lines was a two step process involving the image operators for thresholding, copying, and pasting. The first step was to threshold the cleaned grey scaled backup image saved in stage 2. Thresholding in Photoshop produces a black and white binary image where all grey tones less than the threshold are black and all others are white. The threshold level utilized was selected and adjusted visually in Photoshop until contour lines in the resulting binary image were one pixel wide. Care must be taken at this step to select a threshold that thins the contour lines without deleting segments of the contour centers. The real time preview option of Photoshop provides a useful tool for quickly adjusting and appraising the suitability of each threshold level.

The second step in data reduction required copying the white area of the thresholded binary image and pasting it into the encoded elevation image. Perfect registration between the two images allowed the white space of the binary image to mask off the sides of the contours in the encoded image in one quick and precise step. The final processed and encoded image was then written to disk as a raw binary image file.

Before the fifth and final stage of the data acquisition could proceed, some information had to be visually extracted from the encoded data file. Specifically, UTM coordinates of the relevant region of the image had to be determined. The UTM easting and northing dimensions of the image pixels were calculated from row and column values of the extreme UTM registration marks in the image. The equation used to calculate cell dimensions was:

$$\text{UTM meters per cell} = (\text{UTM_Max} - \text{UTM_Min}) / (\text{Cell_Max} - \text{Cell_Min})$$

Knowing the pixel dimensions in UTM coordinates permitted proper determination of UTM values for the pixels in the corners of the image based on the internal location of the UTM registration marks. The information on the relationship between UTM values and pixel locations was utilized in stage five.

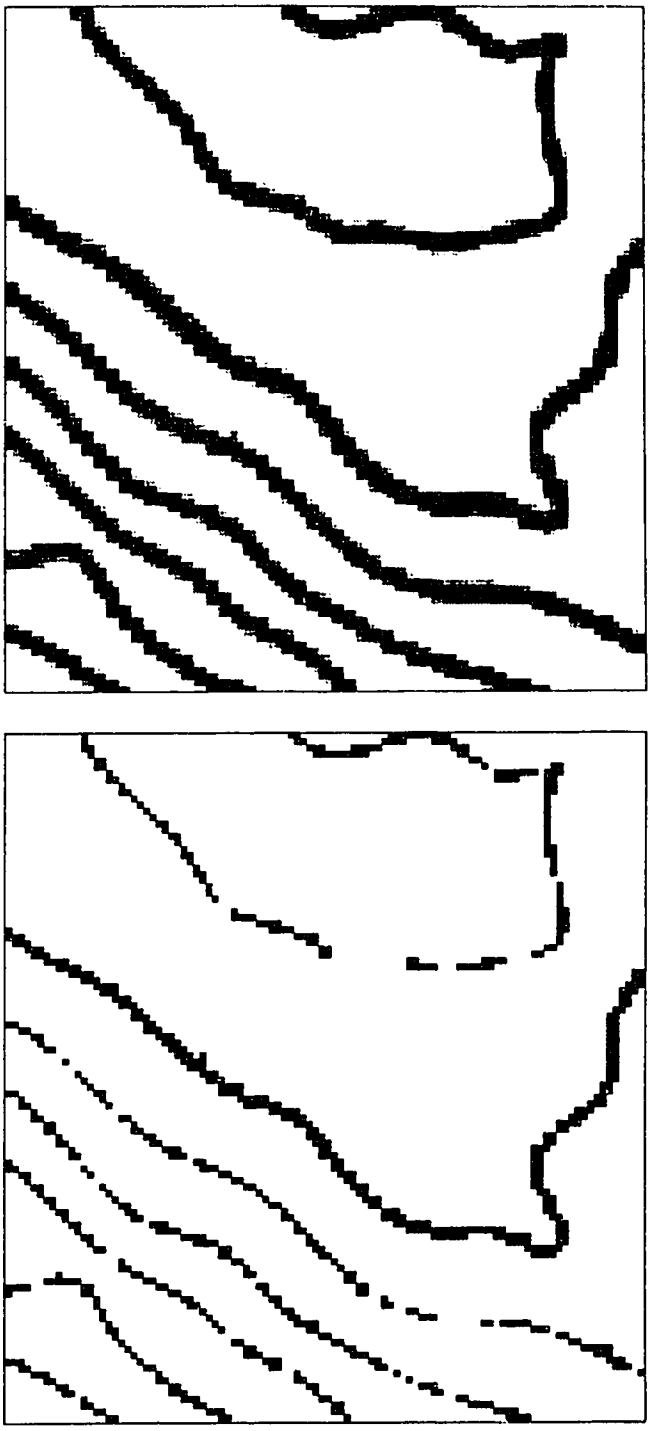

Figure 4.4. A contour mask is created by thresholding a copy of the scanned image. The mask is pasted over the final encoded image to thin the contours to their centers.

Extracting Elevation Information from a Raster Image

The fifth and final stage of capturing digital elevation data required extracting elevation locations from the implied location format of the raster to explicitly defined XYZ locations. A program was developed which automatically performed the necessary data conversions. The program prompts the operator for information defining the dimensions of a single cell in the raster, total size of the image raster, world coordinate values of the first cell in the raster, and the grey tone to elevation encoding used. The program was designed to ignore grey tone values of 0 and 255, which allows registration marks to be left in the image without compromising the encoding scheme. Once the required information is entered, the program proceeds to extract all encoded elevations as explicitly defined coordinate triplets. Depending on the resolution of the image scan, and on the degree of data reduction performed in stage four, the resulting file of elevation points may become very large and contain literally hundreds of thousands of values. In the case where the number of points becomes unmanageable for the computing resources available, a further reduction of data will be required before the actual surfacing program can be executed.

Chapter 5
Data Management for Small Computers

Surfacing DEMs using DOS based operating systems can be a challenging endeavor due to the potentially large number of data points involved, combined with the restrictive segmented memory architecture of the computer. A program designed to generate DEMs under these conditions must efficiently and effectively handle not only thousands of data values, but also the thousands of requests for data retrieval based on approximated spatial locations. Retrieval locations are described as approximated locations due to the fact that retrieval requests are in the form of "which N points are closest to location L". The spatial nature of digital elevation values, given in the form of XYZ triplet coordinates, suggest that a multi-dimensional handling of the data may be advantageous for purposes of rapid searching and retrieval. Several highly sophisticated and efficient techniques for handling multi-dimensional data have been developed in the field of computer science (Aho, 1983). The general classification under which these multi-dimensional algorithms are identified is "range searching" (Sedgewick, 1983).

Range Searching

The general premise of range searching as applied to geographic elevation data is that elevation values constitute records in a database indexed by two attributes representing the spatial location (Sedgewick, 1983, p. 335). Items are located through a search for all records which satisfy all attribute requirements as bounded by range conditions. For DEM surfacing, bounding range conditions are simply the X and Y limits identifying a rectangular area of interest. Elevation values which correspond to X and Y attributes located within the rectangular range are selected for processing. Many computer science texts explain in detail the merits of various range searching algorithms (Aho et al., 1983; Claybrook, 1983). For the purpose of this research, a multi-dimensional enhancement to the simple binary tree searching algorithm was employed.

Two Dimensional Binary Search Trees

Binary search trees are simple, efficient, dynamic searching methods based on one of the most fundamental algorithms in computing science (Sedgewick, 1983). Two-dimensional trees are dynamic, adaptable data structures which are very similar to binary trees but divide up a geometric space in a manner convenient for use in range searching (Sedgewick, 1983). Multi-dimensional binary trees are nearly identical to traditional binary trees with the difference being that at each level in the tree a different attribute is identified as the key to determine branching. In a simple two-dimensional search tree of geographic positional data the X and Y attributes function as branching keys on alternate levels (Figure 5.1).

A pre-processing algorithm is used to create the two-dimensional binary search tree from a data file before the actual range searching algorithm can be used. The code to construct a two-dimensional binary search tree is a straight forward modification of standard binary tree construction code which has been published in many computer science and algorithm texts (Tremblay and Bunt, 1979; Aho et al., 1983). The modification involves a switch to alternate the testing of X and Y coordinates on alternate levels of the tree. Published statistics for the efficiency of creating a binary search tree (Claybrook, 1983; Sedgewick, 1983) state that the average time to create a tree using randomly distributed points is proportional to NlogN, where N is the total number of points to be added to the tree. An important note is that randomly distributed points are used to determine the average construction efficiency. For specific combinations of data points the construction efficiency can hit a worst case scenario of an N^2 proportionality. Statistics for creating a two-dimensional binary search tree are the same as the statistics for creating the traditional binary tree, namely NlogN. Statistical similarity is consistent with the nearly identical algorithms required to create the two types of binary trees. As with the traditional binary search tree, a worst case scenario for creating a two-dimensional binary search tree can hit a proportionality of N^2.

Algorithms for traversing a binary search tree typically employ recursion to control branching and returning between levels of the tree. Recursive search routines are easy to design and are very easy to implement in most programming languages. The problem with recursion, however, is

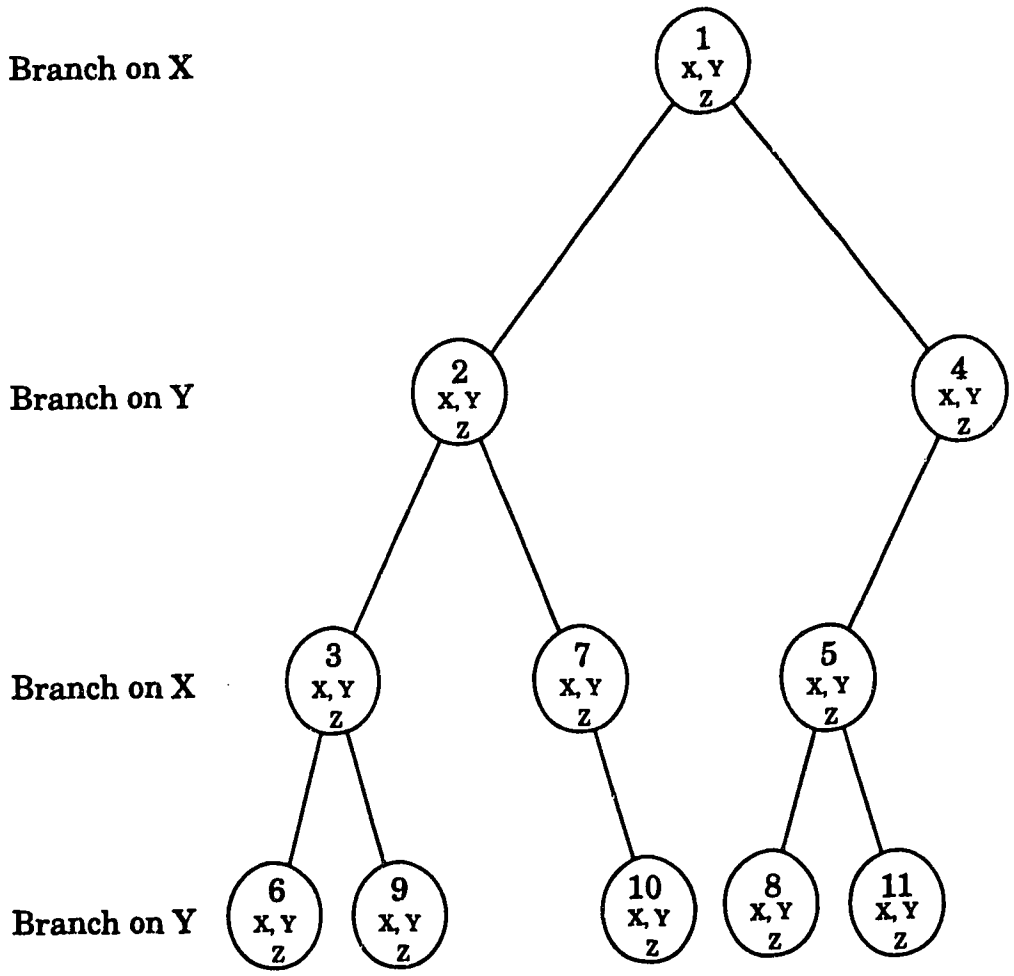

Figure 5.1. Sample two dimensional binary search tree with 11 nodes containing XYZ coordinate information.

that space in a computer's memory stack must be available to store system values every time a recursion call takes place. On a DOS based computer the stack space is at a premium and memory problems can rapidly develop when hundreds of recursion calls are made into a binary search tree containing tens of thousands of data values.

A non-recursive post-fix traversal algorithm for two-dimensional binary search trees was developed during the course of this research. The non-recursive search routine eliminated the stack problems on DOS based computers without impacting on the performance characteristics of the binary search tree algorithm. The branching logic of the non-recursive routine matched the branching logic in the traditional recursive search routine, however, an internal loop and two boolean flags were utilized to control traversal directions. Comparison of the non-recursive branching logic with the traditional recursion logic indicates that performance of the non-recursive routine matches performance of the recursive method. Published statistics for the efficiency of binary search tree traversals (Aho et al., 1983; Sedgewick, 1983) reveal that the number of checks needed to locate one point in a tree containing N points is proportional to logN. Therefore, the efficiency of searching for the R points contained in a defined range using a two-dimensional binary tree containing N points would be proportional to R+logN. These efficiency values indicate the average performance characteristics for binary search trees and would not be valid if points in the tree are distributed such that the worst case scenario developed. Random distribution of points helps to prevent the worst case scenario from developing.

Chapter 6
An Analytical Tiling Approach To Surfacing

Prediction, interpolation, and representation of topographic surfaces from initial sets of irregularly distributed location data has resulted in the development of many analytical and numerical surface-fitting methodologies. Franke (1979) and Hein (1979: cited in Schiro and Williams, 1983) investigated 29 and 8 different surfacing approaches respectively with the goals of evaluating the efficiency and accuracy of each method. A clear definition of what constitutes a surface is necessary to evaluate the characteristics of any surface generating process. Schiro and Williams (1983) proposed the following statement for defining a surface in terms of a model:

> Given the points (X_k, Y_k, Z_k), k=1,..,N over some domain (D(X,Y)), a function is desired which reproduces the given points and produces a reasonable estimate of the surface (Z) to all other points (X,Y) in the given domain.

Two key conditions of this definition provide limits which can be used to classify and evaluate the functionality of surfacing methodologies. The condition that a surfacing method "reproduces the given points" defines a boundary for classifying the method as either an approximation or an interpolation approach (Schumacher, 1976). Approximation approaches assume a degree of measurement error in the initial data making exact reproduction of the initial data undesirable. Least-squares based techniques are a common example of an approximation approach. Interpolation approaches assume that initial irregular data contain exact measurements of the topographic surface. Interpolation approaches preserve the exact measurements and can reproduce original sample data precisely.

The condition that a surfacing approach "produces a reasonable estimate of the surface" is a difficult condition to define or quantify since the intended application of a surface may strongly influence how reasonable the estimated results are. In both the Franke (1979) and Hein (1979) investigations, surfaces generated using a technique of multiquadric interpolating were judged the best in terms of surface accuracy and

computation time. Topographic surface generation using multiquadric interpolation is developed and evaluated in this work.

Multiquadric Equations

Multiquadric interpolation was developed by Dr. Rolland Hardy at Iowa State University (Hardy, 1971, 1972, 1975). Mathematically, a "quadric" is identified as a locus of points which satisfy a second degree polynomial equation. Spain (1960) defined a quadric surface as a locus of points whose coordinates satisfied any general equation of second degree. Multiquadric interpolation describes the process of evaluating multiple quadric surfaces defined in a common spatial domain to produce a solution common to each separate quadric surface. Mathematically a multiquadric-based method for surface generation can be written as:

$$Z = \sum_{i=1}^{n} C_i [Q(X,Y,X_i,Y_i)]$$

where each Q is a quadric surface (Schiro and Williams, 1984). The C_i's are obtained by evaluating the individual quadric surfaces (Q) resulting from substitutions of (X_i, Y_i, Z_i); i=1..N. The N resulting quadric equations are solved as a set of N simultaneous equations. Hardy (1971) provides an extensive analysis of the mathematical steps and principles involved with implementing multiquadric surface interpolations. Eyton (1974) provides a complete example solution for a simplified set consisting of three data points (Figure 6.1). The algorithms designed to implement multiquadric surfacing in this research solved the systems of simultaneous equations using a lower-upper (LU) triangular decomposition routine (Press et al., 1988). The LU decomposition technique was chosen for its characteristic of allowing new interpolation points to be evaluated through back substitution into the solved matrix (Johnston, 1982). A special note should be made that the LU decomposition method for solving simultaneous equations fails when the system is ill conditioned (Johnston, 1982; Press et al., 1988). When dealing with multiquadric equations, the system will become ill conditioned when

1. DATA:

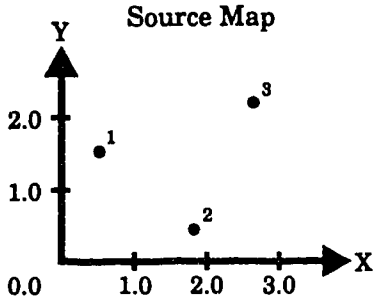

Sample Data

Obs.	Coord.	Z Value
1	X1 , Y1	Z1
2	X2 , Y2	Z2
3	X3 , Y3	Z3

2. MULTIQUADRIC HEIGHT SURFACE EQUATION:

General form: $Z = \sum_{j=1}^{n} C_j [(X_j - X)^2 + (Y_j - Y)^2]^{1/2}$

3. SOLUTION:

General form: $[C_j] = [a_{i\,j}]^{-1} [Z_j]$

Expanding $[a_{i\,j}]$ for sample data:

$$\begin{aligned} a_{11} &= [(X_1 - X_1)^2 + (Y_1 - Y_1)^2]^{1/2} \\ a_{12} &= [(X_1 - X_2)^2 + (Y_1 - Y_2)^2]^{1/2} \\ a_{13} &= [(X_1 - X_3)^2 + (Y_1 - Y_3)^2]^{1/2} \\ &\vdots \qquad\qquad \vdots \\ a_{33} &= [(X_3 - X_3)^2 + (Y_3 - Y_3)^2]^{1/2} \end{aligned}$$

Solution for sample data:

$$\begin{bmatrix} C_1 \\ C_2 \\ C_3 \end{bmatrix} = \begin{bmatrix} a_{11} & a_{12} & a_{13} \\ a_{21} & a_{22} & a_{23} \\ a_{31} & a_{32} & a_{33} \end{bmatrix}^{-1} \begin{bmatrix} Z_1 \\ Z_2 \\ Z_3 \end{bmatrix}$$

4. MULTIQUADRIC HEIGHT SURFACE EQUATION FOR SAMPLE DATA:

$$Z = C_1 [(X_1 - X)^2 + (Y_1 - Y)^2]^{1/2} + C_2 [(X_2 - X)^2 + (Y_2 - Y)^2]^{1/2} + C_3 [(X_3 - X)^2 + (Y_3 - Y)^2]^{1/2}$$

Where: Z = Elevation at any location X,Y

Table 6.1. Example summary for evaluating a multiquadric solution. Source: Eyton, 1974

two data points used in the solution of a system are located at the same (X,Y) spatial location. Care must be taken with multiquadric methods to ensure no points are duplicated in the initial data set.

Tiling

Approximation and interpolation methods for predicting surfaces may be classified as either global or local (Schiro and Williams, 1983) based on selection and relative weights assigned to points used in evaluating the surface. Local methods generate a modelling function utilizing just data points which provide the most influence nearest a location to be evaluated. Global methods employ all data values to determine a modelling function. Multiquadric equations are a global method for modelling topography as every data value entered into the equations may make a significant contribution to the final modelling function. A problem occurs when the number of data values becomes large. Each data value selected adds another simultaneous equation to the system. Solving a system of N simultaneous equations requires solving an N by N matrix of equation coefficients. Few computers are available (or accessible) which can solve the matrices that result when thousands or tens of thousands of data values are considered.

The computational problems raised by large numbers of data points can be resolved by treating the topographic surface being generated as a set of smaller overlapping surfaces defined by smaller, separate sets of data points. The small sets of data points can then be modelled by multiquadric equations to interpolate topographic subsets which are combined to form the complete DEM. The key to partitioning a set of data points into smaller subsets in an efficient and effective manner lies in the ability to adapt to unpredictable density changes in the distribution of the data. An early attempt at partitioning data points to support non-overlapping surface tiles was successfully developed by Eyton (1974): this methodology generated surfaces that did not contain artifacts where data density was uniform, but produced boundary effects around tiles where data density varied strongly.

Tile Boundary Effects

Experience through years of periodic investigations into surfacing research has shown that partitioning data point distributions into uniformly sized, contiguously spaced tiles or neighborhoods of points produced reasonable results for DEM surfaces where point distributions were dense. In areas where the point distribution was thin or sparse, partitioning points into uniformly sized tile units produced very undesirable results along the boundaries of each tile. In areas of thinly distributed points, seams appeared along the boundaries of each tile where the evaluated surfaces from adjoining tiles did not agree. The seams result from a lack of control when defining the edges of evaluated surface tiles due to the sparseness of data points in each partitioned region. The seams may be exaggerated or very subtle in the DEM surface but are recognizable by their perfect alignment along row and column directions.

Adaptive Tiling

Attempts to minimize effects of tile boundaries resulting from unpredictable variations in data point distributions resulted in an adaptive tiling scheme which takes advantage of the variations in data distribution to improve overall computational efficiency of the process. The basic tenet of adaptive tile partitioning is to subset data points dynamically based on local data distributions centered on the surface tile under evaluation at any given time. A surface tile is then interpolated only in the area which is well defined and controlled by the partitioned data values.

Tile boundaries are further reduced by selecting subsequent tile centers along the edges of previously evaluated tiles. The practice of selecting new tile centers along these edges guarantees up to 50% overlap between old and new tile surfaces. Tile overlaps are combined as a weighted blend based on a cell's distance to the new tile's center. Blending tile boundaries with the centers of subsequent tiles removed nearly all traces of tile boundaries in the resulting DEMs. Computational efficiency of the adaptive tiling method is improved relative to the uniform tiling method due to increased surface coverage generated from the solution of single sets of multiquadric equations in sparse locations. The sizes of systems of simultaneous multiquadric equations were coded to be the same for both

adaptive and uniform tiling methods, however, the variable tile size of the adaptive method permitted greater topographic surface interpolation in regions of low data point distributions and therefore less numbers of tiles needed to be evaluated.

Directional Point Selection

Adaptive tiling based on point density distributions reduces computational time and reduces the effects of tile boundaries within sparsely represented data regions; however, tile boundaries are still a problem along transition zones between densely and sparsely distributed regions. Tile boundaries which appear along these transitional zones result from disproportionate control across the area being interpolated due to sudden increases or decreases in the representation of data points (Figure 6.2). Investigations into ensuring balanced representation and control of data points throughout a particular partition produced a points partitioning based on directional modifications to the previously defined density modifications. In the directional representation scheme, points are selected for a partition based on proximity to the center of a tile and on location in one of eight sectors radially arranged around the tile center (Figure 6.3). Approximately equal numbers of points are selected from each sector giving uniform representation and control to all sides of a tile partition. The area interpolated by the multiquadric equations within the directional partition is determined by the shortest distance to the farthest point found in each of the sectors to ensure control of the tile surface, even at the edges. Tight control over the entire tile surface ensures smooth blending with adjacent overlapping tiles. Directional data point selection within an adaptive tiling scheme produced a multiquadric surfacing approach which was computationally efficient and generated DEM surfaces which were essentially boundary free, even when extremely high variations in point distribution densities were observed.

Post-Processing

Despite the reduction in tile boundaries produced on most data sets when using the adaptive tiling approach, specific arrangements of point distributions were found which would still generate small tile boundary

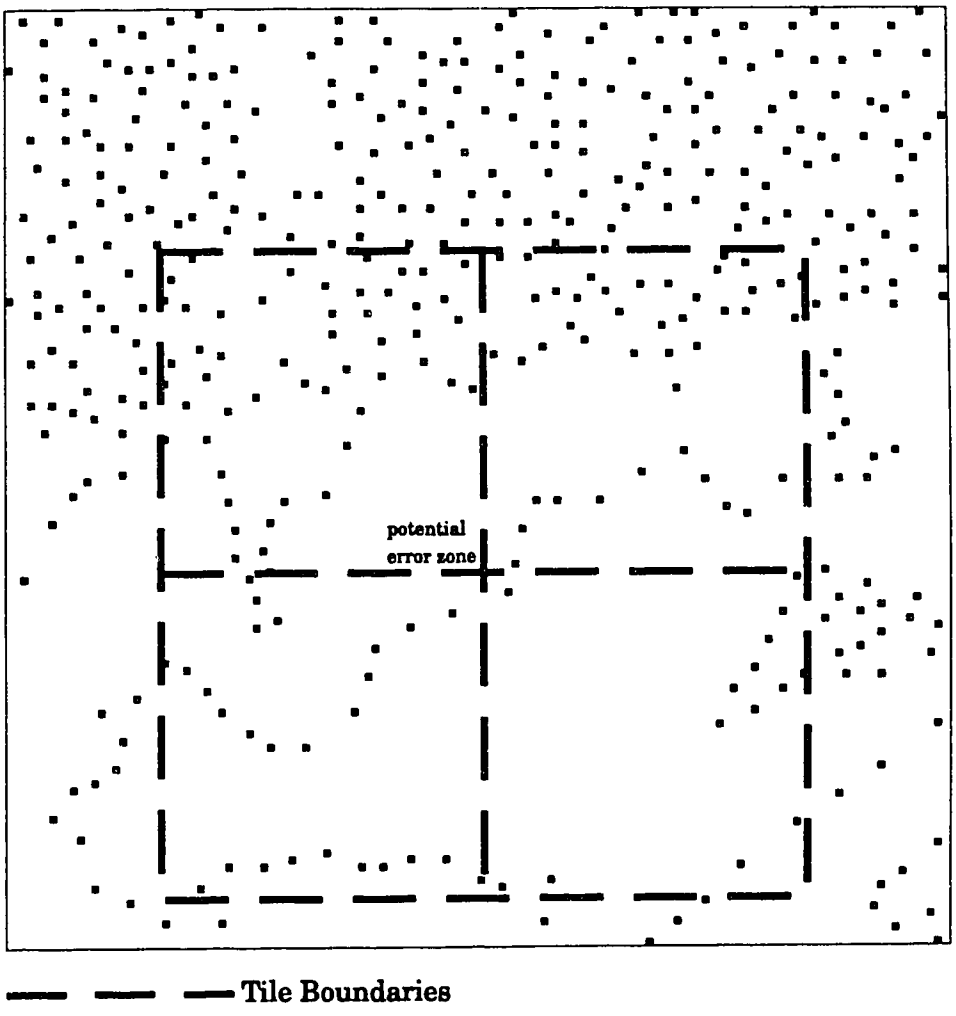

Figure 6.2. Point density variations over the area of a uniform tile may cause surface discontinuities with adjacent tiles.

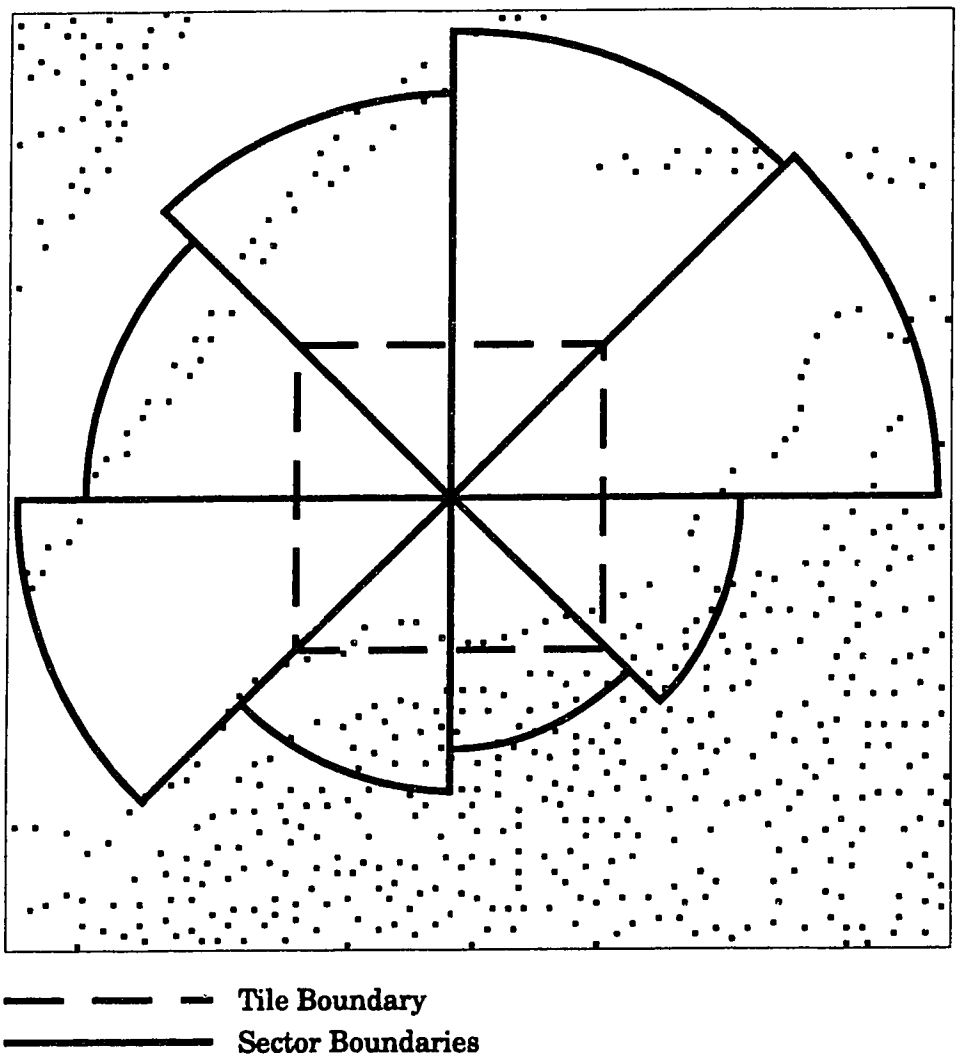

Figure 6.3. For adaptive directional tiling, similar numbers of points are selected from eight sectors radiating around the tile center. Sector sizes adapt to local density variations in data point distributions.

effects. The persistent tile boundaries were subtle and required highly thresholded derivative surfaces to detect. The tile boundaries were due to the spatial arrangement of specific data points causing the directional selection process to fail (Figure 6.4). When the directional selection process failed, a corner of the generated surface tile would not blend cleanly with adjacent tile surfaces of other evaluated point partitions. Investigations of these persistent boundary corners produced a hypothesis that corner boundary effects were a consequence of poor tile locations relative to the distribution pattern within the data points. In all boundary effects identified, moving the tile center from its computer selected location to the location of the boundary corner, fixed the break in the directional selection process and produced a DEM surface with no detectable boundary problems.

Testing the movement of tile centers while investigating boundary errors resulted in development of a post-processing program which is a companion program to the main DEM generating program. The post-processing program uses multiquadric equations to re-interpolate and blend an adaptive tile partition into a previously generated DEM. The new tile location is specified by the operator through an interactive interface. The test DEM generated in this research did not require use of the post-processing program; however, the unpredictable nature of point distributions made development of the post-processing program necessary.

Qsurf

The multiquadric equation methodology, efficient memory management, and adaptive tiling approach to surfacing as discussed previously were brought together in the form of a main program called Qsurf. Qsurf was the end product of many revisions of code, all aimed at maximizing computational efficiency while producing the cleanest and most reliable representations of surfaces from a variety of data sets. The program was developed on an Intel based 486/33 computer running the Microsoft DOS 6.2 operating system. The program was designed to work as efficiently as possible within the 640 kb memory restriction of the DOS operating system without resorting to DOS specific memory handlers. Qsurf was written in ANSI standard C using the Borland C++ version 4.0 compiler. Restricting code development to ANSI standard C permitted the program to be tested without modification on a wide range of computer platforms. Systems on

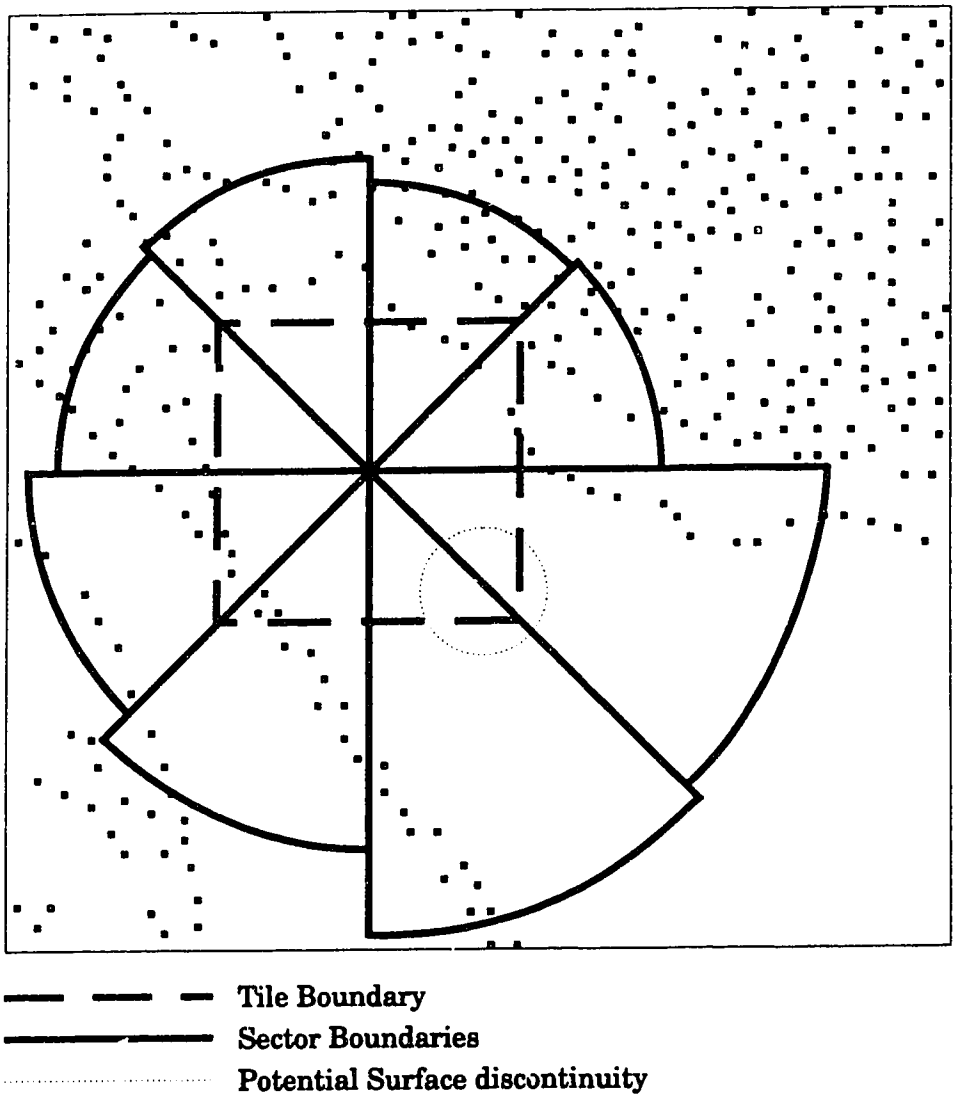

Figure 6.4. Even with adaptive directional tiling, specific patterns in data point distributions can cause surface discontinuities at tile boundaries.

which Qsurf was tested include an IBM RS/6000 running AIX, a Silicon Graphics Indigo running IRIX, a NeXT Station running the NeXT version of UNIX, an Intel based 486DX2/66, and an Intel based Pentium 90. In all tests, a numerically consistent surface was produced from common data test points attesting to the stability and reliability of the program with variations in operating environments.

Qsurf uses a non-recursive two-dimensional binary search tree data structure to optimize memory accesses with the potentially high volume of data points selected to define a surface. The generated surface is stored directly to disk where it is updated through random access routines. Storing the surface directly to disk eliminates memory problems which may result when very large surfaces are generated, while allowing maximum memory space for storing, selecting, and manipulating initial data points. The data points partitioned for evaluating a given tile are identified through a range search in the binary search tree. Identification of points in each of the eight sectors nearest the center of a tile is determined by a sorted list of distances. The program will allow initial data points to be entered as cartesian coordinate units or as spherical coordinate units. Permitting data values to be entered in both cartesian and spherical units ensures that surfaces generated by Qsurf are correct and suitable for both local and regional applications.

The number of points used in calculating a tile surface is controlled in Qsurf by a global constant definable by the operator at the start of program execution. The default value of 20 points per sector (160 per complete system of equations for one tile) was set to optimize program performance on the slowest DOS based computer used in testing. The number of points was set small enough to allow the entire two dimensional array of coefficients used in solving the simultaneous equations to be stored in a single 64 kb memory block. The same limiting value was maintained for tests on the high performance UNIX workstations to permit valid comparisons between all surfaces generated on DOS and UNIX computers while verifying the reliability and stability of the program. The impact that varying the number of points in a partition has on the performance of Qsurf is presented in Figure 6.5. The number of points selected for inclusion in a set of simultaneous equations determines the DEM surface area evaluated in the resulting tile. As the number of points increases the size of the tile increases producing a lower total number of tiles and sets of equations which must be solved. The

Surfacing Time vs Sector Points

Compiled on an Intel 486/33 computer
Note: Test File contained 7434 points

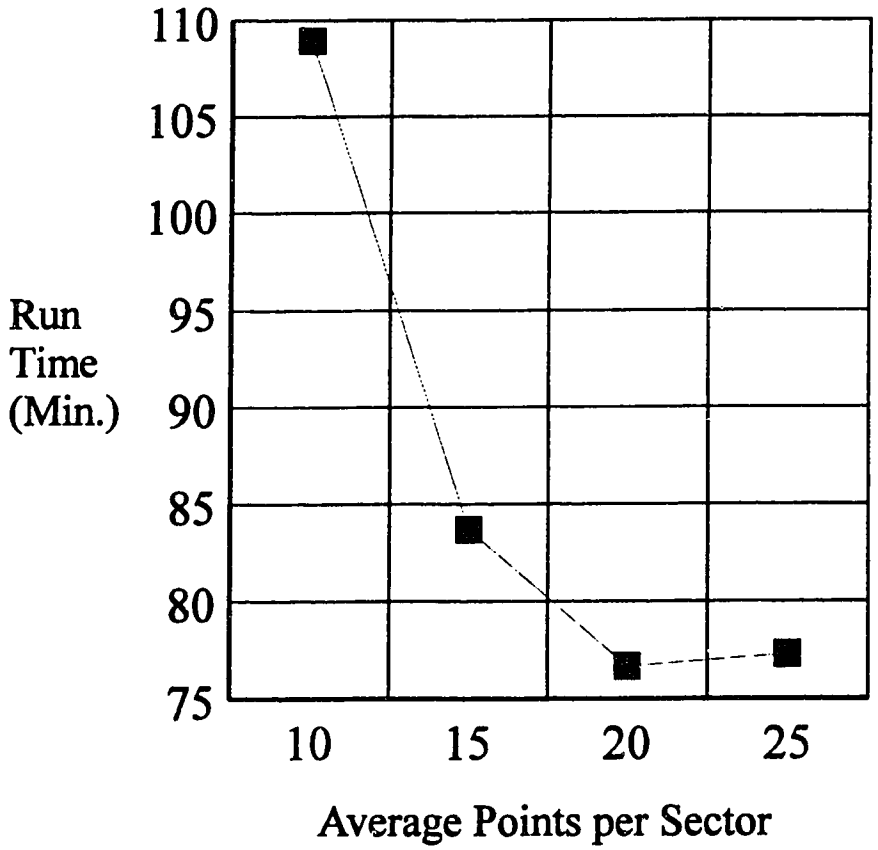

Figure 6.5. Performance chart indicating the relationship between total surfacing time and average number of points selected from each sector of a tile partition.

lower number of sets of simultaneous equations is reflected in Figure 6.5 where the execution time decreases as the number of points increases. When the number of points increases to the value where the size of a set of simultaneous equations exceeds a 64 kb memory block, execution time begins to increase as the time savings obtained by processing a lower number of equations sets is more than offset by the increase in time spent on memory swapping.

Chapter 7
Comparisons with the Alberta 1:20,000 DEM

The DEM surface representing the test area as produced by Qsurf was checked for validity and reliability through comparisons with a DEM supplied by the Provincial Government of Alberta. The Government of Alberta DEM was produced at a scale of 1:20,000 using a commercial program called SCOP. The data supplied to the SCOP program was obtained from direct measurements of stereo ortho-photo images. Numerical and visual comparisons between the two DEM products provided a rigorous, though potentially unfair, evaluation of the Qsurf methodology. The unfair nature of the comparisons is a consequence of using primary source data for the SCOP DEM and secondary source data for the Qsurf DEM. The primary source data used for the SCOP DEM provided a much higher level of terrain specific information than was available from the secondary source. Comparisons between the products was considered valid despite the different data sources because the SCOP product presented a quality controlled base-line surface upon which to evaluate the unknown product generated by Qsurf. The comparisons demonstrated that multiquadric interpolation, combined with an adaptive tiling approach, produced a DEM that was a valid and reliable representation of an actual terrain surface. In nearly all cases, differences between the SCOP DEM and the Qsurf DEM could be explained by the different levels of high frequency detail contained within the primary and secondary data. The programs which generated the derivative surfaces used in the comparisons were developed specifically for DEM analysis by Eyton (1991, 1995) and are released under the collective package name of TERRA FIRMA. In the comparisons presented, derivative surfaces generated from the SCOP DEM are displayed at the top of the figures and the corresponding surfaces generated from the Qsurf DEM are presented at the bottom.

Edge Contours

Edge contour images of the DEMs (Figure 7.1) were generated using a base reference elevation of 1300 meters and a contour interval of 50 meters. The major difference between these two images results from the smoother

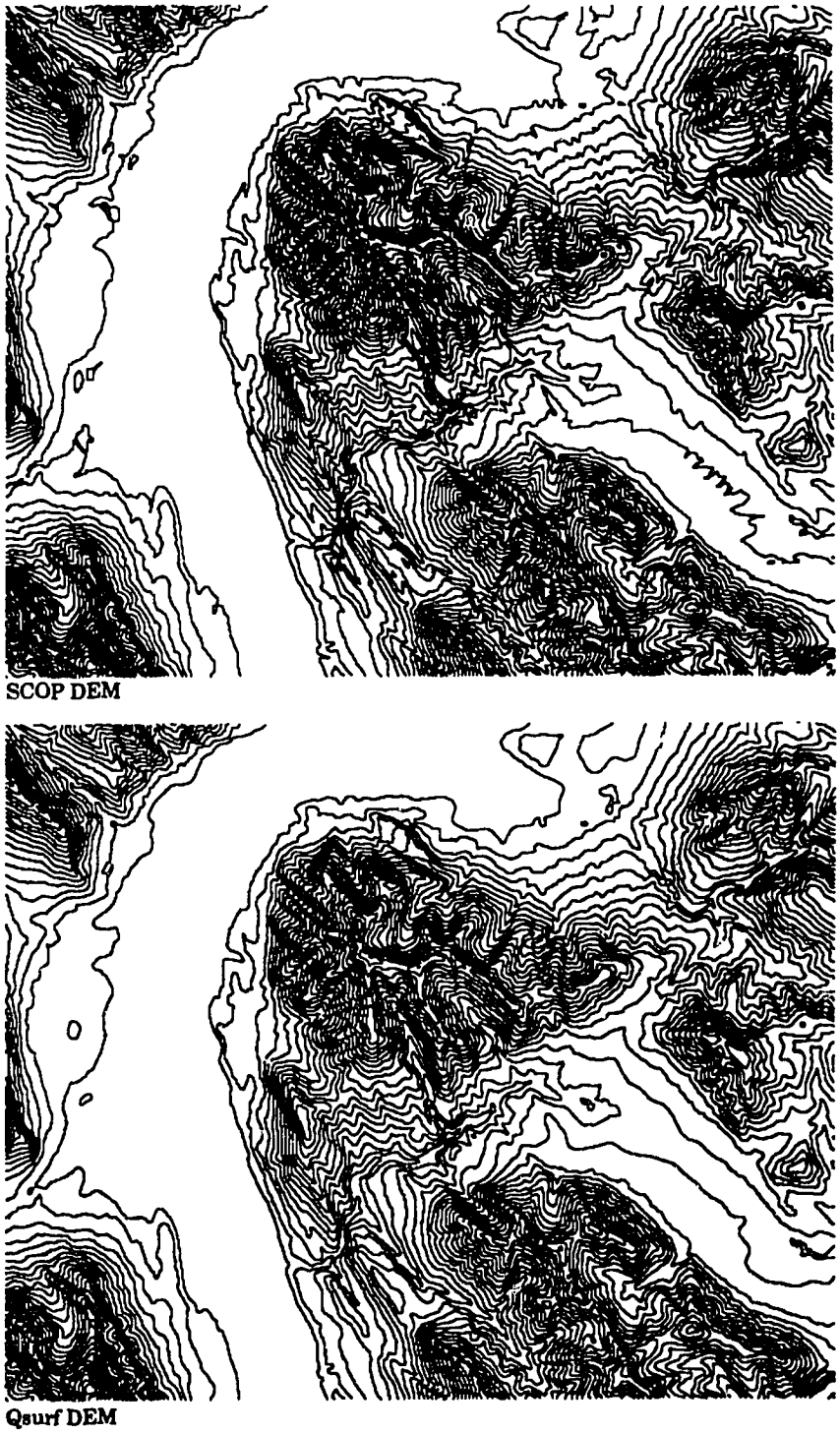

Figure 7.1. Edge contour images. Base reference elevation is 1300m. Contour interval is 50m.

nature of the Qsurf DEM. Contours extracted from the Qsurf DEM are more fluid than the angular contours of the SCOP DEM. Sharper angularity in the SCOP DEM surface resulted from the application of high frequency surficial information in the primary source data. The high frequency data provided information for defining breaklines, divides, and surficial modulations when the surface was generated.

Lambertian Light Model

Lambertian lighting models of the two DEMs show both the similarities and differences between the surfaces (Figure 7.2). The SCOP DEM appears sharper and more defined due to small surficial features like the shallow drainage channels in the lower right area of the image. Details such as the shallow channels were not available in the secondary data and are not present in the Qsurf DEM. Structurally the two surfaces appear identical. The artificial sun used to illuminate the surfaces was placed at an azimuth of 300 degrees and at an altitude of 30 degrees. The light models were clipped at 5% on each tail of the Lambertian light values distribution to enhance the internal detail of the resulting images.

Slope Magnitude

Gray scale images of the slope distributions for the DEMs were almost identical in appearance (Figure 7.3). Small areas of discernable differences between the two images were a product of small deviations in the slopes along shallow drainage channels located in the SCOP DEM. Shallow channels were not present in the initial Qsurf data which accounts for the absence of the corresponding slope changes in the Qsurf DEM. Transitions of slope magnitude are not as sharply defined in the Qsurf DEM image as they are in the SCOP image due to differences in DEM sharpness and definition as previously explained.

Across Slope Curvature

Images of across slope curvature derivatives (Figure 7.4) present the first significant differences between the SCOP and Qsurf DEMs. Across slope

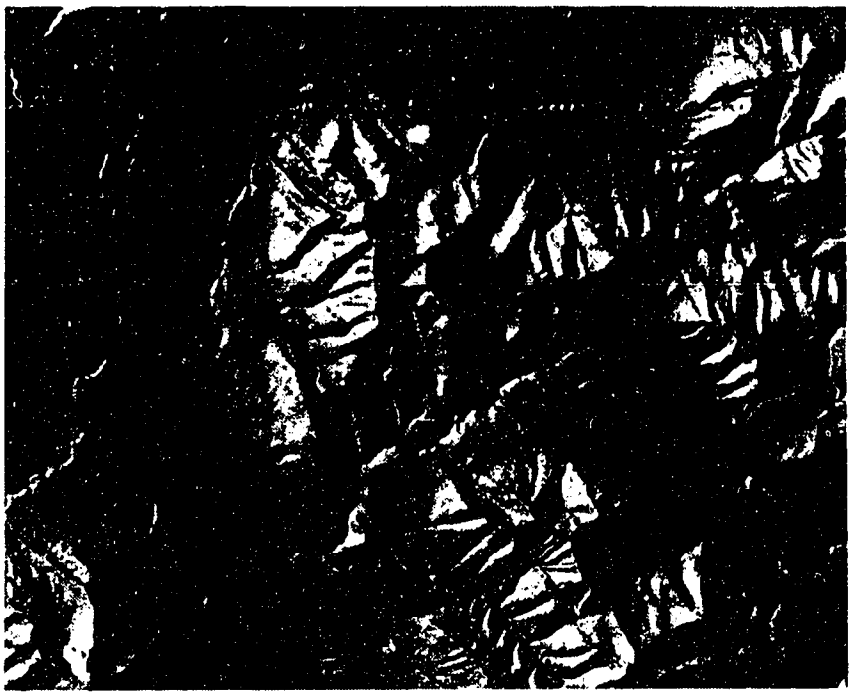

SCOP DEM

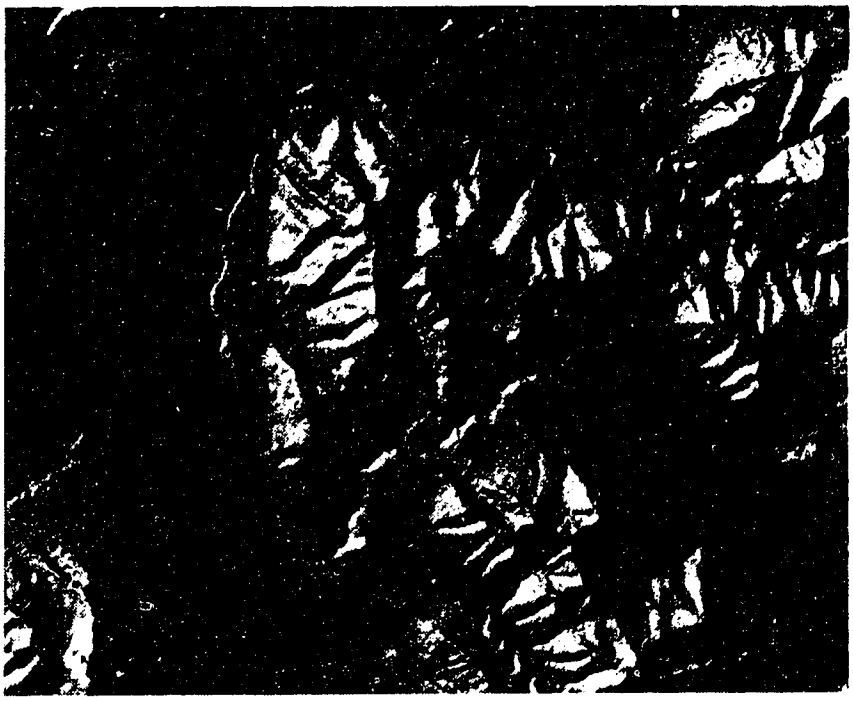

Qsurf DEM

Figure 7.2. Relative radiance images using a Lambertian Light model. Solar illumination is from 300° at an elevation of 30°.

SCOP DEM

Qsurf DEM

Figure 7.3. Slope magnitude images. Maximum magnitudes were clipped at 48° of slope to enhance low-magnitude slope details.

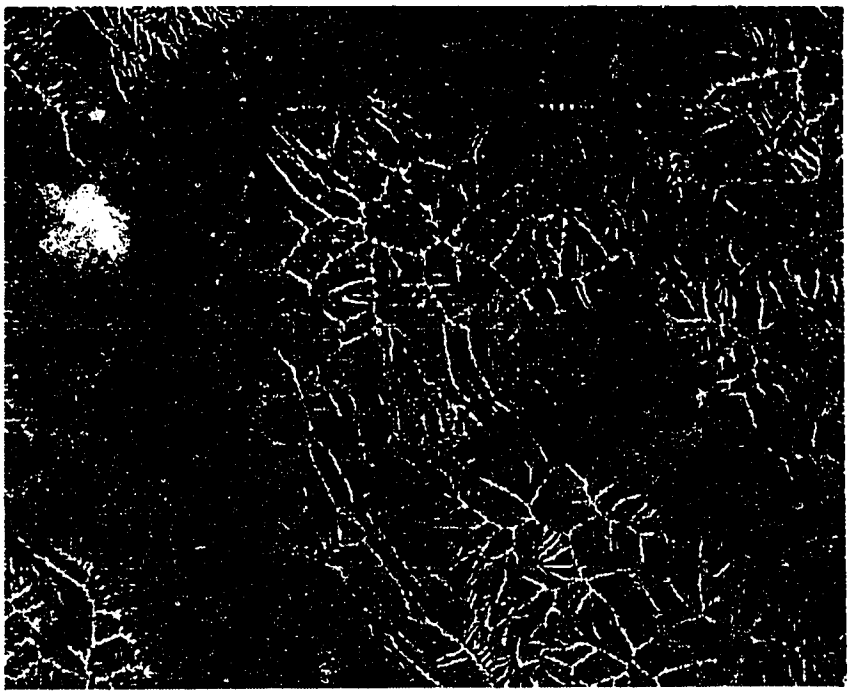

SCOP DEM

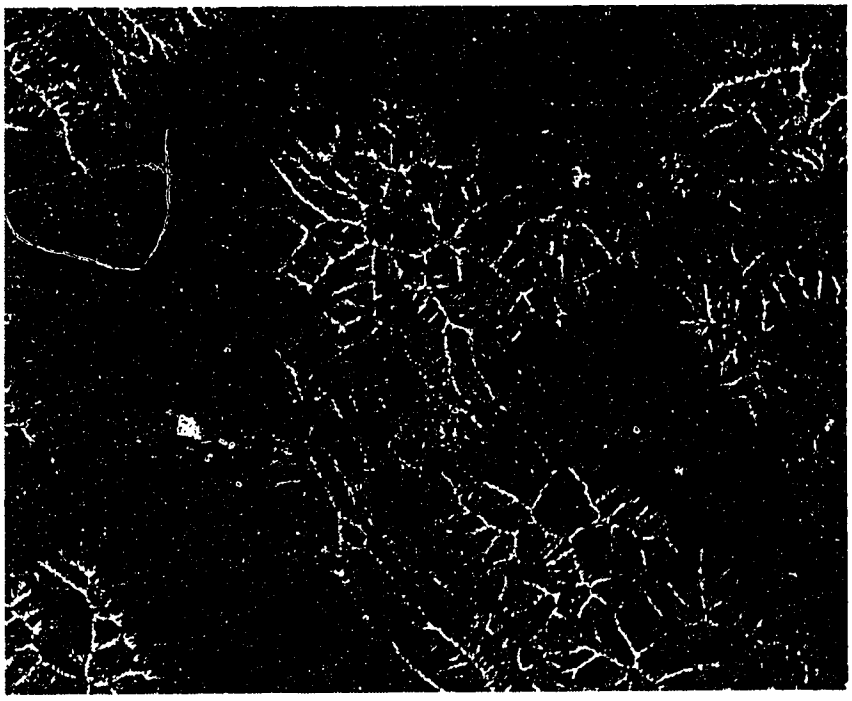

Qsurf DEM

Figure 7.4. Across slope curvature scaled between -80° and 80° of change in slope per 100m.

curvature derivatives reveal the concave and convex curvatures across a slope face at each location in the DEM. Curvature units in these images are defined as degrees of curvature per 100 meters. The images were produced by scaling the curvatures between -80.0 and 80.0 which represented a 3% clipping of the most extreme concave and convex curvatures. The images show that curvatures along the channels and divides are very similar between the two DEMs. The Qsurf DEM across slope curvature image presents smooth transitions of curvature between divides and channels with little or no change in across slope curvature through level and flat areas. The across slope curvature image of the SCOP DEM also presents smooth transitions between the divides and channels. However, the SCOP DEM image also reveals artifacts in the DEM resulting from the initial data sampling and the interpolation method evaluated in generating the DEM.

Across slope curvature through flat and level areas of the SCOP DEM show the location of sample points use to interpolate the DEM as well as uniformly spaced curvature discontinuities resulting from linear interpolation of cell values along row and column directions. When linear interpolation is utilized for interpolating unknown elevation values, the curvature over the interpolated range drops to zero. Discontinuities caused by sudden drops in curvature are evident in the second derivative products such as across slope or down slope curvature. Discontinuities caused by linear interpolation are not desirable and can drastically interfere with curvature calculations or estimations subsequently extracted from the DEMs. Curvature discontinuities did not occur in the Qsurf DEM due to the smooth, neutral, and non-linear interpolations that result from utilizing a multiquadric equation approach.

Down Slope Curvature

Down slope curvature derivatives present information similar to that presented by across slope curvature derivatives. Down slope curvature derivatives describe curvature down the face of a slope as the rate of change of slope per 100 meters. The SCOP and Qsurf down slope curvature images (Figure 7.5) were produced by scaling the derivatives between values -80.0 and 80.0. The images show smooth transitions between convex down slope curvature at the tops of divides and concave down slope curvature at the

SCOP DEM

Qsurf DEM

Figure 7.5. Down slope curvature scaled between -80° and 80° of change in slope per 100m.

bottom of drainage channels. As in the across slope curvature comparison, the Qsurf DEM contained smooth curvature continuity across flat and level areas where the SCOP DEM contained discontinuities resulting from linear interpolations of elevation. Sharp definitions of the artifacts resulting from curvature discontinuities in the SCOP DEM image are strong enough to visually interfere with the valid curvature information being presented.

Statistical and Numerical Comparisons

Numerical comparisons between the SCOP and Qsurf DEMs provided some favorable and surprising results. A regression analysis in which the Qsurf DEM was regressed onto the SCOP DEM produced a coefficient of correlation of 0.9999. The coefficient of correlation was higher than anticipated in light of the differences in surface detail between the DEMs. The high correlation coefficient, combined with the visual information presented, gives strong support to the validity of the developed surfacing methodology of generating DEM surfaces from secondary data sources. The comparison results support use of Qsurf generated DEMs as high quality and reliable substitutes to DEMs generated from primary data sources when such DEMs are not available or affordable.

A residual difference surface was created to evaluate how closely the interpolated QSURF elevations approximated the corresponding SCOP values. The residual surface was produced by subtracting the Qsurf DEM from the SCOP DEM. Resulting difference values were presented in an image form (Figure 7.6) by scaling the differences within a range of 10 meters on either side of an exact approximation. The selected range of 10 meters represented one half the contour interval obtained from the topographic map. An important characteristic of the residual difference image supports the distinctions between the DEMs as a consequence of the two types of data sources used. Results of the residual difference image indicate that in all cases drainage channels were shallower in the Qsurf DEM than in the SCOP DEM, while tops of drainage divides were lower in the Qsurf DEM than in the SCOP DEM. The displacement of the channels and divides is evident in the image where all divides appear in light tones, while all channels appear in dark tones. The characteristic displacement of channel bottoms and ridge tops are a result of the SCOP program having access to information defining

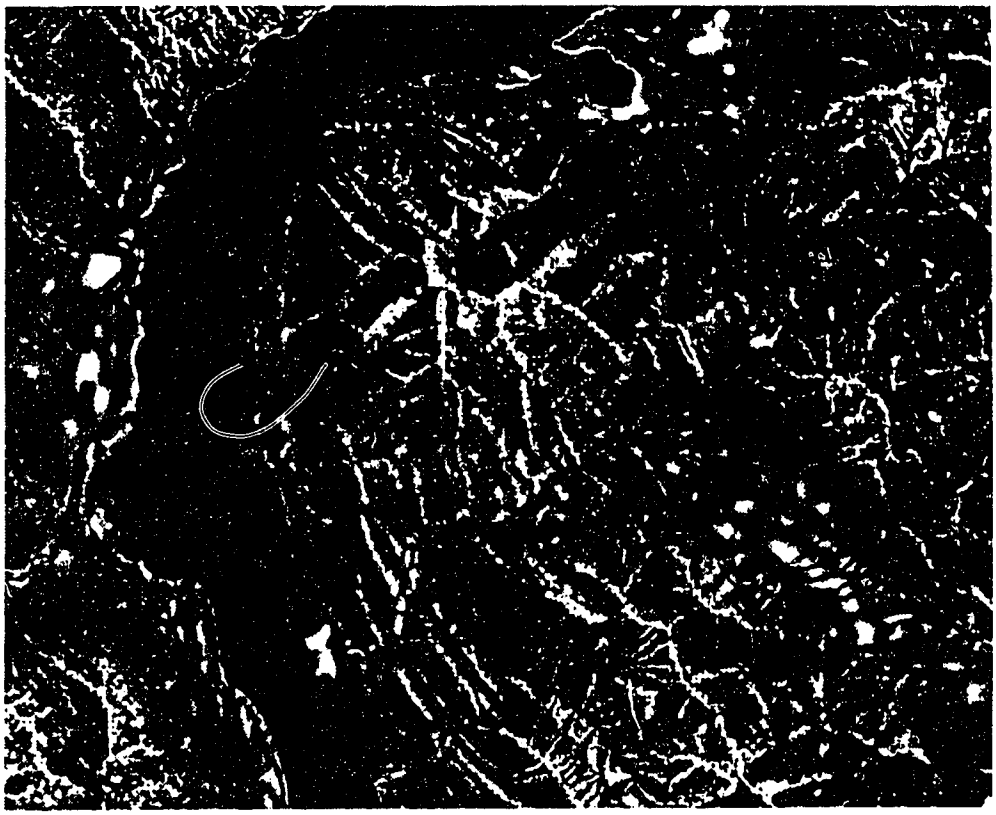

Figure 7.6. Residual difference image produced by subtracting the Qsurf DEM from the SCOP DEM. Differences are scaled between -10m (black) and +10m (white).

exact locations of these features, while the Qsurf program had to interpolate the location of these features based on the nearest contour levels. Neutral interpolation of these features when using the multiquadric equation method produced channel bottoms at slightly higher elevations than in the SCOP DEM and ridge tops at slightly lower elevations. A cumulative breakdown of the residual differences between the SCOP and Qsurf DEMs is presented in Table 7.1. Numerical evaluations of residual differences between the DEMs indicated that 94.4% of the elevations generated by Qsurf were within one half a contour interval of their corresponding elevations in the SCOP DEM. The one half contour interval break point meant that 94.4% of the Qsurf generated elevations were within 10 meters of the base-line elevations. A stricter evaluation of the differences concluded that 78.15% of the Qsurf generated elevations were within 5 meters or one quarter contour interval of the base-line elevations.

Table 7.1. Residual Surface Cumulative Frequency Distribution.

CLASS	LOWER CLASS LIMIT	UPPER CLASS LIMIT	FREQUENCY	PERCENT FREQUENCY	ACCUMULATED PERCENT FREQUENCY
1	-10.5000	-10.0000	9237	2.488	2.488
2	-10.0000	-9.5000	1431	.385	2.874
3	-9.5000	-9.0000	1609	.433	3.307
4	-9.0000	-8.5000	1853	.499	3.806
5	-8.5000	-8.0000	2110	.568	4.374
6	-8.0000	-7.5000	2435	.656	5.030
7	-7.5000	-7.0000	2768	.746	5.776
8	-7.0000	-6.5000	3158	.851	6.627
9	-6.5000	-6.0000	3593	.968	7.594
10	-6.0000	-5.5000	4194	1.130	8.724
11	-5.5000	-5.0000	4638	1.249	9.973
12	-5.0000	-4.5000	5362	1.444	11.418
13	-4.5000	-4.0000	6101	1.643	13.061
14	-4.0000	-3.5000	7038	1.896	14.957
15	-3.5000	-3.0000	8060	2.171	17.128
16	-3.0000	-2.5000	9456	2.547	19.675
17	-2.5000	-2.0000	11044	2.975	22.650
18	-2.0000	-1.5000	12413	3.344	25.993
19	-1.5000	-1.0000	14498	3.905	29.898
20	-1.0000	-.5000	16311	4.394	34.292
21	-.5000	.0000	18632	5.019	39.311
22	.0000	.5000	73138	19.700	59.011
23	.5000	1.0000	19861	5.350	64.361
24	1.0000	1.5000	17327	4.667	69.028
25	1.5000	2.0000	15104	4.068	73.097
26	2.0000	2.5000	13216	3.560	76.656
27	2.5000	3.0000	11014	2.967	79.623
28	3.0000	3.5000	9697	2.612	82.235
29	3.5000	4.0000	8304	2.237	84.472
30	4.0000	4.5000	7202	1.940	86.412
31	4.5000	5.0000	6384	1.720	88.131
32	5.0000	5.5000	5631	1.517	89.648
33	5.5000	6.0000	4845	1.305	90.953
34	6.0000	6.5000	4186	1.128	92.081
35	6.5000	7.0000	3838	1.034	93.115
36	7.0000	7.5000	3240	.873	93.987
37	7.5000	8.0000	2753	.742	94.729
38	8.0000	8.5000	2404	.648	95.376
39	8.5000	9.0000	2225	.599	95.976
40	9.0000	9.5000	1869	.503	96.479
41	9.5000	10.0000	1582	.426	96.905
42	10.0000	10.5000	11489	3.095	100.000

Chapter 8
Summary

Digital elevation models have become a familiar and often vital database for studying, planning, and mapping landforms. Our need to better understand the world fuels a demand to provide quality DEM products for an ever widening base of applications. Generating DEMs necessary for many of these applications can be an expensive and time consuming procedure. A method for converting contour information from topographic maps into high quality DEMs both accurately and efficiently was investigated and developed. Explorations of an analytical tiling approach to surfacing resulted in a DEM generating tool adaptable to nearly any computer system and capable of processing nearly any size elevation data set. The DEMs generated by this program were shown to be comparable in quality to DEMs generated directly from ortho-photo models.

Image processing tools for computer systems have evolved significantly both in quality and affordability in recent years. Rudimentary image processing tools are even available as shareware or freeware on many computer bulletin boards. Adapting the tools and techniques of image processing to fulfil the traditional role of contour digitizing provides a means for even the most inexperienced of users to acquire digital topographic information in an accurate and affordable manner. Although specialized tools are available which can convert scanned maps to digital products using hybrid scanners and pattern recognition software, the use of generic scanners and image processing tools to acquire topographic information is thought to be both a novel and a timely approach.

Analytical methodologies for surface generation have been reviewed and reported for decades (Hardy, 1971; Eyton, 1974; Franke, 1979; Schiro and Williams, 1984). Although capable of generating DEM surfaces superior to surfaces produced using numerical methods (Eyton, 1974; Franke, 1979; Hein, 1979; Schiro and Williams, 1984), analytical surfacing methodologies are rarely used in geographical applications. The intense allocation of computational resources necessary to effectively utilize analytical methods may be a contributing factor to their lack of popularity. Techniques for efficiently implementing multiquadric interpolation methodologies in a tool for generating DEM surfaces have been proposed. The developed analytical

tiling approach to surfacing resulted in a DEM generator that produces exact fitting surfaces which are nearly free of all artifacts. The implementation of two dimensional binary search trees for data storage, and the development of directionally adaptive data partitioning with dynamic sensitivity to data densities were key factors in the successful completion of the goals set out for this research. Strict adherence to hardware generic coding ensured the portability of the tools developed through this work.

Comparisons between the DEMs produced through this research and DEMs produced from ortho-photo models may appear unfair given the superior quality of data available from ortho-photos, however, such comparisons are necessary to fully evaluate and appreciate the quality of DEMs which can be obtained from simple contour maps. Although lacking in some high-frequency surficial details, the test DEM produced through this work generated derivative surface products which reproduced characteristics of the actual terrain. Comparisons of second derivative images extracted from the two DEMs demonstrated the improved curvature results produced through analytical interpolations as compared to numerical interpolations.

Techniques and methodologies for performing a task or accomplishing a goal are always the potential victims of future enhancements and innovations. The methodologies and tools developed in this research are no exceptions. Eventually, new or improved methods of dealing with cartographic and topographic information will obviate the need for manually producing DEMs. For the present, however, the innovative techniques and tools presented in this paper provide an alternative means for producing high quality digital elevation models.

References

Aho, A.V., J.E. Hopcroft and J.D. Ullman: 1983, Data Structures and Algorithms, Addison-Wesley Publishing Co. Inc.

Claybrook, B.G.: 1983, File Management Techniques, John Wiley & Sons Publishing, Inc.

Davis, J.C.: 1973, Statistics and Data Analysis in Geology, Second Ed., John Wiley & Sons Publishing, Inc.

Eyton, J.R.: 1974, An Analytical S[illegible]ethodology for Application to the Geometric Measurement and Anal[illegible]forms, Unpublished Ph.D. dissertation, University of Illinois a[illegible]Champaign.

Eyton, J.R.: 1987, Morphometrics of [illegible] Chasquis Invitational Rocky Mountain Road Race, Sport Place, Technical Notebook: 39-47.

Eyton, J.R.: 1991, Rate-of-Change Maps, Cartography and Geographic Information Systems 18(2): 87-103.

Eyton, J.R.: 1995, TERRA FIRMA: A display and analysis package for raster data, Unpublished software, Department of Geography, University of Alberta, Edmonton.

Franke, R.: 1979, A Critical Comparison of Some Methods for Interpolation of Scattered Data, Report # NPS-53-79-002, Naval Postgraduate School, Monterey, Calif.

Hardy, R.L.: 1971, Multiquadric Equations of Topography and Other Irregular Surfaces, Journal of Geophysical Research 76(8): 1905-1915.

Hardy, R.L.: 1972, The Analytic Geometry of Topographic Surfaces, Proceedings, American Congress on Surveying and Mapping 32: 163-181.

Hardy, R.L.: 1975, Research Results in the Application of Multiquadric Equations to Surveying and Mapping Problems, Surveying and Mapping 35(4): 321-332.

Hein, G. and K. Lenze: 1979, Zur genauigkeit und prodiktionsmethoden, Zeitschrift fuer Vermessungswesen 104: 492-505.

Johnston, R.L.: 1982, Numerical Methods, A Software Approach, John Wiley & Sons Publishing, Inc.

Kumler, M.P.: 1994, An Intensive Comparison of Triangulated Irregular Networks (TINs) and Digital Elevation Models (DEMs), Cartographica 31(2), Monograph 45.

Press, W.H., B.P. Flannery, S.A. Teukolsky and W.T. Vetterling: 1988, Numerical Recipes in C, The Art of Scientific Computing, Cambridge University Press.

Schiro, R. and G. Williams: 1983, An Adaptive Method for Numerically Modeling Large Numbers of Irregularly Spaced Data, Auto-Carto Six 2: 252-261.

Schiro, R. and G. Williams: 1984, An Adaptive Application of Multiquadric Interpolants for Numerically Modeling Large Numbers of Irregularly Spaced Hydrographic Data, Surveying and Mapping 44(4): 365-381.

Schumaker, L.L.: 1976, Fitting Surfaces to Scattered Data, Approximation Theory II, Academic Press, New York.

Sedgewick, R.: 1983, Algorithms, Addison-Wesley Publishing Co. Inc.

Spain, G.: 1960, Analytical Quadrics, International Series of Monographs in Pure and Applied Mathematics 14, Pergamon Press, New York.

Stephanovic, P.: 1988, Digital Elevation Models, Data Presentation, ITC Class Manual.

Tremblay, J. and R.B. Bunt: 1979, An Introduction to Computer Science: An Algorithmic Approach, McGraw-Hill Book Co. Inc.

National Library
of Canada

Acquisitions and
Bibliographic Services Branch

395 Wellington Street
Ottawa, Ontario
K1A 0N4

Bibliothèque nationale
du Canada

Direction des acquisitions et
des services bibliographiques

395, rue Wellington
Ottawa (Ontario)
K1A 0N4

Your file Votre référence

Our file Notre référence

NOTICE

The quality of this microform is heavily dependent upon the quality of the original thesis submitted for microfilming. Every effort has been made to ensure the highest quality of reproduction possible.

If pages are missing, contact the university which granted the degree.

Some pages may have indistinct print especially if the original pages were typed with a poor typewriter ribbon or if the university sent us an inferior photocopy.

Reproduction in full or in part of this microform is governed by the Canadian Copyright Act, R.S.C. 1970, c. C-30, and subsequent amendments.

AVIS

La qualité de cette microforme dépend grandement de la qualité de la thèse soumise au microfilmage. Nous avons tout fait pour assurer une qualité supérieure de reproduction.

S'il manque des pages, veuillez communiquer avec l'université qui a conféré le grade.

La qualité d'impression de certaines pages peut laisser à désirer, surtout si les pages originales ont été dactylographiées à l'aide d'un ruban usé ou si l'université nous a fait parvenir une photocopie de qualité inférieure.

La reproduction, même partielle, de cette microforme est soumise à la Loi canadienne sur le droit d'auteur, SRC 1970, c. C-30, et ses amendements subséquents.

Canada

University of Alberta

PALEOBOTANY AND PALEOECOLOGY OF THE JOFFRE BRIDGE ROADCUT LOCALITY (PALEOCENE), RED DEER, ALBERTA

by

Georgia Lynne Hoffman

A thesis submitted to the Faculty of Graduate Studies and Research in partial fullfillment of the requirements for the degree of Master of Science

Department of Biological Sciences

Edmonton, Alberta

Fall 1995

National Library
of Canada

Acquisitions and
Bibliographic Services Branch

395 Wellington Street
Ottawa, Ontario
K1A 0N4

Bibliothèque nationale
du Canada

Direction des acquisitions et
des services bibliographiques

395, rue Wellington
Ottawa (Ontario)
K1A 0N4

Your file Votre référence

Our file Notre référence

THE AUTHOR HAS GRANTED AN IRREVOCABLE NON-EXCLUSIVE LICENCE ALLOWING THE NATIONAL LIBRARY OF CANADA TO REPRODUCE, LOAN, DISTRIBUTE OR SELL COPIES OF HIS/HER THESIS BY ANY MEANS AND IN ANY FORM OR FORMAT, MAKING THIS THESIS AVAILABLE TO INTERESTED PERSONS.

L'AUTEUR A ACCORDE UNE LICENCE IRREVOCABLE ET NON EXCLUSIVE PERMETTANT A LA BIBLIOTHEQUE NATIONALE DU CANADA DE REPRODUIRE, PRETER, DISTRIBUER OU VENDRE DES COPIES DE SA THESE DE QUELQUE MANIERE ET SOUS QUELQUE FORME QUE CE SOIT POUR METTRE DES EXEMPLAIRES DE CETTE THESE A LA DISPOSITION DES PERSONNE INTERESSEES.

THE AUTHOR RETAINS OWNERSHIP OF THE COPYRIGHT IN HIS/HER THESIS. NEITHER THE THESIS NOR SUBSTANTIAL EXTRACTS FROM IT MAY BE PRINTED OR OTHERWISE REPRODUCED WITHOUT HIS/HER PERMISSION.

L'AUTEUR CONSERVE LA PROPRIETE DU DROIT D'AUTEUR QUI PROTEGE SA THESE. NI LA THESE NI DES EXTRAITS SUBSTANTIELS DE CELLE-CI NE DOIVENT ETRE IMPRIMES OU AUTREMENT REPRODUITS SANS SON AUTORISATION.

ISBN 0-612-06482-4

Canada

University of Alberta

Library Release Form

Name of Author:	Georgia Lynne Hoffman
Title of Thesis:	Paleobotany and Paleoecology of the Joffre Bridge Roadcut Locality, Red Deer, Alberta
Degree:	Master of Science
Year This Degree Granted:	1995

Permission is hereby granted to the University of Alberta Library to reproduce single copies of this thesis and to lend or sell copies for private, scholarly, or scientific research purposes only.

The author reserves all other publication and other rights in association with the copyright in the thesis, and except as hereinbefore provided, neither the thesis nor any substantial portion thereof may be printed or otherwise reproduced in any material form whatever without the author's prior written permission.

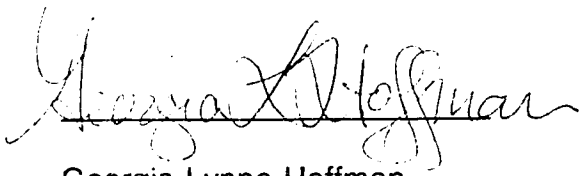

Georgia Lynne Hoffman
1914 Fifth Street S.W.
Calgary, Alberta
Canada T2S 2B3

28 August 1995

University of Alberta

Faculty of Graduate Studies and Research

The undersigned certify that they have read, and recommended to the Faculty of Graduate Studies and Research for acceptance, a thesis entitled Paleobotany and Paleoecology of the Joffre Bridge Roadcut Locality (Paleocene), Red Deer, Alberta by Georgia Lynne Hoffman in partial fulfillment of the requirements for the degree of Master of Science.

Dr. Ruth A. Stockey
Supervisor

Dr. Randall J. Bayer

Dr. Mark V.H. Wilson

Date: August 28, 1995

Dedicated to the memory of Henry and Carol Faul of the University of Pennsylvania, for teaching me my first courses on geology and paleontology, a long time ago.

ABSTRACT

Fossil plant remains representing more than 15 families have been recovered from Joffre Bridge Roadcut in south-central Alberta. Strata lie within the Paskapoo Formation. Faunal remains, palynology and magnetostratigraphy have established a middle Paleocene age (Middle Tiffanian, Ti_3) for the strata, and allowed them to be correlated beyond the Alberta Basin with confidence. The succession of sedimentary layers records the gradual abandonment of a river channel and its development into an oxbow lake. Plant remains are common, but assemblages vary according to the environment of deposition. Foliage and reproductive structures from riparian and floodplain trees are common in most layers, and delicate aquatic plants are found in the lacustrine beds. Systematic study of the material has identified more than 25 taxa, including a new genus (Araceae), and new species of a liverwort (Ricciaceae) and the samara of an Acer-like tree (Sapindaceae/Aceraceae).

ACKNOWLEDGEMENTS

This work was supported in part by NSERC (Natural Sciences and Engineering Research Council of Canada) grant A6908 to Dr. Ruth A. Stockey. Thanks are given to Dr. Stockey for guidance and financial support throughout the course for this study, as well as for instruction and encouragement in karate, and for many a fine dinner.

Special thanks are due to Mrs. Betty Speirs of Red Deer, Alberta, whose diligent collecting activities, spanning a period of more than 15 years, produced most of the plant fossils that have been the subject of this work, as well as many insect and vertebrate fossils that have been studied by others. The many specimens that she has recovered have expanded our understanding of the Paleocene of central Alberta, and her continuing efforts will keep many paleontologists busy for a long time to come.

Dr. Mark V.H. Wilson and Dr. Randall J. Bayer are thanked for serving on my Committee, a dreary task, I'm sure. Dr. Wilson shared his knowledge of the geology of the site, gained during the excavation of vertebrate fossils, and endured many questions about the insect and fish fossils. Dr. Bayer was subjected to many questions about angiosperms and plant taxonomy, and contributed in many informative discussions of botany and other topics.

Dr. Art R. Sweet of the Geological Survey of Canada helped the author recover and study the pollen of the Spirodela-like plant, and kindly provided the palynological report included in Appendix C, as well as many informative discussions about the Paleocene of western North America.

The following people are also thanked for providing helpful information, either in person, by letter or by electronic mail: Mr. K.R. Aulenback, Dr. J.F. Basinger, Dr. C.P. Daghlian, Dr. T.D. Demchuk, Dr. D.M. Erwin, Dr. R.C. Fox, Dr. L.J. Hickey,

Dr. K.R. Johnson, Dr. S. Jovet-Ast, Dr. J.F. Lerbekmo, Dr. B.A. LePage, Mr. A. Lindoe, Dr. E.E. McIver, Ms. A.M. Murray, Dr. J.M. Osborn, Dr. H.W. Pfefferkorn, Dr. K.B. Pigg, Dr. R.J.H. Richardson, Dr. G.W. Rothwell, Mr. R. Serbet, Mrs. A.E. Speirs, Dr. D.H. Vitt, Mr. W.C. Wehr, Dr. S.L. Wing, and Dr. J.A. Wolfe.

The loan of specimens for this study is greatfully acknowledged. Dr. Michael Grayum of the Missouri Botanical Garden kindly provided specimens of extant Spirodela intermedia and Pistia stratiotes, as well as helpful comments about the Lemnaceae and Araceae. The type specimens of Azolla stanleyi were loaned by Dr. D.L. Dilcher of the Florida Museum of Natural History. Specimens of Spirodela scutata were loaned by Dr. T.E. Bolton of the Geological Survey of Canada; and specimens of Spirodela scutata and Pistia corrugata were loaned by Dr. E.E. McIver and Dr. J.F. Basinger of the University of Saskatchewan Department of Geology.

The assistance of Mr. G.D. Braybrook with the scanning electron microscopy, and Dr. J.M. Osborn and Mr. D.C. Fernando with transmission electron microscopy, are greatly appreciated. Mr. Robert A. Wilson is thanked for surveying assistance and computing advice. Dr. David Frishman is thanked for field assistance, computing advice and assistance with preparation the text-figures. Both are thanked for their encouragement, as are Mr. Dennis Nikols, Mr. John Priegert, and Ms. Carol Rushworth.

Surveyed elevation data, maps, and permission to trench the site were obtained from Alberta Transportation and Utilities personnel in Edmonton and Red Deer. Backhoe services were provided by Mr. Mike Palulis of Red Deer. The final word processing was performed by Mrs. Sandra Gilday and is much appreciated.

TABLE OF CONTENTS

CHAPTER 1.	INTRODUCTION	1
	Location	1
	Background	3
	Materials and Methods	6
CHAPTER 2.	REGIONAL STRATIGRAPHY AND AGE	12
	Stratigraphic Position of Joffre Bridge Roadcut	17
	Age of the Strata	21
CHAPTER 3.	SITE STRATIGRAPHY AND DEPOSITIONAL HISTORY	25
	Summary	25
	Unit 1: The Lower Level Bed	31
	Unit 2: The Fluvial Channel Sandstone	33
	Unit 3: The Channel-Fill Siltstone	34
	Unit 4: The Lower Lacustrine Sequence	35
	Unit 5: The Mollusc Layer	35
	Unit 6: The Upper Lacustrine Sequence	36
	Unit 7: The Crossbedded Sandstone	39
CHAPTER 4.	SYSTEMATIC DESCRIPTION OF FLORA	41
CHAPTER 5.	CONCLUSIONS	110
REFERENCES		112
APPENDIX A.	GEOLOGICAL DESCRIPTIONS	160
APPENDIX B.	CATALOG OF FAUNAL REMAINS	172
APPENDIX C.	PALYNOLOGY	174

LIST OF TABLES

TABLE 1. Systematic list of taxa from Joffre Bridge Roadcut. 7

TABLE 2. Generalized stratigraphic section for Joffre Bridge Roadcut. 26

LIST OF TEXT FIGURES

FIGURE 1.	Map of fossil localities of the Red Deer Valley area.	2
FIGURE 2.	Map of the Joffre Bridge area showing roadcut and trenches.	4
FIGURE 3.	Stratigraphy of uppermost Cretaceous and Tertiary sediments.	13
FIGURE 4.	Correlation of uppermost Cretaceous and Tertiary strata.	14
FIGURE 5.	Geophysical logs of Drillhole ARC 81-8.	18
FIGURE 6.	Summary of biostratigraphic and magnetostratigraphic data.	22
FIGURE 7.	Correlation of layers at Joffre Bridge Roadcut.	27
FIGURE 8A.	Diagrammatic illustration of the fluvial channel.	29
FIGURE 8B.	Diagrammatic illustration of channel abandonment.	29
FIGURE 8C.	Diagrammatic illustration of the oxbow lake.	30
FIGURE 8D.	Diagrammatic illustration of the crevasse splay.	30
FIGURE 9.	The Joffre Bridge Roadcut paleoenvironment and plant community.	32

LIST OF PLATES

PLATE 1	130
PLATE 2	132
PLATE 3	134
PLATE 4	137
PLATE 5	139
PLATE 6	141
PLATE 7	143
PLATE 8	145
PLATE 9	147
PLATE 10	149
PLATE 11	151
PLATE 12	153
PLATE 13	155
PLATE 14	157
PLATE 15	159

LIST OF SYMBOLS AND ABBREVIATIONS

Measurement of Distance:

Å	angstrom
μ	micron
m	metre
mm	millimetre
km	kilometre

Measurement of Accelerating Potential:

kV	kilovolts

Latin Words and Abbreviations:

al.	alia (others)
cf.	confer (compare)
gen.	genus
nov.	novum (new)
sp.	species
incertae	uncertain
sedis	seat (affinity)
sensu	sense

Miscellaneous Abbreviations:

API Unit	A standard for natural gamma radiation count-rates set by the American Petroleum Institute, used in downhole geophysical logging
ARC	Alberta Research Council
GSC	Geological Survey of Canada
SEM	Scanning Electron Microscopy
TEM	Transmission Electron Microscopy
UALVP	University of Alberta Laboratory for Vertebrate Paleontology
UAPC-ALTA	University of Alberta Paleobotanical Collection

Geological Symbols and Abbreviations:

Fm	Formation
Ti_3	Middle Tiffanian Land-Mammal Age

Lithological symbols - see Appendix A

Legal Descriptions (Township and Range System):

LSD	Legal Subdivision
Sec.	Section
Tp.	Township
Rg.	Range
W4M	West of Fourth Meridian

CHAPTER 1

INTRODUCTION

Joffre Bridge Roadcut is a highly productive Paleocene fossil locality in the Red Deer River valley of south-central Alberta (Fig. 1). It was discovered by Mrs. A.E. (Betty) Speirs of Red Deer when fossiliferous beds were exposed during the relocation of Provincial Highway 11 in 1978. Numerous plant, vertebrate and insect specimens have been recovered from the site through the efforts of Mrs. Speirs, Dr. R.A. Stockey of the University of Alberta Department of Botany, and Dr. R.C. Fox, Dr. M.V.H. Wilson, Mr. D.C. Wighton, and Mr. A. Lindoe of the University of Alberta Laboratory for Vertebrate Paleontology (UALVP).

This thesis describes the stratigraphy of the site, which includes a series of distinct fossiliferous layers, and presents a systematic analysis of the megaflora. The paleoenvironments represented by the different layers, as indicated by the nature of the sediments and their included plant and animal remains, are also discussed.

LOCATION

The site is usually called the Joffre Bridge locality (e.g., Stockey and Crane, 1983; Taylor and Stockey, 1984; Demchuk, 1987). Fox (1990) called it Joffre Bridge Roadcut to distinguish it from several other sites near the bridge (Fig. 1), and that name is used in this thesis.

The Joffre Bridge Roadcut site occupies an area of roughly 10,000 square metres on the south side of Alberta Provincial Highway 11 where the road

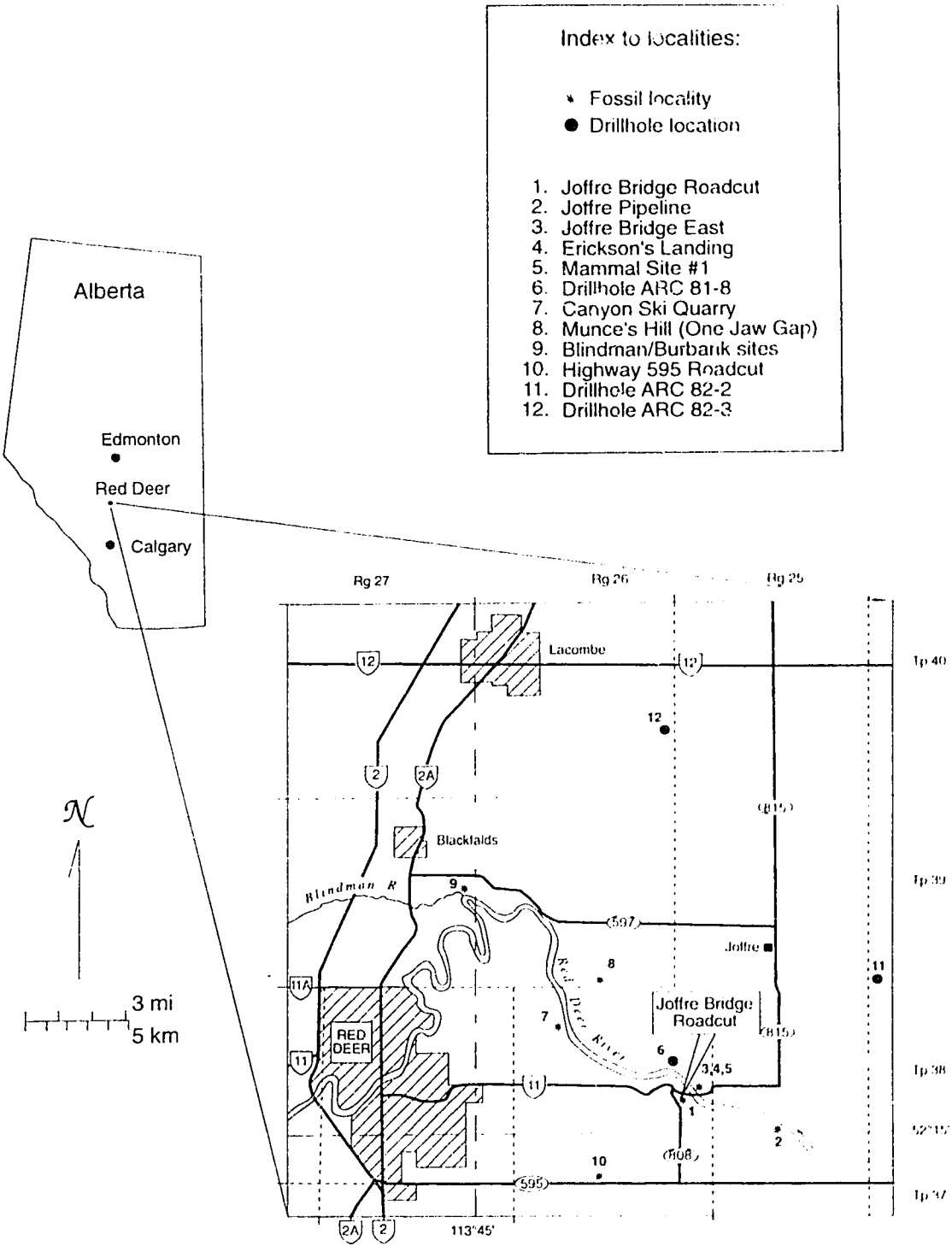

Figure 1: Map showing fossil localities and drillholes in the Red Deer Valley area of south-central Alberta, Canada.

descends to Joffre Bridge, about 14 km west of the city of Red Deer (Figs. 1, 2). The site lies within the right-of-way for Highway 11 adjacent to farmland owned by Mr. J.D. Kaiser of Red Deer. Topographic map Red Deer 83A/5, 2nd edition (1975) (1:50,000); and Alberta Department of Highways and Transport Grading Mosaic, Highway 11:14 (1:4800), cover the site.

The site lies at 52° 16′ 10" North latitude, 113° 36′ 00" West longitude (Universal Transverse Mercator Grid 12UUN226940), Legal Subdivisions 9 & 16 of Section 14, and Legal Subdivision 12 of Section 13, Township 38, Range 26, West of 4th Meridian (Fig. 2). The Upper Level Beds (elevation about 845 m) have been quarried on the west side of the site (Section 14); the Lower Level Bed (elevation about 830 m) was quarried on the east side (Section 13).

BACKGROUND

Geologic Setting: The strata at Joffre Bridge Roadcut are of middle Paleocene age and lie within the lower Paskapoo Formation. They are part of a sequence of flat-lying Upper Cretaceous and Paleocene strata exposed along the Red Deer River valley in south-central Alberta. Those outcrops have attracted the attention of geologists and paleontologists since their first description by Tyrrell over a hundred years ago (Tyrrell, 1887). Numerous studies of the regional stratigraphy have been undertaken since that time, and large numbers of vertebrate, plant and other fossils have been recovered from a series of sites along the valley in the area where Joffre Bridge now stands (Fig. 1). Recent studies of the stratigraphic context (e.g., Richardson et al., 1988; Lerbekmo et al., 1992), faunal succession (Fox, 1990, 1991), palynology (Demchuk, 1987, 1990; Demchuk and Hills, 1991), and magnetostratigraphy (Lerbekmo et al., 1992) have established the ages of the fossil localities and their correlation with

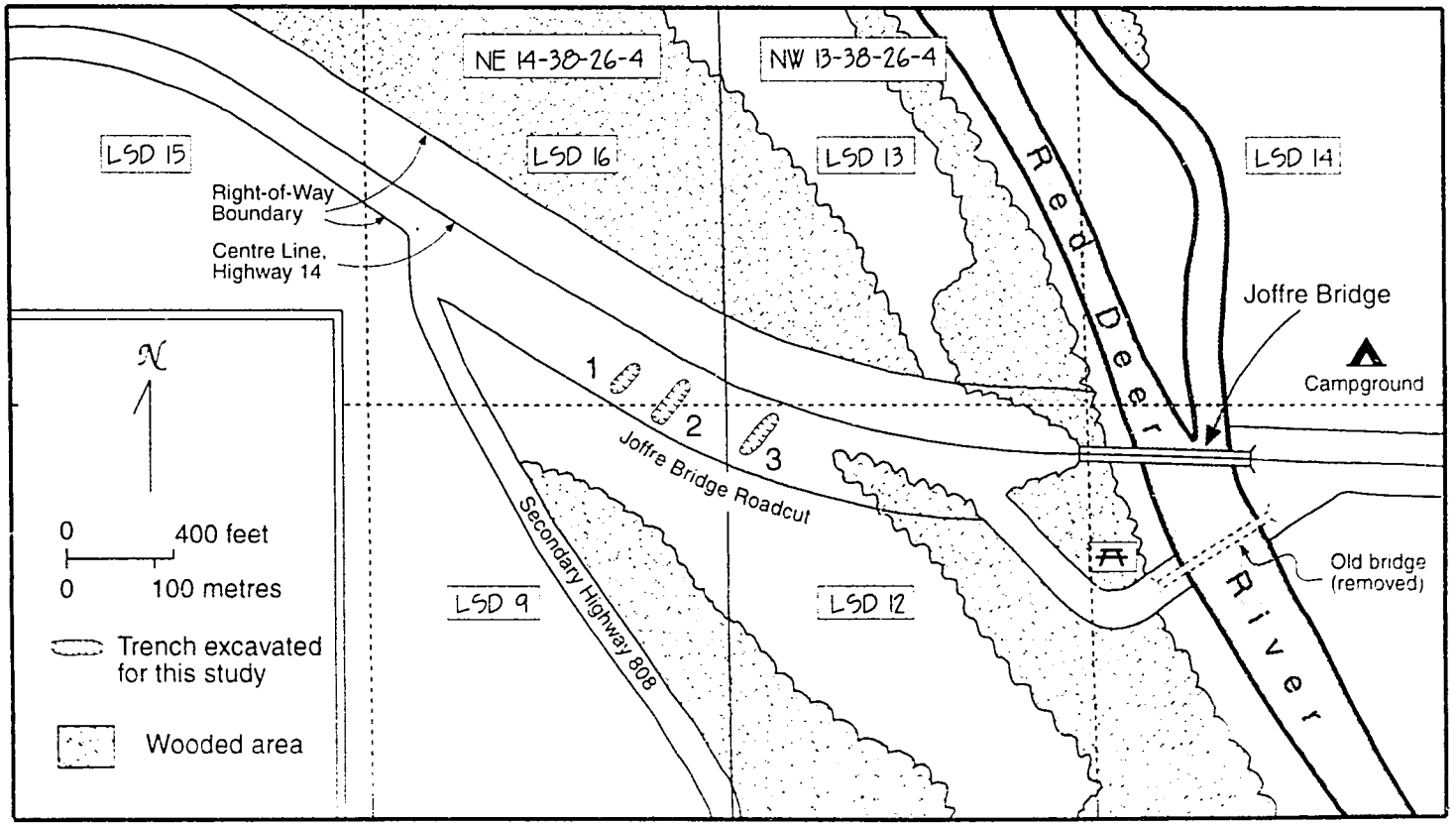

Figure 2: Map of Joffre Bridge area showing location of of roadcut and trenches. Base from Alberta Department of Highways and Transport. Highway 11:14 Grading Mosaic. 1:4800. aerial photography dated 26/07/75.

Paleocene sites beyond the Alberta Basin (Lerbekmo et al., 1992; Fox, 1991). Details of the regional stratigraphy and age relationships are discussed in Chapter 2.

Field Work: Paleontological work at Joffre Bridge Roadcut began in the summer of 1978. Realignment of the highway and construction of the new bridge were in progress when Mrs. Speirs noted the fossiliferous beds and began to recover specimens. She informed Dr. Stockey at the University of Alberta, and was soon joined by field parties from the Department of Botany and the UALVP. Two zones have been productive, referred to as the Lower Level and Upper Level by Fox (1990). The Lower Level (or Lower Vertebrate) Bed was worked intermittently from 1979 to 1982, and in 1986 (Fox, 1990). The Upper Level Beds, which produced the plant material described in this thesis, have been worked every summer since 1978 (Speirs, pers. comm.). Most of the quarrying has been done by hand, but the Upper Level Beds were partially cleared of brush, overburden, and accumulated waste rock by a bulldozer prior to a field trip sponsored by the Second International Organization of Paleobotany Conference in August 1984 (Taylor and Stockey, 1984), and again during work for this thesis in August, 1993 (Fig. 2 of Plate 1).

Faunal Remains: Remains of Paleocene mammals recovered from the Lower and Upper Level Beds at Joffre Bridge Roadcut have been described by Fox (1990). Remains of reptiles and amphibians (Fox. pers. comm.; M.V.H. Wilson, pers. comm.), fish (Wilson, 1980; Williams and Wilson, 1988; Wilson and Williams, 1991; Murray, 1994), insects (Kevan and Wighton, 1981; Wighton, 1982; Wighton and Wilson, 1986), and freshwater molluscs have also been recovered and reside in the UALVP Collections. Faunal remains are summarized in Appendix B.

Previous Paleobotanical Publications: Taylor and Stockey (19840 published an overview of plant remains from Joffre Bridge Roadcut. The cercidiphyllaceous plant Joffrea speirsii and its seedlings were described by Crane and Stockey (1985, 1986) and Stockey and Crane (1983). The platanaceous remains were described by Pigg and Stockey (1991). Remains of Azolla stanleyi were described by Hoffman and Stockey (1992, 1994), and the Spirodela-like plant was reported by Hoffman et al. (1995).

MATERIALS AND METHODS

The University of Alberta Paleobotanical Collection (UAPC-ALTA) currently contains more than 15,000 specimens of fossil plant remains from Joffre Bridge Roadcut, representing more than 15 families (Table 1). Most are the remains of isolated organs, but some (e.g., Ricciopsis, Azolla and the Spirodela-like plant) are whole plants. The specimens come from a succession of layers of clastic sediment ranging from claystone to medium-grained sandstone. The layers and the depositional environments that they represent are described in Chapter 3.

Compression/Impression Specimens: Almost all of the specimens are preserved as compression/impressions, and many display detailed features such as venation. The strata at Joffre Bridge Roadcut tend to break easily along bedding planes, so little preparation work is required in the laboratory. However, most of the layers are soft, poorly cemented and closely jointed, so the material tends to be rather fragile and large specimens like Platanus leaves are difficult to recover intact.

TABLE 1:
SYSTEMATICS OF PLANT TAXA FROM JOFFRE BRIDGE ROADCUT

DIVISION BRYOPHYTA

CLASS: HEPATICOPSIDA
Order: Marchantiales
Family: Ricciaceae
Ricciopsis Lundblad sp.

CLASS: BRYOPSIDA
Order: incertae sedis
Family: incertae sedis
Muscites Brongniart sp.

DIVISION TRACHEOPHYTA

CLASS: SPHENOPSIDA
Order: Equisetales
Family: Equisetaceae
Equisetum L. sp.

CLASS: FILICOPSIDA
Order: Filicales
Family: Osmundaceae
Osmunda macrophylla Penhallow
Family: Dennstaedtiaceae
Dennstaedtia blomstrandii (Heer) Hollick

Order: Salviniales
Family: Azollaceae
Azolla stanleyi Jain & Hall

CLASS: GYMNOSPERMOPSIDA
Order: Ginkgoales
Family: Ginkgoaceae
Ginkgo L. sp.

Order: Coniferales
Family: Taxodiaceae
Glyptostrobus europaeus (Brongniart) Heer
Metasequoia occidentalis (Newberry) Chaney

SUBDIVISION: ANGIOSPERMOPHYTINA

CLASS: MAGNOLIOPSIDA

SUBCLASS: MAGNOLIIDAE
Order: Ranunculales
Family: Sabiaceae
cf. *Meliosma rostellata* (Lesquereux) Crane et al.

SUBCLASS: HAMAMELIDAE

Order: Hamamelidales
Family: Cercidiphyllaceae
Joffrea speirsii Crane & Stockey
Family: Platanaceae
Platanus nobilis Newberry
Macginicarpa manchesteri Pigg & Stockey
Platananthus speirsae Pigg & Stockey

Order: Urticales
Family: Ulmaceae
Chaeoptelea microphylla (Newberry) Hickey

SUBCLASS: DILLENIIDAE
Order: Salicales
Family: Salicaceae
Populus penhallowi Bell

SUBCLASS: ROSIDAE
Order: Sapindales
Family: Sapindaceae
Deviacer Manchester sp.
"*Acer*" *arcticum* Heer, sensu Wolfe & Tanai

Order: Geraniales
Family: Oxalidaceae
Averrhoites affinis (Newberry) Hickey

SUBCLASS: INCERTAE SEDIS

"Viburnum" cupanioides (Newberry) Brown
Wardiaphyllum daturaefolium (Ward) Hickey
Fortuna marsilioides (Bell) McIver & Basinger
Unidentified aquatic leaf
Unidentified leaf 1
Unidentified leaf 2

CLASS: LILIOPSIDA

SUBCLASS: ALISMATIDAE
Order: Alismatales
Family: Alismataceae
Alismaphyllites grandifolius (Penhallow) Brown

SUBCLASS: ARECIDAE
Order: Arales
Family: Araceae
Spirodela-like plant

SUBCLASS: ZINGIBERIDAE
Order: Zingiberales
Family: Zingiberaceae
Zingiberopsis attenuata Hickey

SUBCLASS: INCERTAE SEDIS
Lilialean monocot

CLASS: INCERTAE SEDIS

Unidentified seed or fruit
Striated seed
Cone-like infructescence
Unidentified branching plant
Unidentified sheathing structure

Permineralized Material: A few of the layers at Joffre Bridge Roadcut are cemented by calcite (i.e., the Mollusc Layer and the Concretion Zone; Chapter 3) but most of the included plant material was completely compressed prior to the mineralization. A few twigs and fragments of wood permineralized with calcite, and a few permineralized with limonite, were found. These were impregnated with Bio-Plastic under vacuum, and then cut and peeled to produce serial sections using an acetate peel technique with 5% HCl (Joy et al., 1956), but no cellular structure could be discerned.

Pollen, Spores and Cuticle: Pollen is not always well preserved at Joffre Bridge Roadcut, likely due to oxidizing conditions prevailing at and/or subsequent to the time of deposition. Pigg and Stockey (1991) succeeded in recovering platanaceous pollen from a crushed staminate inflorescence, but Crane and Stockey (1985) could not find any evidence of pollen in Joffrea anthers, likely due to the delicate nature of the pollen. Demchuk (1987, 1990) and Sweet (Appendix C) recovered pollen from some of the carbonaceous horizons and lacustrine beds.

Compressed Azolla megaspores, some with massulae attached, are preserved in place on many of the sporophyte specimens. Megaspores were lifted individually from sporophytes and demineralized by treatment with 5% HCl for 5 minutes, followed by 49% HF for 24 hours. They were rinsed with distilled water and cleared by treatment with 5% sodium hypochlorite for 5 to 10 minutes. Some were examined without treatment, or with bleaching only, to ensure that details were not being lost during preparation. Additional dispersed Azolla megaspores were recovered from the claystone matrix by using the "Quaternary O" method described by Hills and Sweet (1972), followed by treatment with 49% HF for 24 hours. Megaspores were picked up individually and cleared by treatment with 90% HNO_3 for 3 minutes.

Fragments of cuticle were preserved on some of the Ricciopsis specimens, but little evidence of cellular structure could be discerned in them. Cuticle was seldom found on specimens of other taxa.

Scanning Electron Microscopy (SEM): Materials were mounted on stubs using double-sided tape, coated with 150 Å gold by a Nanotek sputter-coater, and examined using a Cambridge Stereoscan 250 scanning electron microscope at an accelerating voltage of 20 kV.

Transmission Electron Microscopy (TEM): Materials were pipetted onto cellulose filters which were subsequently coated on both sides with agar. The agar-embedded filters were dehydrated in a graded ethanol series, transferred to 100% ethanol (with four changes to ensure complete filter removal), and gradually infiltrated with Spurr low-viscosity epoxy resin and embedded. Ultrathin sections were cut with a diamond knife, collected on uncoated copper slot grids, and dried onto Formvar support films (Rowley and Moran, 1975). Grids were stained with potassium permanganate, 1% uranyl acetate and lead citrate (Venable and Coggeshall, 1965), and examined with a Phillips EM 400T transmission electron microscope at an accelerating voltage of 80 kV.

Loaned Material: The type specimens of Azolla stanleyi Jain & Hall (slide 242-3) were loaned by the Florida Museum of Natural History, Gainesville, Florida, U.S.A. Two specimens of Spirodela scutata Dawson (GSC 3461 & 6135) were loaned by the Geological Survey of Canada, Ottawa, Ontario, Canada. Several specimens of Spirodela scutata and Pistia corrugata Lesquereux were loaned by the University of Saskatchewan Paleobotanical Collection, Saskatoon, Saskatchewan, Canada. Flowering specimens of Spirodela intermedia and stamens of Pistia stratiotes were obtained from the Missouri Botanical Garden Herbarium, St. Louis, Missouri, U.S.A.

Storage: Except for the loaned material above, all plant fossils, slides, stubs and negatives used in this thesis are housed in the University of Alberta Paleobotanical Collection (UAPC-ALTA).

CHAPTER 2

REGIONAL STRATIGRAPHY AND AGE

Flat-lying uppermost Cretaceous and Paleocene nonmarine strata are exposed over a distance of more than 100 km along the Red Deer Valley in south-central Alberta (Lerbekmo and Coulter, 1985). This sequence has received much attention from stratigraphers because of its coal resources (Richardson et al., 1988), latest Cretaceous dinosaur remains (Spalding, 1988) and mammalian fossils (Fox, 1990, 1991). Beginnning with Tyrell (1887), numerous geologists have sought to identify reliable lithostratigraphic and biostratigraphic markers that can be used to subdivide the sequence into formations and members, establish their ages, and facilitate their correlation beyond central Alberta. The history of those efforts has been described by Gibson (1977), Demchuk (1987) and Lerbekmo et al. (1992).

The sequence is divided into two major units: the Edmonton Group and the Paskapoo Formation (modified from the Edmonton Series and Paskapoo Series of Tyrell, 1887). The strata of Joffre Bridge Roadcut lie within the Paskapoo Formation, near the boundary between the Haynes and Lacombe Members (Fig. 3). The correlation of the strata in Alberta and the west-central Interior Plains is shown by Fig. 4.

Edmonton Group: The Edmonton Group is a fluvial-deltaic complex deposited during and after the withdrawal of the Bearpaw Sea from Alberta (Fig. 4). It is comprised of interbedded nonmarine clastic sediments (sandstones, siltstones, mudstones, shales, claystones, bentonites, coal seams, and carbonaceous shales),

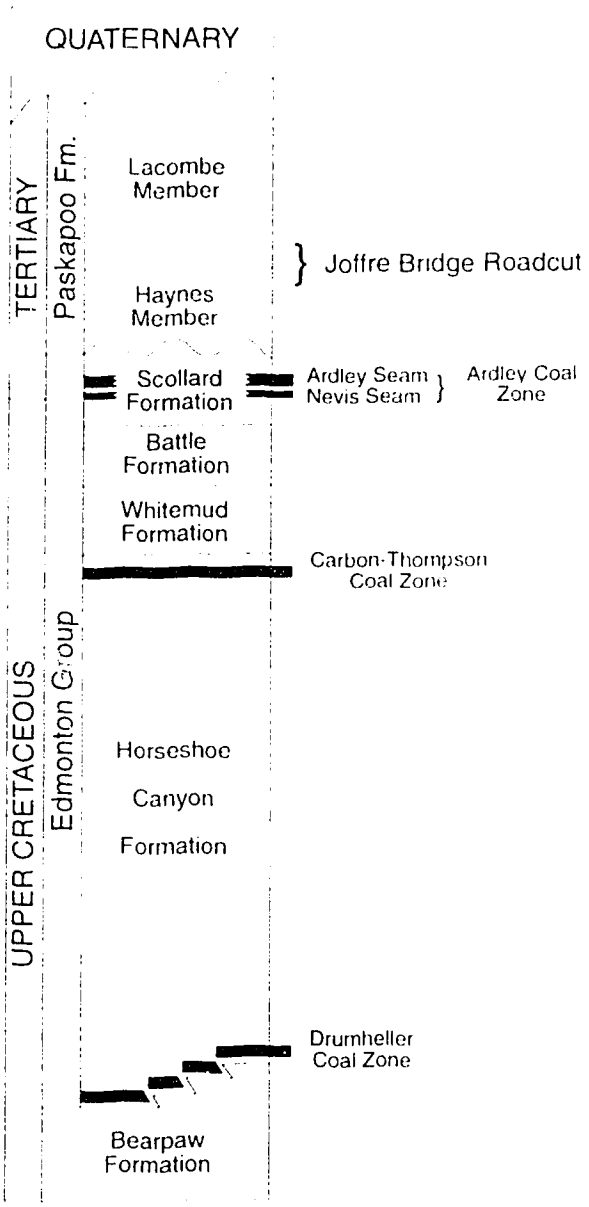

Figure 3: Stratigraphy of uppermost Cretaceous and Tertiary sediments in the Red Deer Valley area of south-central Alberta. Based on Gibson (1977), Demchuk and Hills (1991), and Lerbekmo et al. (1992).

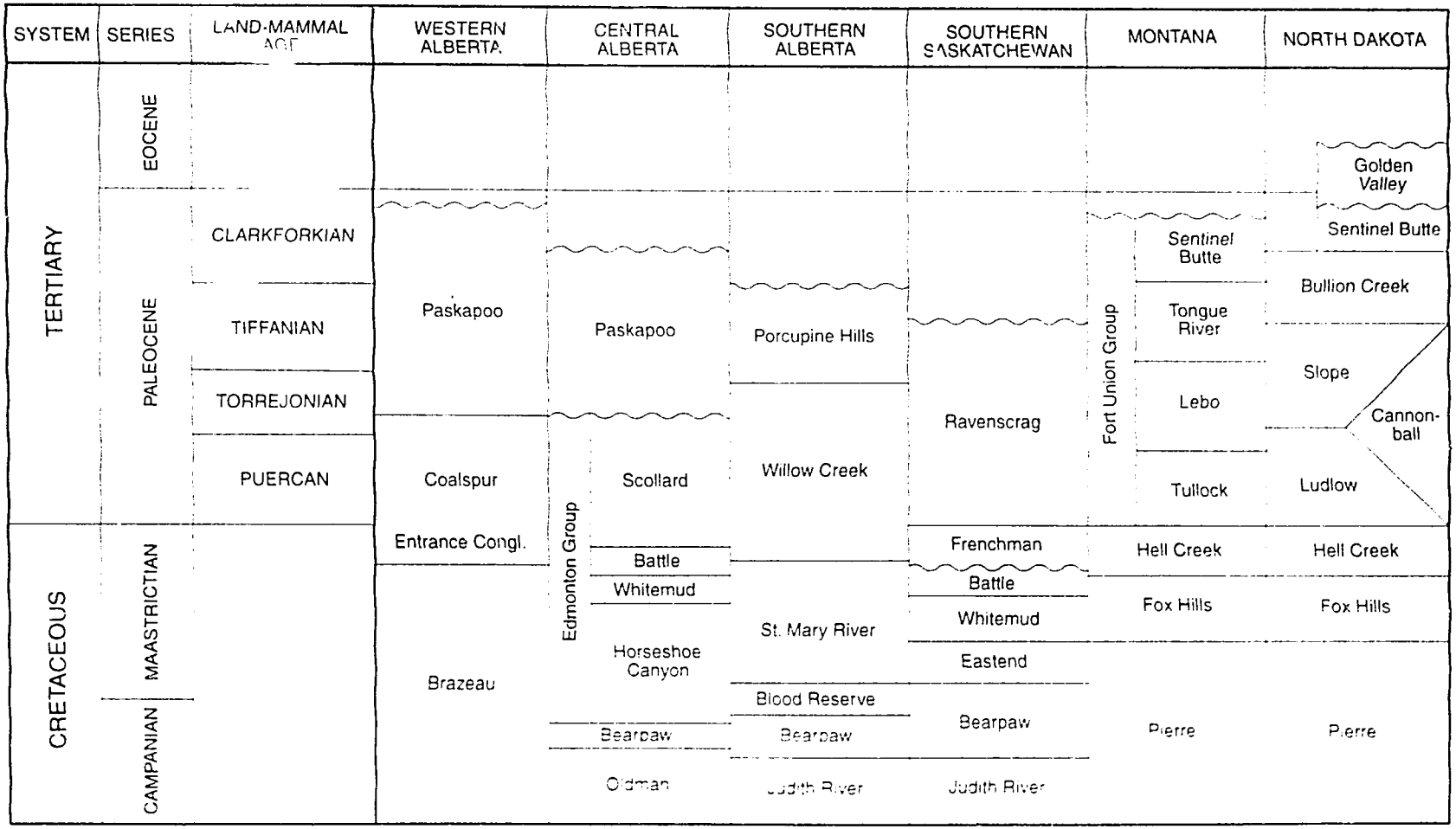

Figure 4: Correlation of uppermost Creatceous and Tertiary strata in Alberta and the west-central Interior Plains. After McIver and Basinger (1993).

and is usually subdivided into the Horseshoe Canyon, Whitemud, Battle and Scollard Formations (Fig. 3) (Gibson, 1977). The Cretaceous-Tertiary boundary lies within the Scollard Formation at the base of the Nevis (No. 13) coal seam of the Ardley coal zone (Fig. 3), as evidenced by faunal and palynofloral extinctions, and the presence of an iridium anomaly (Lerbekmo et al., 1979a,b. 1987, 1990; Sweet and Hills, 1984; Lerbekmo and Coulter, 1985; Lerbekmo and St. Louis, 1986; Sweet et al., 1990).

Paskapoo Formation: The Paskapoo Formation is fluvial in origin, deposited in a tectonically active foreland basin by streams flowing eastward from the Cordillera to the Cannonball Sea (Rahmani and Lerbekmo, 1975; Gibson, 1977; Richardson et al., 1988; Lerbekmo et al., 1992). It includes interbedded fluvial sandstones, siltstones, mudstones, claystones, carbonaceous shales, and generally thin coal seams (thick seams are found only in the Obed area north of Hinton, in the uppermost part of the formation).

The contact between the Paskapoo Formation and the underlying Scollard Formation was defined by Gibson (1977) as "the base of the cliff-forming sandstone marker facies or, in the subsurface, the base of the first prominent thick sandstone unit above the uppermost major coal seam of the Ardley coal zone." However, Richardson et al. (1988) noted that those criteria are not always easy to apply in the subsurface on a regional basis, a problem that is especially pronounced in the western part of the basin where the sedimentary sequence is thickest (Richardson, pers. comm.).

In the Red Deer Valley area the contact is usually consistent with Gibson's definition. It is probably disconformable: magnetostratigraphic work by Lerbekmo et al. (1990, 1992) has demonstrated that a significant hiatus exists at the base of the Paskapoo Formation at several localities. Lerbekmo et al.

(1992) believe that this disconformity may be related to the withdrawal of the Cannonball Sea from North Dakota (Fig. 4), and may be an expression of a global unconformity caused by a mid-Paleocene decline in eustatic sea level (i.e., the Tejas A 1 to 2 supercycle boundary of Haq et al., 1985).

The Haynes Member, recently defined by Demchuk and Hills (1991), includes the thick sandstones that characterize the basal portion of the Paskapoo Formation in the Red Deer Valley area. It is 52 m thick in the type-section (ARC corehole 2-82; Fig. 1), and is composed of resistant medium- to coarse-grained sandstones and minor conglomerates, with subordinate interbeds of finer-grained sediments.

The Lacombe Member (type-section ARC corehole 3-82; Fig. 1), overlies the Haynes Member and consists predominantly of finer grained lithologies: interbedded siltstones, mudstones, shales and thin argillaceous coals, with subordinate interbeds of sandstone and conglomerate (Demchuk and Hills, 1991). Demchuk and Hills (1991) cite Taylor and Stockey's (1984) description of the paleobotany of the Joffre Bridge area in their discussion of the Lacombe Member.

The Dalehurst Member includes the youngest strata in the Paskapoo Formation. It is an erosional remnant and is present only adjacent to the Foothills in the area northeast of Hinton (Demchuk and Hills, 1991). The Dalehurst Member is not present in the Red Deer Valley area and thus is not shown on Fig. 3.

STRATIGRAPHIC POSITION OF JOFFRE BRIDGE ROADCUT

Because the strata of the Red Deer area are essentially flat-lying and undeformed, it is common practice to use elevation to determine stratigraphic position (e.g., Lerbekmo et al., 1992). This approach has occasionally caused difficulties (Lerbekmo et al., 1979b), but is usually adequate for regional studies when used with consideration of geologic context. Factors such as facies changes and differential compaction, for example, should be taken into account. The Haynes Member sandstones discussed below were deposited by fluvial channels meandering laterally within a slowly thickening floodplain, therefore the elevation of a sandstone deposited by a given channel may change gradually with distance.

The stratigraphic position of Joffre Bridge Roadcut can be illustrated by comparison with the data from drillhole ARC 8-81 (Richardson et al., 1988). That hole was drilled about 1.4 km north of Joffre Bridge Roadcut, above the cliffs across the river (Fig. 1). It penetrated to a depth of more than 250 m through the lower Paskapoo Formation and the Scollard Formation, reaching the top of the Battle Formation. The hole was not cored, but geophysical logs (natural gamma, focussed resistivity, gamma-gamma density, caliper and neutron-neutron) were recorded. Fig. 5 shows the natural gamma and focussed resistivity logs.

On Fig. 5 the thin Nevis coal seam that marks the Cretaceous-Tertiary boundary can be seen within the Scollard Formation at an elevation of 706 m above sea level. The thicker Ardley seam lies in the interval 721-725 m (coal is characterized by low count-rates on natural-gamma logs, and high resistivity responses; Hoffman et al., 1984). The Scollard Formation strata overlying the Ardley seam (in the interval 725-773 m) exhibit higher natural gamma responses and lower resistivities, indicating that they contain significant proportions of clay and silt.

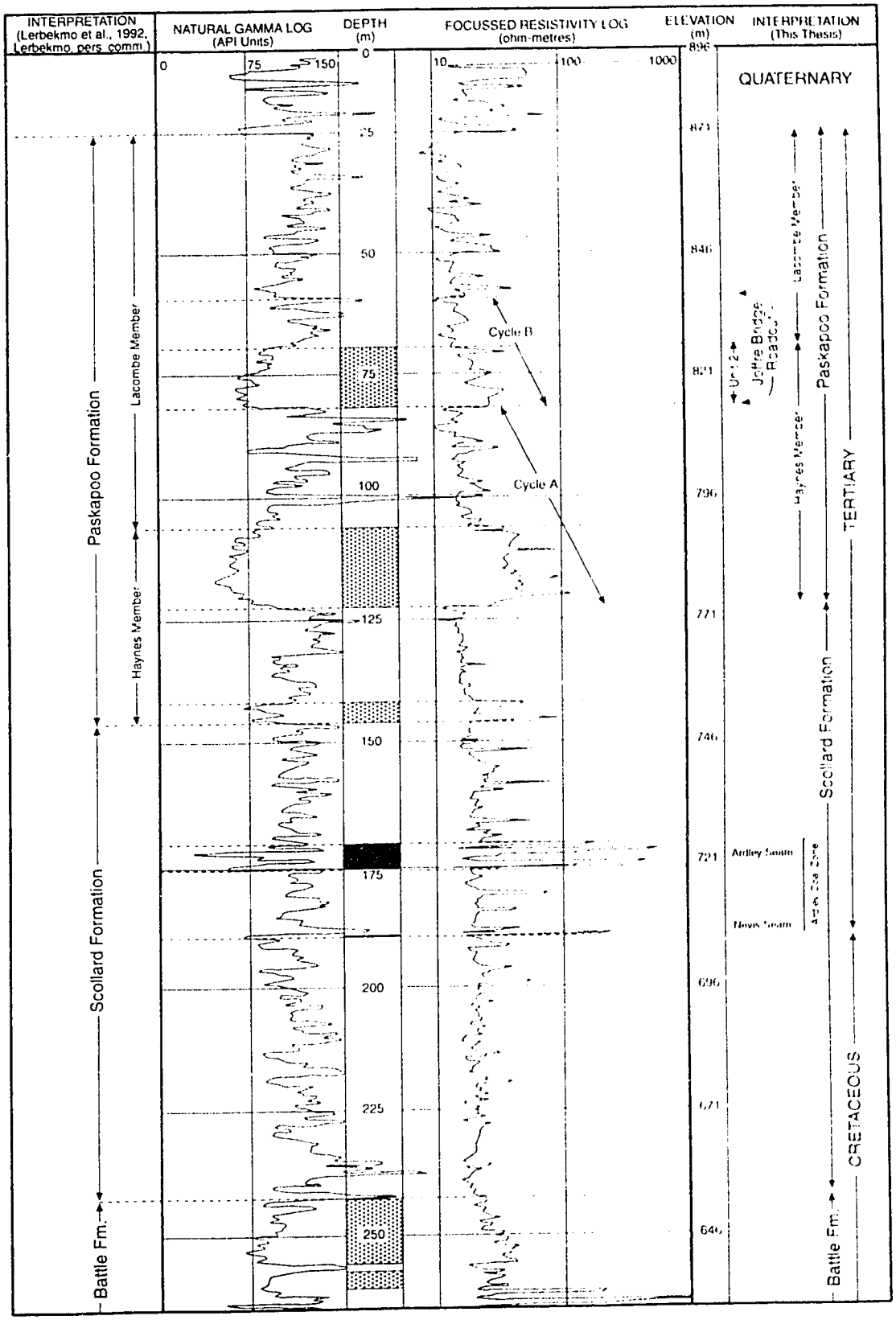

Figure 5. Geophysical logs of Drillhole ARC 81-8. See text for explanation.

The base of the Paskapoo Formation is more difficult to determine in drillhole ARC 8-81 than in other drillholes in the region (Lerbekmo, pers. comm.). An abrupt and conspicuous change to sandstone can be seen at an elevation of 773 m on Fig. 5 which is interpreted in this thesis to be the base of the Paskapoo Formation. This is consistent with the observation of Demchuk and Hills (1991) that the Haynes Member (basal Paskapoo) is easily recognized in the subsurface by its "blocky signature on gamma-ray and resistivity logs (extremely low gamma-ray and high resistivity)". However, Lerbekmo et al. (1992) placed the base of the Paskapoo at 750 m (at the base of the silty sandstone in the interval 750-754 m) because the base of the Paskapoo occurs at 750 m elevation in other drillholes in the region. The choice depends upon the amount of relief that is envisioned on the pre-Paskapoo disconformity surface, and whether a significant disconformity is considered likely to be present at the base of the silty sandstone. No core samples were taken from the drillhole, so there are no core descriptions or magnetostratigraphic data that might resolve the question. Fig. 5 compares the two interpretations.

On Fig. 5 two fining-upward cycles (sandstone to claystone) can be seen in the lower Paskapoo Formation (Cycle A at 773-814 m; Cycle B at 814-836 m). The base of each cycle is a thick layer of sandstone, but clay content increases and grain-size decreases near the top of each cycle (this evidenced by log signatures that are broad and blocky at the base and taper upward near the top). Fining-upward cycles are characteristic of fluvial channel deposits, and are generated as the river meanders back and forth across its floodplain, reworking the sediments laterally (Walker and Cant, 1984). The number of cycles preserved at any one point depends upon the meandering pattern of the river. In this thesis, Cycle A and the sandstone portion of Cycle B are interpreted as the Haynes Member. In the examples given by Demchuk and Hills (1991), the Haynes Member includes several sandstone cycles, each of

which has eroded and removed most or all of the fine-grained beds at the top of the cycle beneath. On Fig. 5 the fine-grained beds at the top of Cycle A are preserved (788-814 m), but otherwise the log signature compares well with those shown by Demchuk and Hills.

Demchuk and Hills defined the contact between the Haynes and the overlying Lacombe Member as "the abrupt termination of sandstone lithologies and the presence of argillaceous and carbonaceous strata." In this thesis, that is considered to occur at the top of the Cycle B sandstone (826 m). With the base of the Paskapoo at 773 m, the thickness of the Haynes Member on Fig. 5 would then be 53 m, compared to 52 m in the type-section. In the interpretation of Lerbekmo et al. (1992), where 750 m was chosen as the base of the Paskapoo, the top of the Haynes Member was placed at the top of the Cycle A sandstone, giving a thickness of about 40 m. In that interpretation, the Cycle B sandstone was considered to be a localized channel sandstone within the Lacombe Member (Lerbekmo, pers. comm.).

The Unit 2 sandstone at Joffre Bridge Roadcut (see Chapter 3) is likely correlative with the Cycle B sandstone on Fig. 5. The elevation of the Cycle B sandstone (814-826 m) is somewhat lower than that of the Unit 2 sandstone (830-843 m), but is within limits that would be feasible for a fluvial channel meandering across a slowly thickening floodplain, given the distance of about 1.4 km between the drillhole and Joffre Bridge Roadcut. In this case, the fossiliferous Lower Level Bed (Unit 1) that underlies the Unit 2 sandstone would then be part of the Haynes Member, and the Upper Level Beds (Units 4-6) would lie at the base of the Lacombe Member. However, if the top of the Cycle A sandstone is chosen as the top of the Lacombe Member, in accordance with Lerbekmo et al. (1992), then all of the beds would be considered to lie within the lower Lacombe Member.

AGE OF THE STRATA

Ages of Paskapoo Formation strata in the Red Deer Valley area have been determined using three independent approaches: mammalian succession (Fox, 1990, 1991); palynostratigraphy (Demchuk, 1987, 1990); and magnetostratigraphy (Lerbekmo et al., 1992). All of those studies have incorporated material from Joffre Bridge Roadcut and neighbouring fossil localities. The results of the methods are in good agreement with one another, and are summarized by Fig. 6. Radiometric dates are not available for the Paskapoo strata, but in the underlying Scollard Formation potassium-argon dates have been determined using sanadines from bentonites within the Ardley coal zone (Lerbekmo et al., 1979a).

Biostratigraphy: North American Land-Mammal (Mammal) Ages (Wood et al., 1941), which have become the primary chronological reference for Tertiary nonmarine sediments in North America, are based on the rapid evolution and dispersal of mammals during the Tertiary. The time-relations for the fossils are known principally from evolutionary changes, and secondarily from stratigraphic superposition, supported where possible by radiometric dates and, more recently, by magnetostratigraphy (Woodburne, 1987a; Lindsay et al., 1987). Mammal remains from the Red Deer Valley have been collected and studied by Fox (1990) who judged those from Joffre Bridge Roadcut to represent a Mammal Age of middle Tiffanian, Ti_3 zone (Plesiadapis rex/P. churchilli lineage-zone) (Archibald et al., 1987) (Fig. 6).

A number of palynostratigraphic time-scales have been proposed for the Paleocene of the Western Interior of North America, but because palynofloral assemblages can differ in composition depending on local and regional paleoclimatic and paleoenvironmental factors, only a small percentage of taxa

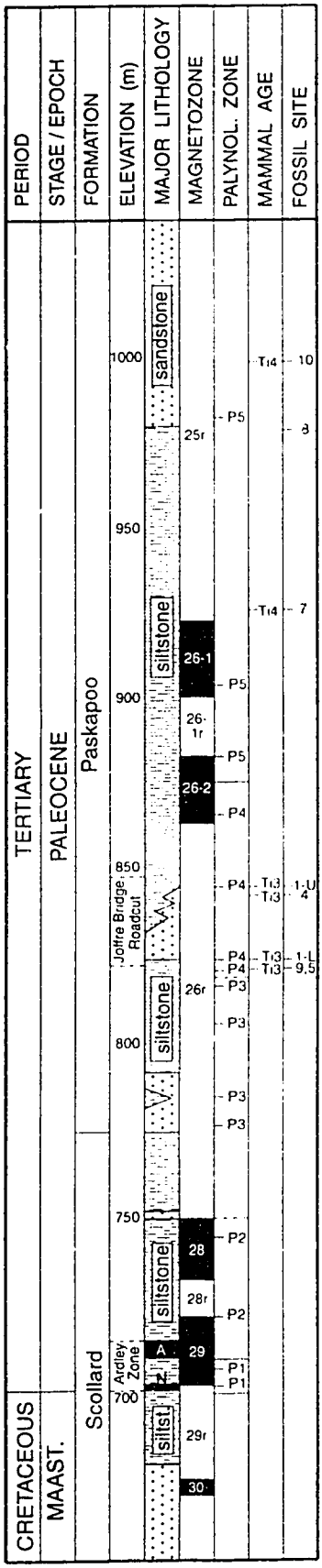

LEGEND

FOSSIL SITES (see also Fig. 1)

- 1-L Joffre Bridge Roadcut, Lower Beds
- 1-U Joffre Bridge Roadcut, Upper Beds
- 4 Erickson's Landing
- 5 Mammal Site #1
- 7 Canyon Ski Quarry
- 8 Munce's Hill (One Jaw Gap)
- 9 Blindman/Burbank
- 10 Highway 595 Roadcut

MAMMAL AGES

- Ti3 - Ti4 After Fox (1990)

PALYNOLOGICAL ZONES

- P1 - P5 After Demchuk (1990)

MAGNETOZONES (Terminology after Harland et al., 1982)

- 28 Normal Polarity
- 28r Reversed Polarity

LITHOLOGIES

- Sandstone, with minor siltstone & mudstone
- Siltstone & mudstone, with minor sandstone
- Coal & carbonaceous shale

Figure 6: Summary of biostratigraphic and magnetostratigraphic data for the Red Deer Valley area, showing the relationship between North American Land-Mammal Ages, palynofloral zones, and magnetozones. Modified from Lerbekmo et al. (1992).

have proven useful for that purpose (Demchuk, 1987, 1990). Using a Momipites-Caryapollenites palynofloral lineage like that proposed by Nichols and Ott (1978) for Wyoming, but also utilizing additional angiosperm taxa, Demchuk recognized five palynofloral zones in the Red Deer Valley area. The samples that he analyzed from Joffre Bridge Roadcut fell within his P4 (Caryapollenites wodehousei) Zone (Fig. 6).

Magnetostratigraphy: The development of the Magnetic Polarity Time Scale was triggered by the discovery that magnetic reversals recorded in igneous rocks are time-dependent (Cox et al., 1963), and that the history of such reversals is recorded in oceanic basalts and marine sediments (Vine and Matthews, 1963). The technique was subsequently extended to nonmarine sediments, including those at critical localities for Mammal Ages (e.g., Lindsay et al., 1987; Butler et al., 1987). Because the magnetostratigraphic approach is independent of the paleoclimatic and paleoenvironmental factors that can affect mammal and pollen distribution, it provides an independent basis for correlation within and between sedimentary basins, as well as between marine and nonmarine strata (Woodburne, 1987a,b). Because many system, series and stage boundaries are defined in terms of marine faunal extinctions, this facilitates the global correlation of nonmarine strata.

Lerbekmo and his colleagues have conducted magnetostratigraphic studies of uppermost Cretaceous to middle Paleocene strata in south-central to southern Alberta, southern Saskatchewan and North Dakota (e.g., Lerbekmo and Coulter, 1984, 1985; Lerbekmo, 1985, 1987, 1989; Lerbekmo et al., 1992), and have used magnetostratigraphy to correlate the Red Deer Valley strata with the well-known marine foraminiferal section at Gubbio, Italy (Lerbekmo and Coulter, 1985; Alvarez et al., 1977). Although the picture in south-central Alberta is complicated by the sub-Paskapoo disconformity which removed variable

amounts of polarity zones 28 and 28r, Lerbekmo et al. (1992) found that Joffre Bridge Roadcut and the other Red Deer Valley Ti_3 sites of Fox (1990) fell within the 26r reverse polarity zone (Fig. 6).

Conclusion: The Red Deer Valley is the first area in North America for which faunal succession, palynostratigraphy and magnetostratigraphy have been integrated for the middle Paleocene (Lerbekmo et al., 1992). Thus, contrary to the assertion of Gingerich (1991) that the Red Deer Valley sites are "isolated localities of uncertain age", these fossil localities are part of a well-documented stratigraphic sequence that can be correlated throughout much of the world with confidence.

CHAPTER 3

SITE STRATIGRAPHY AND DEPOSITIONAL HISTORY

The bedrock at Joffre Bridge Roadcut is now poorly exposed because the slope was backfilled, recontoured and seeded after highway construction was completed. The geological history described below is based on observations that were made in quarries and trenches that were dug by hand, and in two trenches that were dug by a track-mounted backhoe. Measured sections from the trenches are included in Appendix A.

A generalized stratigraphic section for Joffre Bridge Roadcut is shown by Table 2. The depositional units are discussed below and described in detail in Appendix A. Facies relationships between the units are illustrated by Fig. 7.

SUMMARY

The lowermost Paskapoo Formation (Haynes Member) in the Red Deer Valley area includes thick sandstones deposited by meandering river systems that flowed eastward across the foreland basin, draining the tectonically active Cordillera. Complex factors influenced the shifting drainage and sedimentation patterns at that time: episodes of thrust-faulting and uplift in the Cordillera; interference from newly rising ridges in the front ranges; subsidence of the foreland basin; and changes in eustatic sea level.

The Red Deer Valley area lay east of the mountain-building activity and appears to have been a broad floodplain with little topographic relief during the deposition of the Haynes Member. The floodplain deposits grew gradually

TABLE 2:

GENERALIZED STRATIGRAPHIC SECTION FOR JOFFRE BRIDGE ROADCUT

TYPICAL UNIT THICKNESS	NAME	DESCRIPTION	(cm)
-	Quaternary	Glacial till.	-
7	Crossbedded Sandstone	Sandstone, fine-grained, crossbedded.	>150
6d	Fish Layer	Mudstone, grey, silty; fish remains.	1
6c	Barren Zone	Mudstone, tan, becoming siltstone at top; scattered small molluscs.	60
6b	Aquatic Plant Zone	Mudstone & claystone, with aquatic plants & conifer fragments; molluscs; insects.	10
6a	Concretion Zone	Mudstone, grey, with calcite-cemented concretions; dicot leaves & conifer fragments.	15
5	Mollusc Layer	Mudstone & coal, dark grey & black, calcite-cemented; many small molluscs; dicot leaves & fruits; conifer fragments; mammal remains.	10
4	Lower Lacustrine Sequence	Mudstone, tan, silty; dicot leaves & fruits; molluscs; mammal & insect remains.	30
3	Channel-fill Siltstone	Siltstone, tan, yellow & green, with thin sand beds; seedlings; dicot leaves, fruits.	50
2	Fluvial Channel Sandstone	Sandstone, medium-grained, grey; mudstone clasts at base; scattered seeds, fragments of leaves.	1400
1	Lower Level Bed	Claystone, grey, soft, overlain by thin coal; mammal remains.	7
-	Grey Mudstone	Mudstone, grey; shell fragments; root traces.	

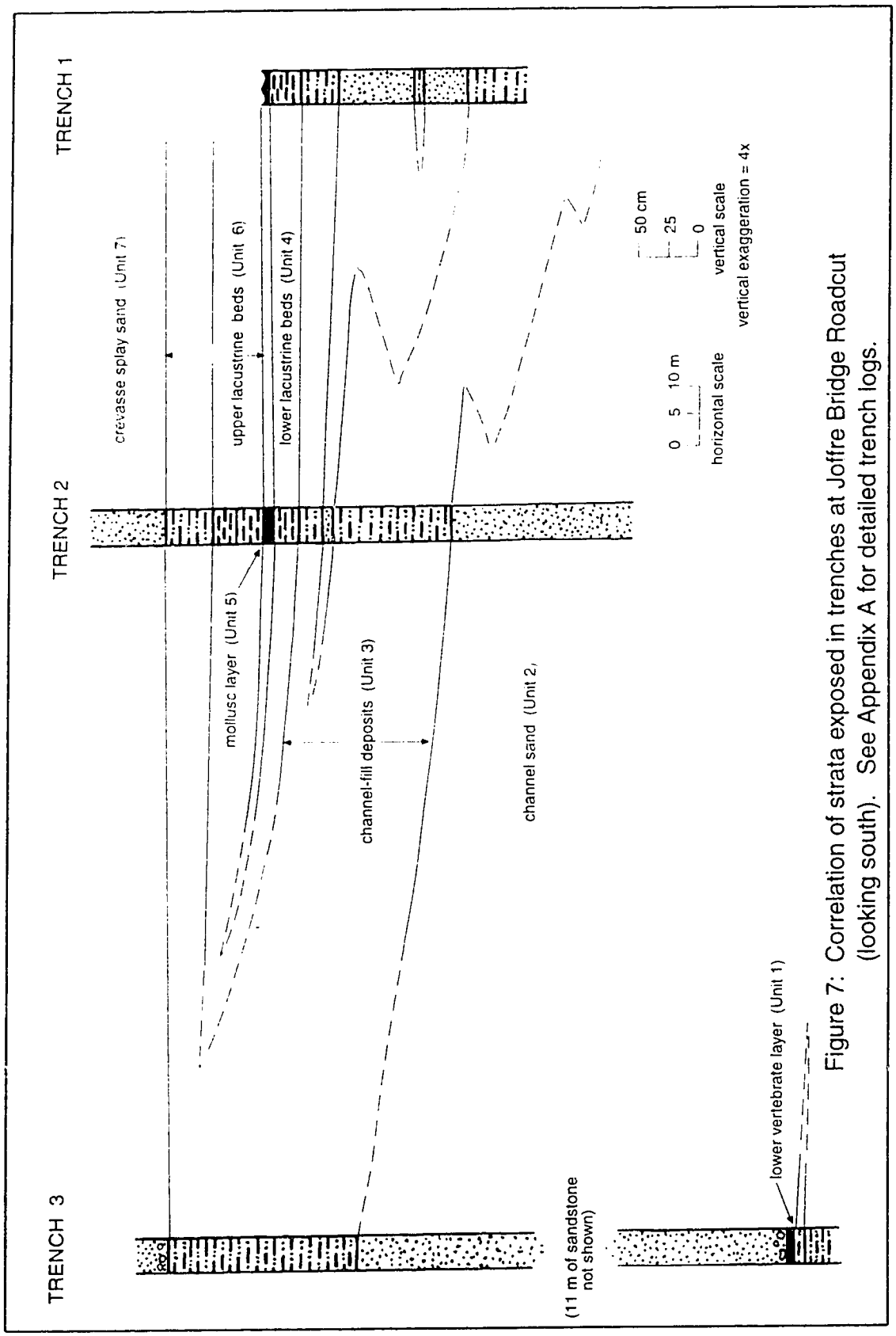

Figure 7: Correlation of strata exposed in trenches at Joffre Bridge Roadcut (looking south). See Appendix A for detailed trench logs.

thicker while the river channels meandered laterally across them, reworking the sediments.

The fossiliferous beds at Joffre Bridge Roadcut were deposited on the floodplain in association with a river channel. The interpreted depositional history is shown diagrammatically in Figs. 8a-d. The drawings are oriented looking south (into the outcrop) but are not to scale. The river flowed roughly eastward but the direction of flow varied locally due to meandering. The geometry of the meanders shown in the drawings is arbitrary.

The Lower Level Bed (Unit 1 below) is a thin bed of clay and coal that includes scattered bones of small vertebrates. It was deposited prior to the onset of fluvial activity at the site. The river channel itself (Fig. 8a) is represented by a thick deposit of medium-grained sandstone (Unit 2) that rests directly on top of the Lower Level Bed.

When the active channel eventually shifted eastward (Fig. 8b), deposition of the Upper Level Beds (Units 3-6) began in the abandoned channel (Fig. 8b-d). As the site became increasingly isolated from the active channel, water flow and energy levels declined, and the sediments became increasingly fine-grained, creating an environment that was well-suited to the preservation of plant and animal fossils.

The Upper Level Beds record the gradual in-filling of the abandoned channel and its development into an oxbow lake, here named Lake Speirs in honor of Mrs. Betty Speirs who collected most of the fossils from Joffre Bridge Roadcut. The channel sandstone (Unit 2) grades upward into siltstone (Unit 3; Fig. 8b), and then into lacustrine mudstones and claystones (Unit 4; Fig. 8c). The coaly mudstone of the Mollusc Layer (Unit 5) likely represents a swamp that formed

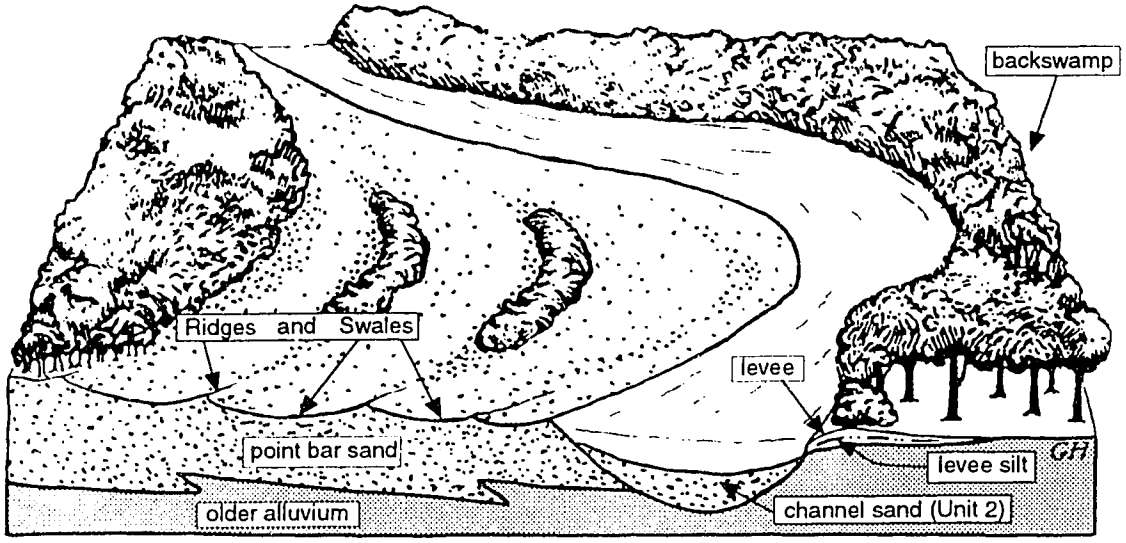

Figure 8a: Diagrammatic illustration of sand (Unit 2) being deposited by the fluvial channel. Not to scale. See text for full explanation. Vegetation cover inspired by Wing (1984).

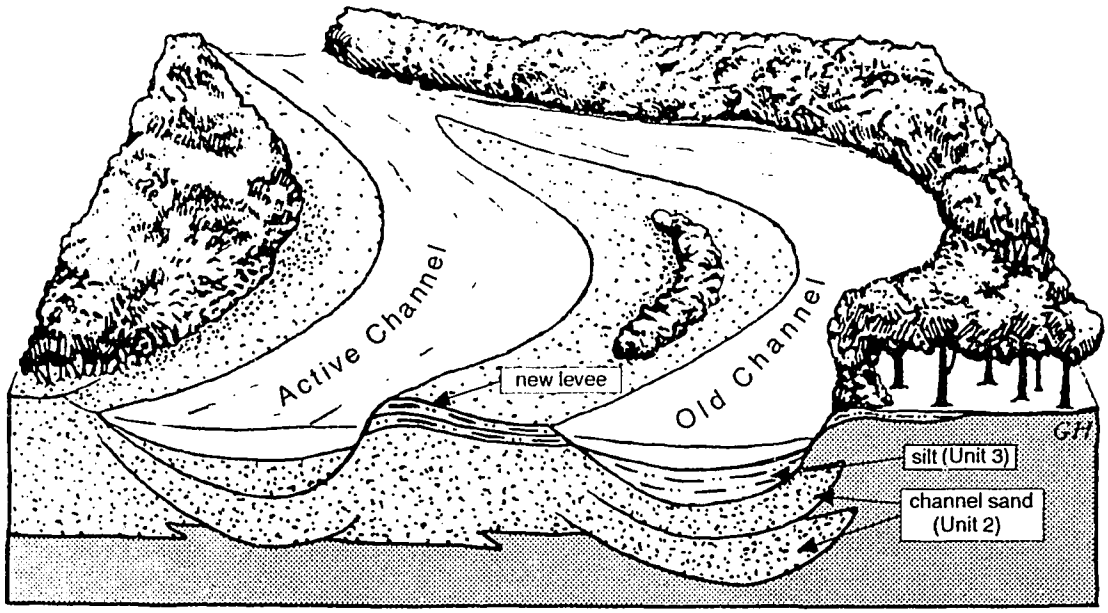

Figure 8b: The active channel reoccupies an old swale. Silt (Unit 3) is deposited in the old channel during gradual abandonment.

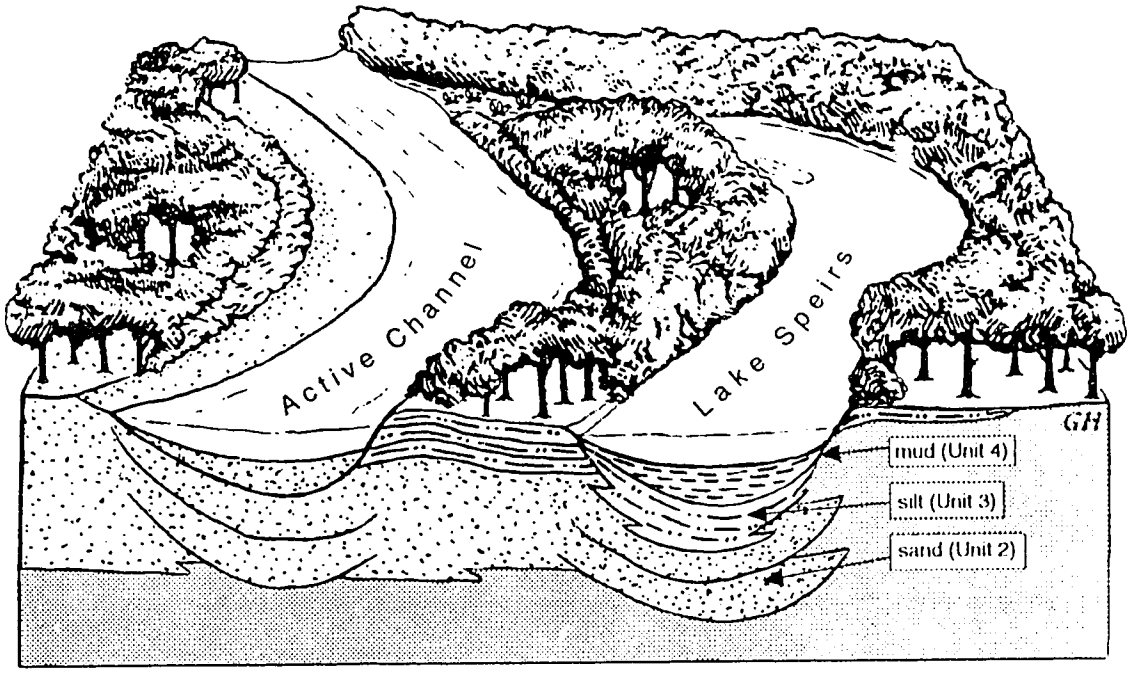

Figure 8c: The old channel becomes an oxbow lake after complete abandonment and mud (Unit 4) is deposited in the lake.

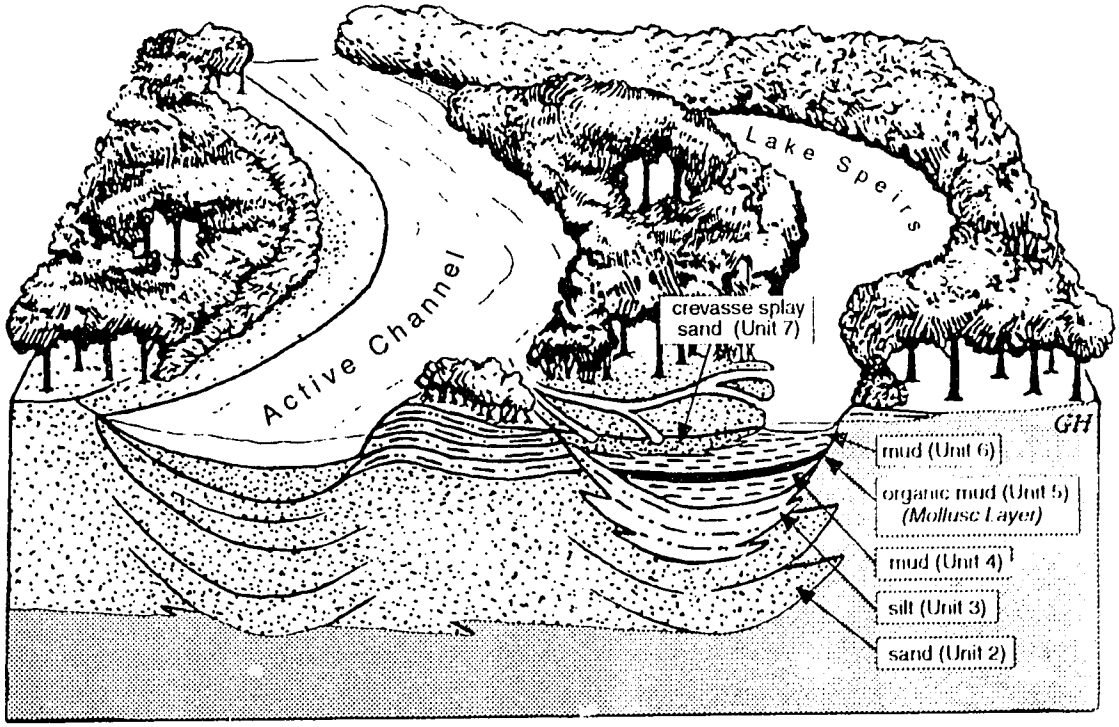

Figure 8d: The levee of the active channel is breached and a crevasse splay (Unit 7) progrades into the lake over the lacustrine sediments.

during a period of low water-level in the lake. Water levels then increased again, drowning the swamp and depositing a new sequence of lacustrine mudstones and claystones (Unit 6). The sequence is capped by a crevasse-splay sandstone (Unit 7; Fig. 8d) that is unconformably overlain by glacial till.

The fossil assemblages are consistent with floodplain and oxbow lake environments (Fig. 9). Leaves and reproductive structures from large trees that preferred riparian (e.g., Joffrea and Platanus), moist (e.g., Metasequoia) and swampy (e.g., Glyptostrobus) environments can be found throughout the Upper Level Beds. Free-floating aquatic plants (Azolla, Ricciopsis, and the Spirodela-like plant) are found in some of the lacustrine beds. Shells of freshwater bivalves and gastropods are very common throughout the lacustrine and swamp layers (Units 4-6). Impressions of wings and larvae of insects that usually live near water (e.g., craneflies, dragonflies, and caddis flies) also occur in those layers. Vertebrate remains include scattered bones of soft-shelled turtles and crocodilians (Fox, pers. comm.), scales and skeletons of freshwater fish, and bones of small mammals (Appendix B).

UNIT 1: THE LOWER LEVEL BED

A bed of soft, grey clay about 4-8 cm thick forms the base of the sequence of interest at Joffre Bridge Roadcut. The clay is topped by 1-2 cm of coal. Named "Joffre Bridge Roadcut, Lower Level" by Fox (1990), this bed was quarried intermittently during 1978-1982 and 1986, producing isolated bones and teeth of small mammals, jaw fragments with teeth, and scattered reptile bones (Fox, 1990, 1991; Appendix B). Some of the jaws were oriented more or less vertically in the clay (Lindoe, pers. comm.), indicating that the bedding was disturbed by bioturbation, rooting or soil processes during or prior to the deposition of the peat that eventually became the overlying coal.

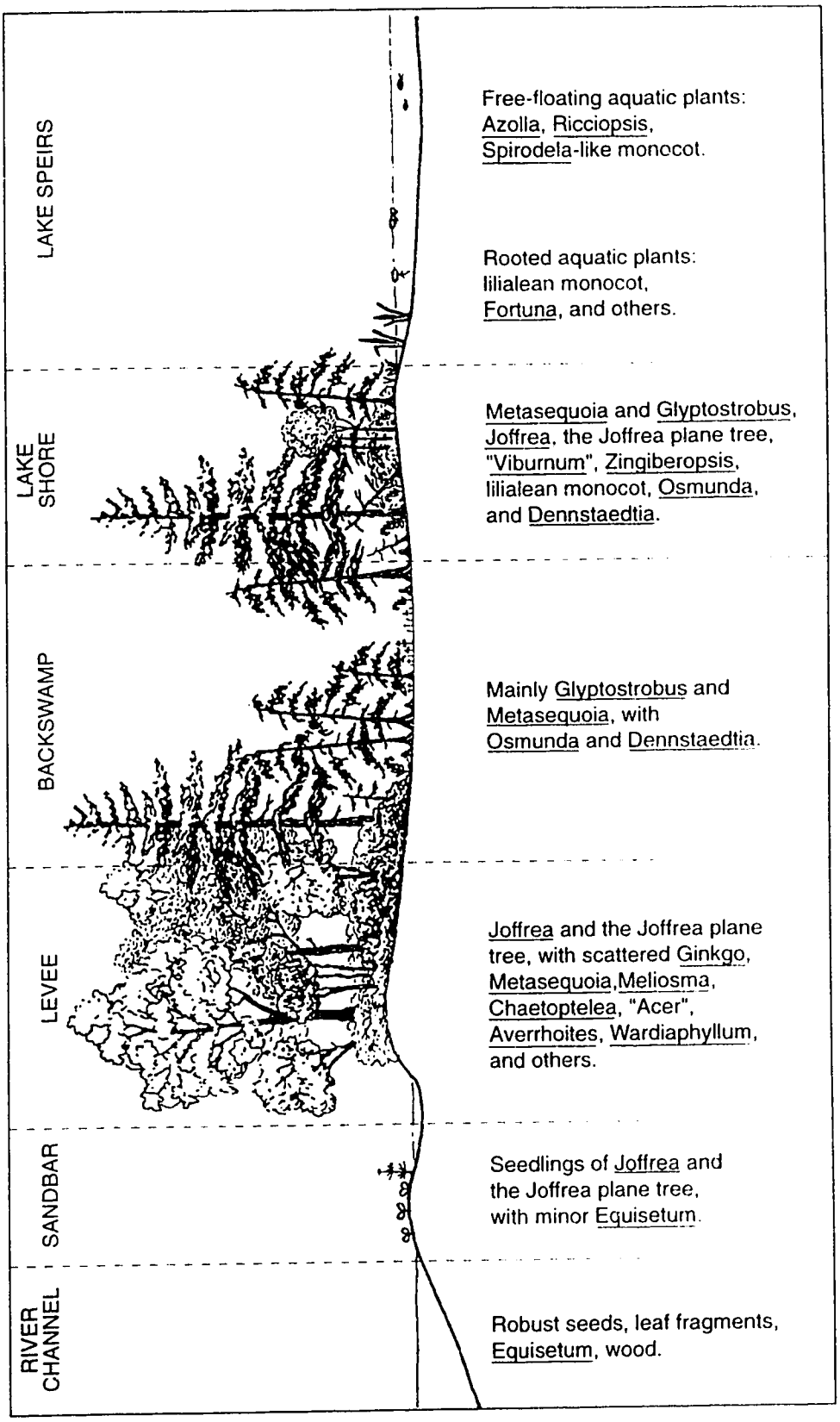

Figure 9: The paleoenvironments and plant communities at Joffre Bridge Roadcut.

A thick sandstone (Unit 2) representing the bed-load of a river channel rests directly on top of the Lower Level Bed. Unit 1 may have resisted erosion during the onset of fluvial activity because of the cohesiveness of the clay and the interlocking structure of the peat material.

The Lower Level Bed is currently difficult to expose and was seen only in Trench 3 (Fig. 7). Lying near the base of the roadcut, it has become covered by slumped sediment (Fig. 2 of Plate 1).

UNIT 2: THE FLUVIAL CHANNEL SANDSTONE

The river channel at Joffre Bridge Roadcut is represented by a thick deposit of massive, medium-grained sandstone (Unit 2 in Fig. 7, 8a). As seen in Trench 3 the sandstone is about 14 m thick, with the overall fining-upward change in grain-size that is typical of sediments deposited by meandering river channels (Walker and Cant, 1984). It is coarsest at the base, where it typically includes scattered mudstone clasts and fairly robust fragments of riparian and floodplain plants such as Joffrea follicles, fragmentary dicot leaves, and coalified wood (Fig. 6 of Plate 2). It grades into siltstone near the top.

The Unit 2 sandstone at Joffre Bridge Roadcut is probably correlative with the sandstone exposed along the cliffs directly across the river. That sandstone is medium-grained and more than 10 m thick, with large-scale crossbedding in the basal portion (Fig. 5 of Plate 1). It becomes finer grained with planar bedding near the top. That sandstone overlies a thin bed of claystone similar to Unit 1, and the erosional nature of the basal contact is apparent in some of the exposures.

UNIT 3: THE CHANNEL-FILL SILTSTONE

In the western portion of the site the channel was gradually abandoned, probably by the process of chute cut-off (Walker and Cant, 1984) in which a river gradually reoccupies an old swale (Fig. 8b). Flow gradually decreases in the old channel, where deposition becomes limited to suspended or wash-load sediments (fine sand, silt and clay). The process often culminates in the formation of an oxbow lake (Fig. 8c). At Joffre Bridge Roadcut, this type of sequence was deposited in the western part of the site after the active channel shifted eastward (Unit 3 in Figs. 7, 8b). This environment was better suited to the accumulation and preservation of plant material than was the active channel.

The siltstone is tan to light green, and thin-bedded, with frequent thin interbeds of fine-grained sand. As seen near Trenches 1 and 2, the siltstone is about 35 cm thick and commonly includes scattered leaves and fruits of Joffrea and Plantanus/Macginicarpa as well as lenses of Joffrea and platanaceous seedlings. Other dicot leaves, seeds and fruits, and fish scales are also present. The lenses of seedlings indicate that parts of these sediments were occasionally emergent, perhaps as bars or mudflats that were subsequently innundated, burying the seedlings in place.

Siltstone exposed near the top of Trench 3 (Fig. 7) may be part of the Unit 3 channel-fill sequence. However, because that area lay closer to the active channel, that exposure could also represent part of a levee deposit (Fig. 8b).

UNIT 4: THE LOWER LACUSTRINE SEQUENCE

The abandoned river channel gradually became more isolated, eventually developing into an oxbow lake (Lake Speirs; Fig. 8c) with little or no direct connection to the active channel. Plant parts tended to fall or be blown in from the lakeshore plant community. Periodically the lake would have received fine sediment from the active channel during periods of high water flow and overbank flooding, during which times additional plant material would have been washed in from the active channel and the backswamps (Fig. 8c).

The Lower Lacustrine sequence (Unit 4) is present in the western part of the site (Fig. 7), where it is about 30 cm thick. It is tan to light green, thin-bedded, and silty near the base, with scattered shells of small freshwater bivalves and gastropods. It includes scattered parts of Joffrea and platanaceous remains, as well as various seeds and fruits. Insect remains include impressions of larvae and wings (Speirs, pers. comm.; Appendix B).

UNIT 5: THE MOLLUSC LAYER

Named the Mollusc Layer by Taylor and Stockey (1984), Unit 5 is a distinctive, dark grey to black, carbonaceous mudstone 6-12 cm thick that is present throughout the western part of the site (Fig. 7). It includes numerous shells of small freshwater bivalves and gastropods, and thin (0.5-2.0 cm) lenses of coal. It is well-indurated with calcite cement and very hard. The Mollusc Layer is a useful marker-bed at the site. Its dark-coloured coaly sediments contrast strongly with the lighter-coloured fluvial and lacustrine beds, and the numerous white mollusc shells give it a distinctive speckled appearance (Figs. 3, 4 of Plate 1).

The Mollusc Layer represents a swamp environment that formed during a period of low water-level in the lake. The area was isolated from the active channel, and clastic sedimentation was minimal. Small amounts of peat formed, but sufficient oxygen was available to support the population of small molluscs.

Metasequoia foliage and cones are abundant in the Mollusc Layer, as are the remains of Glyptostrobus and Platanus, and various seeds. A few fragmentary Ginkgo leaves are also found. Given the isolation of the swamp, it is unlikely that the plant remains were transported over any great distance; these taxa probably grew in or adjacent to the swamp. Isolated mammal jaws (Fox, 1990) and larvae of craneflies are also found in the Mollusc Layer (Appendix B).

UNIT 6: THE UPPER LACUSTRINE SEQUENCE

Water levels and clastic sedimentation rates in the area increased, the Mollusc Layer swamp was drowned, and a new sequence of lacustrine strata was deposited on top of it (Fig. 3 of Plate 1). The Upper Lacustrine Sequence (Unit 6) is present in the western part of the site, where it is about 85 cm thick (Fig. 6). It includes several important fossiliferous beds and has therefore been subdivided into four zones: the Concretion Zone (Unit 6a) at the base; overlain by the Aquatic Plant Zone (Unit 6b); and the Barren Zone (Unit 6c); with the Fish Layer near the top (Unit 6d) (Table 2). The overall lithology and history of the upper lacustrine sequence is summarized below, followed by detailed descriptions of the individual zones.

Initially the lake was shallow, and the lowermost mudstones and claystones contain abundant remains of swamp and shallow water plants (Unit 6a), overlain by remains of shallow water plants and free-floating aquatic taxa (Unit

6b). Insect and mammal remains have also been recovered from those beds (Appendix B).

The sediment in the overlying beds becomes coarser toward the top and is largely devoid of plant material (Unit 6c), likely due to an increasing supply of oxygenated water and coarser sediment from the active channel.

Unit 6a: The Concretion Zone

The Concretion Zone (called the Hard Layer by Taylor and Stockey, 1984) rests directly on top of the Mollusc Layer. It is about 10-15 cm thick and consists of light to medium grey mudstone with well-preserved plant and animal remains. In the westernmost part of the site (near Trench 1) the mudstone is commonly cemented into concretions by calcite; it is usually uncemented in the east (near Trench 2). Faunal remains collected from this zone (Appendix B) include insect wings and larvae (M.V.H. Wilson, pers. comm.); the skull and postcranium of a large Pantodont that Speirs found just above the Mollusc Layer (Fox, 1990; Speirs, pers. comm.); one fish (a small osteoglossomorph) and scales of a large bowfin (M.V.H. Wilson, pers. comm.).

The Concretion Zone records the inundation of the Mollusc Layer swamp by the growing lake, with increasing water levels and deposition of mud. Fragments of Glyptostrobus are abundant at the base of this zone, which may reflect the drowning of those swamp-dwelling trees. Osmunda pinnules, Metasequoia foliage, Joffrea leaves, "Viburnum" leaves, and scraps of Zingiberopsis leaves are also found, as are remains of emergent aquatic plants that grew rooted in shallow water also appear (e.g., the lilialean monocot and Fortuna).

Unit 6b: The Aquatic Plant Zone

The Aquatic Plant Zone (Unit 6b) is usually about 10 cm thick and consists of light grey to light green mudstone and claystone, with plant and insect fossils. Whole liverworts (Ricciopsis) and Spirodela-like plants, and fragments of Typha-like leaves, are found in the lower part of the zone. Scattered Azolla sporophytes, many of which are fertile, are found near the top. Insect wings (dragonfly, caddisfly and beetle) have also been found in this zone (Speirs, pers. comm.; Appendix B).

The lake was still fairly shallow when these sediments were deposited. The Spirodela-like plant and Azolla were free-floating plants that would have accumulated near the lake margins; the Lilialean monocot grew at the lake margin; and the Ricciopsis likely had free-floating and attached forms like the modern Riccia fluitans L.

Unit 6c: The Barren Zone

The Barren Zone (Unit 6c) includes about 60 cm of light green to tan mudstone, grading into siltstone in the upper half. The sediments are mildly bioturbated, and include scattered small molluscs and fish scales, but almost no plant material.

The lake appears to have grown deeper during the deposition of this zone, and was probably better connected with the active channel. Water levels and sedimentation rates increased as oxygenated water and coarser sediment flowed in from the channel, and the unit grades into siltstone at the top.

Unit 6d: The Fish Layer

A mass-death layer of fish remains lies near the top of the lacustrine sequence. The Fish Layer consists of about 1 cm of medium grey, rust-stained silty mudstone, containing the skeletons of freshwater fish. It lies a few centimetres below the crossbedded sandstone (Unit 7). The Fish Layer has been quarried by UALVP since 1984. Between 1984 and 1991, UALVP recovered 45 specimens of an osmerid (smelt), 1,795 specimens of a paracanthopterygian, two articulated specimens of an osteoglossomorph, a few disarticulated bones of an amiid, and one articulated crustacean (Murray, 1994; Wilson and Williams, 1991; Williams and Wilson, 1988).

Because modern osmerid species often spawn on beaches or in streams or ponds during spring or early summer, Wilson and Williams (1991) felt that the presence of both male and female osmerids, with apparent breeding tubercules in some of the males, indicates that the fish may have died during or after an attempt to spawn, probably in spring or early summer. The increasing coarseness of the sediment in Units 6c and 7 indicates connection between the lake and an active channel, which would facilitate the passage of fish as well as water and sediment (Fig. 8d). The UALVP is continuing to work on the Fish Layer, and further taphonomic and phylogenetic studies are in progress.

UNIT 7: THE CROSSBEDDED SANDSTONE

The crossbedded sandstone (Unit 7) appears to represent a crevasse splay that prograded into the lake (Fig. 8d). Crevasse splays form when the levee of an active channel is breached, allowing sediment-laden water to escape into the adjacent floodplain, backswamps and lakes (Davis, 1992). The sediment is deposited as a delta with its own system of distributaries leading away from the

channel. Unless the breached levee heals, a crevasse splay can remain active for many years, and its deltaic deposits continue to grow.

In the western part of the site the crossbedded sandstone is fine-grained and crossbedded, with climbing ripples, a few large molluscs, and scattered large concretions (Fig. 1 of Plate 1). It contains no significant plant material (Speirs, pers. comm.; Lindoe, pers. comm.). The crossbeds and ripples indicate that the sediment was prograding roughly westward from a source to the east.

In the eastern part of the site (at Trench 3), the sandstone has an erosional base, is coarser grained, and includes mudstone clasts. This coarser part of the deposit may represent one of the distributary channels near the breached levee.

The crossbedded sandstone is the youngest Paleocene unit preserved at Joffre Bridge Roadcut. It is unconformably overlain by glacial till. Younger Paleocene strata are exposed along the Red Deer Valley to the west, and are present in the upper portion of drillhole ARC 8-81 across the river (Figs. 1 and 5).

CHAPTER 4

SYSTEMATIC DESCRIPTION OF FLORA

The suprageneric classification used in this thesis has been adapted from Cronquist (1981), Parker (1982), and Stewart and Rothwell (1993). Descriptions of leaf architecture are based on Hickey (1973, 1979), Dilcher (1974), and Hickey and Wolfe (1975).

Where the material is not sufficiently well preserved to identify with confidence, the designation considered most likely is preceeded by cf. (i.e., cf. Meliosma rostellata). A generic name in quotations (e.g., "Acer" arcticum) indicates that the generic assignment is generally believed to be incorrect, but the name is valid, and the proper designation has not been established. Material for which no affinity could be determined is described as incertae sedis (i.e., unidentified aquatic leaf).

A number of new taxa have been recognized, and it is the intention of the author to describe, name and validly publish them after the submission of this thesis, but they are unnamed in the thesis itself. They include the Spirodela-like plant, which represents a new genus; a new species of Ricciopsis, designated Ricciopsis sp. in this thesis; and a new species of Deviacer, designated Deviacer sp. in this thesis.

Division BRYOPHYTA
Class HEPATICOPSIDA
Order MARCHANTIALES
Family RICCIACEAE
Ricciopsis Lundblad
Ricciopsis sp.
(Plate 2, Figs. 8-10)

Description: The thallus is flat, linear, ribbon-like, and dichotomously branched, with a distinct dorsal sulcus, and rounded terminal segments (Fig. 7). Generally the thallus is consistently about 1.7-2.0 mm wide, but it is occasionally abruptly constricted to 0.7 mm, and abruptly dilated to as much as 5.5 mm proximal to a dichotomy (Figs. 8, 9). The sulcus is acute, deeply impressed, and persistent (Fig. 10). The margin is smooth and lacks papillae or "cilia" (Schuster, 1992) (Fig.10). Dichotomous branching occurs in a single plane, usually with about 3-5 mm between branches, forming branched ribbons or loose, incomplete rosettes (Fig. 8). Segments up to 55 mm long with 7 dichotomies have been recovered. Fragments of cuticle adhering to the specimens show no evidence of pores or modified epidermal cells. No spores were recovered.

Occurrence: About 65 specimens have been recovered from the Upper Lacustrine Sequence, at the base of the Aquatic Plant Zone (Unit 6b).

Discussion: These remains from Joffre Bridge Roadcut have the features of a thallose liverwort gametophyte: small size, prostrate habit, and a flat, leafless body. They resemble living species of the genus Riccia L. that have a slender, dichotomously branched, ribbon like thallus with a dorsal sulcus.

The genus Riccia is large, with more than 200 described species, but phenotypic variability can be extreme and species limits can be difficult to establish satisfactorily (Schuster, 1992). The structure of the thallus is very simple, and has been viewed both as an ancestral type in older theories, and more recently as highly reduced and derived (Schuster, 1966, 1992). The Riccia thallus, which has been well described by MacVicar (1926), Engel (1982), Schuster (1992), and others, is flat and ribbon-like, commonly with a dorsal groove or sulcus, and is strongly branched, often forming rosettes. The dorsal surface includes simple air-chambers that range from narrow fissures completely covered by epidermis, to larger chambers connected to the surface by fissures or rudimentary pores. Where pores are present, the epidermal cells surrounding them exhibit little or no modification. A single row of scales, sometimes rudimentary or inconspicuous, is usually present on the ventral surface. Archegonia and antheridia are scattered within the thallus, and the sporophytes, which are considered to be the most reduced in the Bryophyta (Schuster, 1966, 1992), develop embedded within the thallus. Spores are few and large (well over 50 μm in most species), and are released by the partial decay of the surrounding tissue. Spore ornamentation and wall structure are significant to intrageneric taxonomy and phylogeny (Schuster, 1992; Jovet-Ast, 1987).

Some extant species of Riccia, such as Riccia fluitans L., have two morphologically distinct forms, one terrestrial and one aquatic (MacVicar, 1926; Schuster, 1992). The terrestrial form lives attached to damp soil or mud, and in some species can survive periodic drying and/or shallow submergence. The aquatic form lives free-floating on bodies of quiet or slow-moving fresh water. In most species the floating form is sterile and lacks rhizoids or ventral scales. The thalli develop rhizoids when stranded, attaching themselves to the

substrate, after which the sporophytes may develop. Vegetative propagation by fragmentation occurs in both forms.

Riccia L. and Ricciocarpus Corda are the two living genera of the family Ricciaceae, which, along with the monotypic Oxymitraceae, comprise the suborder Ricciineae of the Marchantiales (Schuster, 1966). Fossil Marchantiales have been known since 1849 when Brongniart described a fertile specimen which he named Marchantites, from Eocene strata of the Paris Basin (Lundblad, 1954). Older marchantialean fossils were subsequently found in Mesozoic sediments (Walton, 1925, 1928, 1949; Steere, 1946; Lundblad, 1954, 1955; Schuster, 1966; Jovet-Ast, 1967). The name Marchantites was emended by Walton (1925) to include only fossils with an undoubted affinity to the Marchantiaceae. For Riccia-like forms, Lundblad (1954) introduced the name Ricciopsis, which she defined to include "sterile fossil thalli of Hepatics showing closer resemblance to the Ricciineae than to any other living group".

The name Ricciopsis is appropriate for the liverwort specimens from Joffre Bridge Roadcut. Their sterile thalli resemble those of Riccia in their slender, branching, ribbon-like habit, dorsal sulcus, and lack of pores. However, because no spores or sporophytes are available, the plant is not known well enough to assign it to a living genus.

The Ricciopsis remains from Joffre Bridge Roadcut are unusual in the abrupt constrictions and dilations of the thallus that are sometimes present proximal to a dichotomy (Jovet-Ast, pers. comm.). A new specific name may therefore be warranted for this fossil.

The thalli are found in a thin bed of claystone near the base of a lacustrine sequence, scattered among the very abundant remains of a Spirodela-like plant,

just as modern Riccia are commonly found floating among Spirodela and other Lemnaceae on ponds and sluggish streams (Hillman, 1961; Schuster, 1992). The deposit appears to represent an assemblage of floating plants that had become stranded together on a mudflat or shoreline immediately prior to burial.

The lack of any visible rhizoids or ventral scales and the geological setting suggest that these specimens may represent a free-floating form, like those seen in modern Riccia fluitans. It is also possible that, like the free-floating form of R. fluitans, the floating form of this plant was sterile. No ricciaceous spores were recovered from thallus fragments or the surrounding matrix despite efforts by the author and A.R. Sweet of the Geological Survey of Canada. Well-preserved lemnaceous pollen from the associated Spirodela-like plant was obtained from the samples, so the absence of spores probably cannot be attributed to poor preservation.

Class BRYOPSIDA

Family INCERTAE SEDIS

Genus Muscites Brongniart

Muscites sp.

(Plate 2, Fig. 11)

Description: Specimens consist of branching stems up to 15 mm long. Stems are about 0.2 mm wide, with branches up to 6 mm long, arising at an angle of about 35°. Leaves are alternately or helically arranged, imbricate, 2 mm long, 0.5 mm wide, symmetrical, narrow-oblong, with acute apices and bases, entire margins, apparently thin laminae, and prominent, straight costae (Fig. 11).

Occurrence: Two fragmentary specimens, UAPC-ALTA S12,519 and S16,645, have been recovered from the Channel-Fill Siltstone (Unit 3).

Discussion: The genus Muscites was established by Brongniart for fossils that are clearly mosses but whose systematic position cannot be more precisely determined (Steere, 1946), as is the case for these fragments from Joffre Bridge Roadcut. They likely represent a moss gametophyte because of their small size, their branched and creeping habit, and their symmetrical, narrow-oblong leaves with distinct, dark costae and apparently delicate laminae. They resemble a specimen from Genesee, Alberta (Lower Paleocene age) that was described by Chandrasekharam (1972, 1974), who suggested a possible relationship to the Dicranaceae or Ditrichaceae. The specimens are too fragmentary and poorly preserved, however, to allow precise identification (D.H. Vitt, pers. comm.).

Division TRACHEOPHYTA

Class SPHENOPSIDA

Family EQUISETACEAE

Genus Equisetum Linnaeus

Equisetum sp.

(Plate 2, Figs. 12, 13)

Description: Specimens consist of whorls of leaves, usually detached or rarely adhering to poorly preserved stem fragments 3-7 mm in diameter. Individual leaves have a prominent midvein, are 0.5-1.5 mm wide and 5-11 mm long, and are fused along more than half of their length (Fig. 12). Free leaf apices are 1-5

mm long, with acute tips. Fragments of axes show longitudinal ridges and furrows (Fig. 13).

Occurrence: More than 25 specimens have been recovered from the Fluvial Channel Sandstone (Unit 2), the Channel-Fill Siltstone (Unit 3), the Lower Lacustrine Sequence (Unit 4), and the Aquatic Plant Zone (Unit 6b).

Discussion: These whorls of small, partially fused leaves and fragments of axes from Joffre Bridge Roadcut are typical of those of the living genus Equisetum L., but the specimens are too incomplete and poorly preserved to consider identification to a species level. Stems and rhizomes are preserved only as short fragments, and no strobili have been found.

Forms resembling the extant genus Equisetum appear in early Mesozoic strata, and Equisetum-like remains are common in most Upper Cretaceous and early Tertiary plant fossil assemblages of the Northern Hemisphere (McIver and Basinger, 1989). Modern species are very widespread, ranging from boreal forests to tropical areas, growing at elevations of up to 4200 m (Tryon and Tryon, 1982). They inhabit a variety of moist or wet environments, including open disturbed soils, bogs, thickets, dense forests, and shores of ponds and streams, often forming dense colonies from their branching underground rhizomes (Tryon and Tryon, 1982). Most of the stratigraphic units at Joffre Bridge Roadcut represent wet environments that would have been suitable for Equisetum, and traces of Equisetum are occasionally found throughout the sequence. None of the Equisetum material is common or well-preserved, however, and most of it appears to have been reworked or transported, rather than buried in place.

Class FILICOPSIDA

Order FILICALES

Family OSMUNDACEAE

Genus Osmunda Linnaeus

Osmunda macrophylla Penhallow

(Plate 3, Figs. 14-16)

Description: The pinnules are alternate on the rachis (Fig. 15). They are narrow-ovate, asymmetrical, up to 38 mm long and 14 mm wide, with acute apices and obliquely truncate bases (Fig. 14). The proximal pinnules have a narrow base of attachment; distal pinnules are attached by broad bases; the terminal pinnule is basally lobed (Fig. 15). Margins are finely toothed with convex, acute-tipped serrations (Fig. 16). Venation is open dichotomous with a distinct midvein; lateral veins dichotomize one to three times before reaching a margin (Fig. 16).

Occurrence: Thirteen specimens, UAPC-ALTA S11,191, S13,007, S16,948-949, S16,952, S16,970-972, S36,908-912 have been recovered from the Upper Lacustrine Sequence, Concretion Zone and Aquatic Plant Zone (Units 6a and 6b).

Discussion: The specimens from Joffre Bridge Roadcut include part of one sterile frond and a number of isolated sterile pinnules that are consistent with Osmunda macrophylla as described by Penhallow (1908). Penhallow's specimens (sterile fronds) were collected "from the Red Deer River, at the mouth of the Blindman", an area which lies about 15 km northwest of Joffre Bridge Roadcut (Fig. 1, site 9) and encompasses strata of the same age (middle Tiffanian, Ti_3) (Fox, 1990). Collecting sites near the mouth of the Blindman

River, including Blindman-Burbank (Taylor and Stockey, 1984), Burbank (Fox, 1990) and Blackfalds (Hickey and Peterson, 1978), consist of exposures along the northwest bank of the Red Deer River on each side of the confluence, and along the north and east banks of the Blindman River immediately upstream of the confluence (Speirs, pers. comm.).

Bell (1949), and Taylor and Stockey (1984) have also described pinnae and pinnules of O. macrophylla that were collected near the mouth of the Blindman River, and the species has been reported from other Paleocene localities in the Ravenscrag Formation in Saskatchewan (McIver and Basinger, 1993), the Fort Union Group in North Dakota and Montana (Brown, 1962), and the Golden Valley Formation in North Dakota (Hickey, 1977). Boulter and Kvaček (1989) referred material from Tertiary localities in Spitsbergen and the Arctic of North America and Siberia to O. macrophylla Penhallow because it is "the earliest published name for this type of foliage."

The Osmundaceae have a long fossil record, first appearing in Mesozoic strata (Miller, 1971; Tidwell, 1992). Osmundaceous rhizomes are known from the Upper Cretaceous (Maastrictian) of central Alberta (Serbet, 1994), and during the Tertiary the genus was common in the swamp forests that occupied northern and Arctic areas (Boulter and Kvaček, 1989). Modern Osmunda grow primarily in habitats that are wet, usually in open or brushy areas, and occasionally in shaded forests (Tryon and Tryon, 1982).

Family DENNSTAEDTIACEAE

Genus Dennstaedtia Bernhardi

Dennstaedtia blomstrandii (Heer) Hollick

(Plate 3, Figs. 17-19)

Description: The frond is twice pinnate, with primary pinnae diverging at angles of about 40° (Fig. 17). Pinnules are alternate on rachis (Fig. 18); they are up to 11 mm long and 55 mm wide, narrow ovate, with acute apices (Fig. 19). Pinnule margins have acute-tipped serrations and acute sinuses. Venation is open dichotomous; there is no midvein, and veins dichotomize up to four times before reaching the margin (Fig. 19).

Occurrence: There are three specimens, UAPC-ALTA S16,950-951, S36-913, from the Upper Lacustrine Sequence, Concretion Zone and Aquatic Plant Zone (Units 6a and 6b).

Discussion: A few fragments of sterile fronds have been referred to Dennstaedtia blomstrandii (Heer) Hollick. Specimens of the same fern, also sterile, collected near the mouth of the Blindman River, were described by Penhallow (1902), Bell (1949) and Taylor and Stockey (1984). Penhallow referred his material to Sphenopteris blomstrandi Heer, which was later incorporated as a synonym of D. americana Knowlton (1910) by Knowlton (1919). Heer's specific name has priority, however, thus the name Dennstaedtia blomstrandii is used (e.g., Hollick, 1936; Bell, 1949; Boulter and Kvaček, 1989).

Like Osmunda, Dennstaedtia was a common fern genus of the swamp forests that occupied northern latitudes during the Tertiary (Boulter and Kvaček, 1989).

Living Dennstaedtia are found in wet mountain forests and forest openings (Tryon and Tryon, 1982).

Order SALVINIALES*

Family AZOLLACEAE

Genus Azolla Lamarck

Azolla stanleyi Jain & Hall

(Plate 4, Figs. 20 - 33)

Description: Plants are small, planar, and triangular, reaching up to 225 mm in length. The main rhizomes are up to 0.2 mm wide and bear alternately arranged lateral branches, with one leaf between succeeding branches (Fig. 21). Leaves are alternate, sessile, and imbricate, each leaf overlapping the next by 10-20%. Leaves reach up to 2 mm in length and are ovate with obtuse bases and apices, entire margins, and papillate surfaces (Fig. 22), frequently showing indications of a single unbranched midvein (Fig. 20). Ventral leaf lobes, if present, could not be discerned due to the imbrication of the leaves. Detached roots near sporophytes are 0.1 mm wide and up to 0.5 cm long; no roots were found attached.

On fertile specimens megaspores are associated with leaves along the entire length of the lateral branches (Fig. 21), occurring singly or in pairs at the bases of leaves (Fig. 22). Megasporocarps and megasporangia appear to have decayed prior to preservation, leaving the resistant megaspores lying naked on the impressions of the leaves, sometimes with massulae attached. Similarly, microsporocarps and microsporangia were not preserved, but free massulae are abundant.

* A version of this section is published in Can. J. Bot. 72: 301-308.

Megaspore complexes are ovate (Fig. 33), ranging from 432-663 μm in length, (average 516 μm). Megaspores are nearly spherical and range from 266-452 μm in diameter (average 334 μm), inclusive of perine. The supraspore is generally as wide as the megaspore and bears more than 15 floats, roughly organized in three tiers (Fig. 23). Floats appear spherical to ovoid in surface view. The upper, innermost floats are conical (Fig. 24). Floats lack filaments and are distinct entities, loosely held by entanglement in filaments from the columella (suprafilosum of Fowler and Stennett-Willson, 1978) (Fig. 24). Megaspore and supraspore are covered by filamentous infrafilosum and suprafilosum, respectively (Fowler and Ste[illegible]n, 1978). Infrafilosum is up to 4.0 μm thick, with filaments about [illegible] in diameter (Fig. 25), arising from the outer perine or experine (Sw[illegible]ls, 1971) (exoperine of Fowler and Stennett-Willson, 1978) (Fig. 27[illegible] here infrafilosum has been removed by degradation (e.g., Fig. 24), the rugulo-reticulate texture of the experine is apparent (Fig. 26). The megaspore wall is distinctly layered. The experine ranges from 2.3-5.0 μm thick (average 3.8 μm) and consists of large sculpturing elements that are more or less solid, fused, rugulate, elongate baculae (Sweet, 1972), separated by pit-like depressions reaching the inner perine (Figs. 12, 13). The inner perine or inperine (Sweet and Hills, 1971) (endoperine of Fowler and Stennett-Willson, 1978) is 1.3-3.4 μm thick (average 2.0 μm) with tangentially oriented alveolae (Saunders and Fowler, 1992, 1993). The exine is 1.8-3.4 μm thick (average 2.3 μm), alveolate and more dense than the inperine (Fig. 27). Apart from occasional effects of degradation, megaspores from the dispersed population did not differ from those found in place on sporophytes.

Massulae adhere to megaspores by entanglement of their glochidia in the filosum (Fig. 28). They are roughly ovate, typically about 125 by 200 μm in size, sometimes entangled together in large clumps. Glochidia 17-33 μm long,

with fluked tips, arise from the massula surface (Figs. 28, 31), in some cases densely covering the massula. Glochidia stalks are about 0.5-1.0 μm wide at the midpoint, flaring to about 3.0 μm at the base and tip (Fig. 31). Flukes are generally 6.0-9.6 μm long. Microspores embedded within the massulae (Figs. 29, 32, 33), are circular in outline, 20-25 μm in diameter, with a rugulate surface texture and distinct trilete suture (Figs. 29, 30). Microspore walls are 0.5-1.0 μm thick and unlayered (Fig. 32). The enclosing massulae have a pseudocellular internal structure (Fowler, 1975a,b; Saunders and Fowler, 1992) (Fig. 32). Because massulae are often partly degraded and adhering to one another, it was not possible to reliably determine the number of microspores per massula.

Occurrence: More than 200 specimens have been catalogued from the Upper Lacustrine Sequence at the top of the Aquatic Plant Zone (Unit 6b).

Discussion: The genus Azolla contains small heterosporous ferns, and is classified in either the Salviniaceae or the Azollaceae. Six or seven extant species are usually recognized (Perkins et al., 1985). Plants live free-floating on the surface of quiet bodies of fresh water. The value of fossil Azolla as an environmental indicator has long been recognized (e.g., Melchior and Hall, 1983; Collinson, 1983).

Species delineation in both living and fossil Azolla is based primarily on the anatomy of the reproductive structures and the ultrastructure of the megaspore wall (Kempf, 1969; Snead, 1969, 1970; Fowler and Stennett-Willson, 1978; Calvert et al., 1983; Perkins et al., 1985). The complex reproductive structures, called megaspore complexes and massulae, are impregnated with sporopollenin (Lucas and Duckett, 1980) and are often preserved in the fossil record (Hall, 1968). Numerous fossil species ranging in age from uppermost

Cretaceous to Pleistocene have been described (Kovach and Batten, 1989; Batten and Kovach, 1990), although most are known only from dispersed megaspores and massulae. The comparatively fragile sporophyte is rarely preserved (Melchior and Hall, 1983; Saunders and Fowler, 1993).

The oldest known Azolla fossils are spore complexes of uppermost Cretaceous age (Batten and Kovach, 1990). The oldest Azolla for which sporophyte remains have been described to date are from Paleocene strata in Alberta, Saskatchewan and North Dakota: A. schopfii Dijkstra (Sweet and Chandrasekharam, 1973; McIver and Basinger, 1993); A. velus (Dijkstra) Jain & Hall (McIver and Basinger, 1993); and A. stanleyi Jain & Hall (Melchior and Hall, 1983). The spore complexes of the well-preserved Azolla from Joffre Bridge Roadcut closely resemble those of A. stanleyi, hence the material is referred to that species. The material is described below and, given the relative rarity of Azolla sporophytes, is compared with the other Paleocene species for which sporophytes are known and discussed in terms of evolutionary trends for the genus.

Azolla stanleyi (Jain and Hall, 1969) is based on dispersed megaspores and massulae from the Paleocene Sentinel Butte Formation of North Dakota. The Joffre Bridge specimens are referred to A. stanleyi because of the rugulo-reticulate texture of the experine of the megaspore wall. The ovate shape of the megaspore complex, the thick filosum arising from the experine and covering the entire megaspore complex, and the multifloated supraspore with the lowermost tier of floats overlapping the top of the megaspore, are also characteristic of A. stanleyi.

Dispersed megaspores and massulae referred to A. stanleyi have been described from the Paskapoo Formation at Wizard Lake, Alberta (Sweet, 1972) and from

the Ravenscrag Formation at Estevan, Saskatchewan (Sweet, 1972; Sweet and Hills, 1976). Fertile sporophytes referred to A. stanleyi from the Paleocene Bullion Creek Formation at Wannagan Creek, North Dakota, have been described by Melchior and Hall (1983). These localities, the type locality and the Joffre Bridge site are all of Tiffanian age (Ti_3 and Ti_4) and A. stanleyi would thus appear to be a good index fossil for that time interval.

The dimensions of the megaspores and massulae of the Joffre Bridge A. stanleyi are quite similar to those reported by Jain and Hall (1969), Sweet and Hills (1976) and Melchior and Hall (1983). Sweet and Hills (1976) discussed size variations between the Alberta, Saskatchewan and North Dakota populations, and pointed out that these are no greater than the intrapopulation variation that they had observed in extant populations of A. pinnata R. Br. (Sweet and Hills, 1974).

Melchior and Hall (1983) described several (eight) "anomalous" megaspores of A. stanleyi "without float apparatus and with generally reduced perines and exinal elements ... frequently associated with groups of microspores that are not confined within massulae." They attributed these features to "significant differences in tapetal behavior". Some of the spores from Joffre Bridge exhibit similar characteristics (e.g., Figs. 24, 26, 29), particularly the dispersed spores that were obtained by maceration of the claystone matrix. It seems likely that these are actually normal megaspores and massulae that were partially degraded prior to burial, probably due to oxidizing conditions at the time of deposition. The megaspores and massulae in the Joffre Bridge sediments are found in varying stages of degradation, a fact that facilitates their observation under SEM. The megaspore in Fig. 24 has lost many of its floats and much of its supra- and infrafilosum. Infrafilosum has also been lost in Fig. 26. The massula in Fig. 28 is [illegible] but has probably lost many of its glochidia. The

megaspore in Fig. 24 has lost some of its infrafilosum, and the attached massulae are partially degraded, exposing the microspores.

The morphological diversity of fossil Azolla megaspores and massulae has become fairly well documented. As of 1965, only 16 fossil species had been described (Hills and Weiner, 1965), but by 1990 over 60 names had been published (Batten and Kovach, 1990). The spores of living species have also become better known through increased application of SEM and TEM since the work of Kempf (1969). Extant Azolla are usually divided into two sections: Section Azolla with three floats and fluke-tipped glochidia; and Section Rhizosperma with nine floats and massulae with few or no glochidia (Fowler, 1975a). Fossil forms with more than nine floats and fluked glochidia like A. stanleyi are referred to section Kremastospora (Jain and Hall, 1969).

Most Cretaceous and Paleocene megaspore species have more than nine floats in the supraspore, and it is now generally accepted by most researchers that a large number of floats is the plesiomorphic state (e.g., Jain and Hall, 1969; Sweet, 1972; Fowler, 1975a; Collinson, 1980; Saunders and Fowler, 1993). Evolutionary trends in massula, glochidium and columella structure remain under discussion (e.g., Fowler, 1975a; Collinson, 1980; Saunders and Fowler, 1993). Little has been written about trends in megaspore wall ultrastructure (Sweet, 1972; Collinson, 1980), despite the general agreement that this is a major taxonomic character for the genus. Modern species are distinguishable from one another on the basis of perine structure alone (Perkins et al., 1985), and the texture of the outer perine and the structure of the megaspore wall is often used to differentiate fossil species (Kempf, 1969, 1973; Snead, 1970). Analysis of the accumulated data and re-examination of other genera of fossil Salviniaceae (Hall, 1974, 1975) would likely be rewarding.

Discussion of evolutionary trends in vegetative morphology has been hampered by the limited number of fossil Azolla species for which vegetative material has been described (Saunders and Fowler, 1993). As of 1973, sporophytes were known for only five fossil species (Sweet and Chandrasekharam, 1973); twenty years later the number remains less than 10 (Melchior and Hall, 1983; Saunders and Fowler, 1993; McIver and Basinger, 1993). Saunders and Fowler (1993) have suggested that the evolutionary trend appears to be one of increasing adaptation to the free-floating aquatic habit, including reduction of the sporophyte, changes to the branching pattern, adoption of a planar habit, reduced vascularization of leaves, and reduced development of roots.

To date the oldest Azolla for which vegetative morphology has been described are from Paleocene localities: A. schopfii from lower Paleocene strata at Genesee, Alberta (Sweet and Chandrasekharam, 1973) and Ravenscrag Butte, Saskatchewan (McIver and Basinger, 1993); A. velus, also from Ravenscrag Butte (McIver and Basinger, 1993); and A. stanleyi from middle Paleocene beds at Wannagan Creek, North Dakota (Melchior and Hall, 1983) and Joffre Bridge, Alberta. A new species represented by fertile whole plants from Cretaceous-Tertiary boundary outcrops in Montana and Wyoming has also been reported (Collinson, 1991a, 1991b), but details are not yet available.

The vegetative structure of A. schopfii exhibits a number of features that Saunders and Fowler (1993) have proposed as plesiomorphic: a large overall size (up to 5 cm long), an elongate alternate branching pattern, a sub-erect growth habit, prominent leaf venation, a pubescent stem, and well developed roots in borne in large fasicles (Saunders and Fowler, 1993; Sweet and Chandrasekharam, 1973). The leaves are widely spaced along the main axis and are imbricate only at branch apices (Sweet and Chandrasekharam, 1973; Saunders and Fowler, 1993; McIver and Basinger, 1993).

In contrast, sporophytes of A. stanleyi indicate that most of the vegetative characteristics of modern Azolla were established by the middle Paleocene. The sporophytes of both A. velus and A. stanleyi seem well adapted to the free-floating habit, and exhibit features that enhance buoyancy. The sporophytes of both species are small (up to about 2 cm long), with a planar growth habit and reduced, fragile and probably solitary roots. Sporophytes of A. stanleyi from Joffre Bridge have a pinnate alternate branching pattern (Figs. 1, 3); those from Wannagan Creek consist of a number of rhizomes arising from a central point and radiating outward (Melchior and Hall, 1983). The leaves of A. velus are closely spaced but not overlapping (McIver and Basinger, 1993), while those of A. stanleyi are crowded and imbricate, like those of modern species. All three Paleocene species have prominent leaf venation, however, a feature not seen in modern species (Saunders and Fowler, 1993).

The Joffre Bridge sporophytes appear to shed the lowermost branches when the plant reaches about 2 cm in length (Fig. 3). While this type of asexual propagation by vegetative fragmentation was likely important in Paleocene Azolla, these plants also appear to have relied heavily on sexual reproduction by sporulation. Spore production can be a rare event in living species (Perkins et al., 1985), but significant percentages of the sporophytes of all three Paleocene species were fertile at the time of preservation. Azolla stanleyi bore sporocarps on each leaf along each lateral branch (i.e., Fig. 3), while A. filiculoides bore sporocarps on the first leaf of each branch, like modern species (Sweet and Chandrasekharam, 1973). Abundant spore production may be a pleisomorphic character, ensuring survival under occasionally dry conditions. This may reflect an origin for heterosporous ferns in temporary pools as suggested by Wagner (1973).

Class GYMNOSPERMOPSIDA

Order GINKGOALES

Family GINKGOACEAE

Genus Ginkgo Linnaeus

Ginkgo sp.

(Pl. 5, Fig. 34)

Description: Leaves are fragmentary, reaching widths of up to about 55 mm at the apical margin. Apical margins are truncate, and undulate or irregularly lobed. Veins are numerous and equal, diverging at very low angles and branching dichotomously toward the apical margin, spaced about 0.2-0.3 mm apart (Fig. 34). No fragments with leaf bases, petioles or cuticle were found.

Occurrence: There are eight fragmentary leaves, UAPC-ALTA S9,549A/B, S11,648 S11662a, S13,072, S13,087, S13,091, S24,521, S33,552, from the Mollusc Layer (Unit 5).

Discussion: The size, apical margins, and radiating, dichotomously branching veins of these fragmentary leaves from Joffre Bridge Roadcut are consistant with those of the petiolate, fan-shaped leaves of Ginkgo L., but the specimens are too incomplete to consider identification to a species level. Fossil leaves as old as Lower Jurassic have been referred to the living genus Ginkgo (Tralau, 1968). Although the generic name Ginkgoites Seward was originally proposed for fossil Ginkgo-like leaves, it was subsequently applied to material that differs significantly from the living genus (Tralau, 1968).

At Joffre Bridge Roadcut, Ginkgo leaves have been found only in the Mollusc Layer (Unit 5), a coaly bed that was deposited in a swamp environment. Their

rarity and fragmentary nature suggest that Ginkgo trees were not common at the site. Well preserved, whole Ginkgo leaves with cuticle have been found near the mouth of the Blindman River, a locality about 15 km northwest of Joffre Bridge Roadcut, where the strata are the same age (Ti_3).

Order CONIFERALES

Family TAXODIACEAE

Genus Glyptostrobus Endlicher

Glyptostrobus europaeus (Brongniart) Heer

(Pl. 5, Figs. 35 - 41)

Description: Fragments of branches range from stout, presumably persistent, twigs up to 100 mm long and 5 in diameter, to thinner twigs that bear alternately arranged, presumably deciduous, branchlets (Fig. 36). Leaves are helically arranged, and five morphologies (Christophel, 1973, 1976) can be recognized. Cupressoid leaves are scale-like with acute apices; the largest ones up to 8 mm long and 3 mm wide, are borne on the stout, persistent twigs; smaller ones 1-2 mm long and 0.5 mm wide occur near the bases of deciduous branchlets (Fig. 36), and on cone-bearing twigs (Fig. 37). Cryptomeroid leaves are acicular to falcate, 3-6 mm long and 0.5-1.5 mm wide with acute apices, and are often present distal to cupressoid leaves on branchlets (Fig. 36). Crypto-cupressoid leaves are intermediate between cryptomeroid and cupressoid leaves. Taxodioid and crypto-taxodioid leaves occur on both persistent and deciduous branches; they are flat and oblong, with decurrent bases and acute to mucronate apices, ranging up to 15 mm long and 2 mm wide (Fig. 37).

Seed-cones are pyriform, up to 20 mm long and 15 mm wide, and are terminal on short twigs 5-25 mm long that bear cupressoid leaves (Figs. 35, 37). They consist of helically arranged, imbricate, nonpeltate scales that are roughly triangular, and range up to 20 mm long and 15 mm wide, depending upon their position in the cone; they broaden from a narrow base to a rounded distal margin bearing up to 11 crenate lobes (Fig. 39). Bracts are obovate, and are about two-thirds as long as the associated scale (Fig. 40). The seeds are winged, asymmetrical, and roughly triangular or "hatchet-shaped" (Silba, 1986; McIver and Basinger, 1993), up to 13 mm long and 7 mm wide (Fig. 41). The seed body is oblong, up to 6 mm long and 2 mm wide, surrounded by the asymmetrical wing. Pollen-cones consist of acute-tipped, incurved, imbricate scales. They are globose, up to 3 mm long and 3 mm wide, and are terminal on short, alternately arranged twigs that bear cupressoid leaves (Fig. 38). Pollen was sought in several cones, but none was found.

Occurrence: More than 350 specimens have been catalogued, including branchlets bearing foliage, seed-cones and pollen-cones, as well as dispersed seed-cone scales and seeds. Glyptostrobus remains are particularly common near the base of the Upper Lacustrine Sequence in the Concretion Zone (Unit 6a) and the Aquatic Plant Zone (Unit 6b); they also occur in the Channel-Fill Siltstone (Unit 3), the Lower Lacustrine Sequence (Unit 4), and the Mollusc Layer (Unit 5).

Discussion: The Glyptostrobus remains from Joffre Bridge Roadcut provide a fairly complete record of the parent plant, including twigs, foliage, seed-cones, seed-cone scales and bracts, and pollen-cones. The material is consistent with that described as Glyptostrobus nordenskioldii (Heer) Brown by Brown (1962) from the Paleocene of the western United States, and with other material assigned to G. nordenskioldii from Paleocene localities in Alberta

(Chandrasekharam, 1972, 1974; Christophel, 1973, 1976), and Saskatchewan (McIver and Basinger, 1993).

Hickey (1977) asserted that the "division of fossil members of the genus Glyptostrobus into a number of species rests on very unreliable criteria", and he questioned the priority of the species name G. nordenskioldii. He assigned Glyptostrobus material from the Paleocene of North Dakota to G. europaeus (Brongniart) Heer, because he considered G. nordenskioldii to be a later synonym of G. europaeus. Brown (1936, 1962) had separated North American Paleocene forms of Glyptostrobus from G. europaeus on the basis of: (1) the cone-scales being "on an average, shorter and broader"; (2) their occurrence as detached scales rather than as complete cones; and (3) their age (older than Miocene). Hickey (1977) reported that the size and shape of the cone-scales from Brown's material "completely overlap" those of G. europaeus; and that complete seed-cones which are "indistinguishable from those of the European form" do occur in the American species. Heer (1870) had noted the resemblance to G. europaeus when he established G. nordenskioldii for material from Spitzbergen that did not include any examples of appressed leaves. It thus seems appropriate to include the Glyptostrobus material from Joffre Bridge Roadcut in Glyprostrobus europaeus.

The anatomy and development of living Glyptostrobus have been described by Henry and McIntyre (1926), and Takaso and Tomlinson (1990). Henry and McIntyre (1926) noted that that Tertiary Glyptostrobus did not appear to differ significantly from the living species, and they remarked that "it is possible that the tree now on the verge of extinction in China is the Tertiary species unchanged". The Glyptostrobus material from Joffre Bridge Roadcut closely resemble that of the living species and does not appear to contradict that view. However, work in progress on permineralized seed-cones of Upper Cretaceous

age from Drumheller, Alberta, suggests that some of the fossils may differ in the structure of the seed-cone scales (Aulenback, pers. comm.).

The genus Glyptostrobus is believed to be extinct in the wild, but a single species survived in southeastern China where Glyptostrobus trees were planted along the swampy banks of rivers and canals to strengthen them against periodic flooding (Henry and McIntyre, 1926). The trees reach heights of up to 25 m and have prominently buttressed, conical bases. They develop "knees" or pneumatophores like those of Taxodium, and like Taxodium they shed short deciduous branchlets annually. They grow on deltaic and fluvial plains, between latitudes 22° and 26°, at elevations "not exceeding a few feet above sea-level" (Henry and McIntyre, 1926). The genus has also been reported from Vietnam at elevations of up to 1000 metres (Silba, 1986).

The geological setting of the Glyptostrobus remains at Joffre Bridge Roadcut is consistent with a wet, floodplain environment, like that favored by the living trees in China. Fragments of leafy Glyptostrobus branchlets occur in most of the stratigraphic units, and are particularly common near the base of the Upper Lacustrine Sequence, in the Mollusc Layer (Unit 5), the Concretion Zone (Unit 6a) and the Aquatic Plant Zone (Unit 6b). Glyptostrobus trees may have dominated the swampy lake margins at that time, shedding their branchlets, cones and seeds into the shallow water. The associated plant remains also indicate a wet environment. They include the taxodiaceous conifer Metasequoia, and free-floating aquatic plants (a Spirodela-like plant, Ricciopsis and Azolla).

Family TAXODIACEAE

Genus Metasequoia Miki

Metasequoia occidentalis (Newberry) Chaney

(Pl. 6, Figs. 42 - 47)

Description: Fragments of branchlets up to 80 mm long have been recovered which bear oppositely arranged leaves spaced 2-3 mm apart. The leaves are "lorate-oblong" (Hickey, 1973), up to 12 mm long and 2 mm wide, with a distinct midvein, petiolate base, and acute tip (Fig. 42). Seed-cones are globose to cylindrical, up to 20 mm in diameter and 25 mm long, with oppositely arranged, peltate scales; they are borne terminally on a leafless stalk about 2 mm in diameter and more than 25 mm long (Fig. 43). Seed-cone scales are triangular, and are generally about 5-7 mm long, 2-6 mm wide, and 2-4 mm thick (Fig. 46). Seeds are winged, flat, and roughly heart-shaped, ranging up to 7 mm in diameter (Fig. 47). The oblong seed-body is 1-2 mm wide, and lies between the two lateral wings. Each wing is usually slightly wider than the seed body at the chalazal end, narrowing toward the micropylar end. The pollen-cones are oppositely arranged on specialized axes, with one cone terminal on the axis (Figs. 44, 45). They are globose to ovoid, up to 3 mm in diameter, and are borne in the axils of scale-like leaves up to 3 mm long. The sporophylls are exserted on one specimen, extending 2.5 mm beyond the enclosing sterile scales (Fig. 44).

Occurrence: More than 250 specimens have been catalogued, including foliage, coalified seed-cones, dispersed seeds, and a few pollen-cones. Metasequoia remains are found scattered throughout most of the stratigraphic section, from the Fluvial Channel Sandstone (Unit 2) to the Aquatic Plant Zone (Unit 6b).

Discussion: The foliage, seed-cones, and pollen-cones described above are typical of those of the genus Metasequoia (Hu and Cheng, 1948; Sterling, 1949; Rothwell and Basinger, 1979; Basinger, 1981, 1984; Takaso and Tomlinson, 1992). They are consistent with material described as Metasequoia occidentalis by Chaney (1951), and with other material assigned to M. occidentalis from Paleocene localities in Alberta (Chandrasekharam, 1972, 1974; Christophel, 1973, 1976) and Saskatchewan (McIver and Basinger, 1993).

The Metasequoia pollen-cones from Joffre Bridge Roadcut are particularly interesting. Each cone appears to consist of sterile scale-like leaves that overarch and enclose the sporophylls, as is typical for the genus (Rothwell and Basinger, 1979). The pollen-cones were likely mature when preserved, being as large as the largest of those described by Chaney (1951), Chandrasekharam (1972, 1974), and Christophel (1973, 1976). On some specimens the sporophylls are exserted beyond the tips of the enclosing scales (Fig. 45) to facilitate pollen escape, as occurs in the living species (Rothwell and Basinger, 1979). Each pollen-cone is subtended by a scale-like leaf that is about as long as the diameter of the cone (Figs 44, 45), although longer subtending leaves may be seen on some of the specimens illustrated by Chaney (1951) and Chandrasekharam (1972, 1974). The subtending leaves are absent on some of the Joffre Bridge specimens, perhaps reflecting Chaney's (1951) observation that those leaves are "rarely persistent."

The genus Metasequoia first appeared during the Late Cretaceous epoch, and became the dominant conifer of North American temperate floras by early Tertiary times (Basinger, 1981). A single species, M. glyptostroboides Hu and Cheng, survived into modern times in remote valleys of south-central China (Hu and Cheng, 1948; Chaney, 1948; Fulling, 1976). It reproduces naturally in

cool, dark, moist forests, and thrives "along the banks of small streams, among rocks and boulders covered thickly by liverworts and mosses", and in "seepage areas at the foot of slopes where there is abundant shade and moisture" (Chu and Cooper, 1950). Associated genera in the wild in China included some closely related to those seen at Joffre Bridge Roadcut: Cercidiphyllum, Acer and Viburnum. A few Ginkgo trees were also present near the Chinese Metasequoia but were "quite certainly planted" (Chu and Cooper, 1950).

Subdivision ANGIOSPERMOPHYTINA

Class MAGNOLIOPSIDA

Subclass MAGNOLIIDAE

Order RANUNCULALES

Family SABIACEAE

Genus Meliosma Blume

cf. Meliosma rostellata (Lesquereux) Crane et al.

(Plate 7, Figs. 48,49)

Description: Subglobose structures, 5-6 mm in diameter, with a prominent keel and pore, and a smooth to slightly papillate surface (Figs. 48, 49).

Occurrence: Two specimens have been recognized (S9,912; S9,909). Their exact stratigraphic position is not known, but the matrix is consistent with the Channel-Fill Siltstone and Lower Lacustrine Sequence (Units 3-4).

Discussion: Crane et al. (1990) described similar structures from the Paleocene Sentinel Butte Formation of North Dakota as Meliosma endocarps, and assigned them to the taxon Meliosma rostellata. The type specimen for Lesquereux's

taxon, Carpites rostellatus, was of Paleocene age from the Denver Formation (Lesquereux, 1878). These structures from Joffre Bridge Roadcut show some resemblance those described by Crane et al. (1990) and are tentatively referred to that taxon, but more specimens are needed to confirm this assignment.

Subclass HAMAMELIDAE
Order HAMAMELIDALES
Family CERCIDIPHYLLACEAE
Genus Joffrea Crane & Stockey
Joffrea speirsii Crane & Stockey

(Plate 7, Figs. 50 - 59)

Stockey and Crane (1983), and Crane and Stockey (1985, 1986) have published detailed descriptions of the cercidiphyllaceous remains and seedlings from Joffre Bridge Roadcut, and their works should be consulted for additional information and illustrations.

Description: Branches (long shoots) up to 130 mm long, with smooth bark and scattered circular lenticels, have been found. They bear short shoots that are usually alternately arranged, 15-45 mm long and 5-13 mm wide, with numerous crowded, diamond-shaped leaf scars. Leaves are simple and petiolate. Laminae are elliptic, ovate or obovate (Fig. 50), and are commonly 30-70 mm long and 30-80 mm wide, or occasionally larger. Margins are crenate, with crenations most prominent in the upper two-thirds of the leaf. Minute glands are set into the lamina at the tips of crenations. Apices are obtuse to rounded. Bases are rounded, cordate or truncate, with the lamina sometimes shortly decurrent down the petiole, and the venation is actinodromous. A midrib and one or two pairs of lateral primary veins diverge radially from a point at or very near the

base (Fig. 50). The midrib and inner pair of primaries are usually more strongly developed than the outermost, basal primaries. Strong secondary veins arise from the midrib at and distal to the midpoint of the leaf, and diverge from the inner primaries toward the leaf margin. Brochidodromous loops are formed by secondaries from the midrib and outer secondaries from the inner primaries (Fig. 50, 51). Higher-order veins form loops closer to the margin. Polygonal areoles with branched, freely ending veinlets are well developed.

Pistillate flowers lack perianth. They are borne in inflorescences produced from axillary buds at the apex of short shoots. Each inflorescence is surrounded at the base by bud scales, and consists of a main axis 1.0-2.0 mm thick at the base and up to 65.0 mm long, bearing approximately 40 carpels, singly or in pairs, on short side branches (Figs. 52, 53). The carpels are narrowly ellipsoidal, 9.0-11.0 mm long and 3.0-4.0 mm wide, with a single longitudinal suture on the ventral surface. An abaxially coiled, persistent style is located at the apex of each carpel (Fig. 53).

Mature infructescences bear follicles spaced 6-11 mm apart on an axis 2.0-3.5 mm thick (Fig. 55). Follicles are ellipsoidal, 18-30 mm long and 5-10 mm wide. Each follicle produced numerous flat, winged seeds. Seeds are 3.5-8.0 mm long and 1.5-3.5 mm wide, and typically crescent-shaped or semicircular, with one margin convex and the other straight to concave (Fig. 56). The seed body, located at the proximal end of the wing, is elliptical to obovate, 2.0-3.5 mm long and 0.5-1.0 mm wide. Germination was epigeal, producing a thin hypocotyl and a pair of opposite, broadly ovate to oblong cotyledons (Fig. 57). Cotyledons are 2.0-4.0 mm long, 1.5-3.0 mm wide, with rounded apices and entire margins. Cotyledon venation is pinnate and camptodromous, with a distinct midrib and 2-3 pairs of opposite to subopposite secondaries (Fig. 57). The first and second seedling leaves are borne in opposite pairs, and are ovate

with acute to rounded apices and obtuse bases (Fig. 58, 59). Their margins are sparsely crenate, with glanduiar teeth (Fig. 59).

Associated staminate inflorescences are bud-like, ovoid, 17.0-25.0 mm long and 11.0-13.0 mm wide, and are composed of about 10-20 tightly packed, helically arranged bracts (Fig. 54). Bracts are triangular, 6.0-15.0 mm long and 5.0-8.0 mm wide, with an acute or acuminate apex, and truncate base. Stamens, borne in the axils of the bracts, consist of anthers 2.0-3.5 mm long and 1.0-1.5 mm wide, without conspicuous filaments. No pollen has been found in the anthers.

Occurrence: Thousands of specimens have been catalogued, including branches, leaves, pistillate and staminate inflorescences, infructescences, follicles, seeds and seedlings. Joffrea remains are common throughout most of the stratigraphic section, from the Fluvial Channel Sandstone (Unit 2) to the Upper Lacustrine Sequence (Unit 6). The seedlings are found in discrete lenses within the Channel-Fill Siltstone (Unit 3).

Discussion: Joffre Bridge Roadcut is the type locality of the Cercidiphyllum-like plant Joffrea speirsii, which was reconstructed by Crane and Stockey (1985). Joffrea speirsii is one of the most completely understood of fossil Cercidiphyllum-like plants. The morphology of its foliage, inflorescences and infructescences is known, and the mode of attachment of the pistillate inflorescences has been demonstrated. It is also one of the few fossil plants for which germinating seeds and seedlings have been found.

Leaves, follicles and seeds that resemble those of Cercidiphyllum are common in the late Cretaceous to Tertiary nonmarine sediments of the Northern Hemisphere, but have been assigned to a large and confusing number of genera

and species (Brown 1939; Hickey, 1977; Crane and Stockey, 1985; McIver and Basinger, 1993). Heer (1876) first noted the resemblance between some fossil leaves which he had described as Grewia crenata, and those of extant Cercidiphyllum. Significant attempts to improve the classification of such leaves and/or correlate them with associated fruits and seeds have been published by Brown (1939), Chandler (1961), Wolfe (1966), Chandrasekharam (1974), Hickey (1977), Crane (1978, 1981, 1984), Tanai (1981), and others. Cercidiphyllum-like material from other Paleocene localities in Alberta and Saskatchewan has been assigned to several genera including Cercidiphyllum (Chandrasekharam, 1972, 1974; Christophel, 1973, 1976; McIver and Basinger, 1993), Trochodendroides (Bell, 1949; McIver and Basinger, 1993), Nyssidium (McIver and Basinger, 1993), and Jenkinsella (Bell, 1949).

Joffrea closely resembles Cercidiphyllum in the morphology and venation of its leaves, seedling leaves and cotyledons. It differs significantly in the morphology of the pistillate inflorescences and their mode of attachment however, as well as in details of the morphology of shoots and staminate inflorescences, and thus Joffrea is considered to be a separate genus within the Cercidiphyllaceae. In Cercidiphyllum, a cluster of two to six free carpels, each subtended by a linear bract, is borne at the apex of a short axis (Swamy and Bailey, 1949; Crane and Stockey, 1986). In Joffrea a much longer axis bears approximately 40 carpels, singly or in pairs. This supports Swamy and Bailey's (1949) suggestion that the cluster of carples in Cercidiphyllum represents a reduced inflorescence, rather than a simple apocarpous flower as suggested by Hutchinson (1964) (Crane and Stockey, 1986).

The habitat of Joffrea appears to have been quite similar to that of living Cercidiphyllum. There are two extant species of Cercidiphyllum Siebold et Zuccarini, C. japonicum Sieb. & Zucc. and C. magnificum (Nakai) Nakai, both

of which are large, wind-pollinated dioecious trees that commonly reach heights of 20-25 m or more (Sargent, 1913; Spongberg, 1979). They are native to Japan and parts of China, and C. japonicum has been introduced in North America and Europe because of its ornamental attributes (Dirr, 1975, 1977). Its seedlings grow quickly and can rapidly colonize suitable areas. Dirr (1975, 1977) reported that seeds "germinated within two weeks at 90 percent plus capacity", and that the seedlings responded very strongly when treated with fertilizer, reaching heights of 1 m by autumn. Joffrea may have been capable of similar performance.

Joffrea seeds are very common in the sediments at Joffre Bridge Roadcut, and were likely produced in large quantities. Evidence from the "Nyssidium arcticum plant" (Crane, 1984) indicates that some Paleocene Cercidiphyllum-like plants produced more than twice as many seeds per follicle as living Cercidiphyllum. Some of the Joffrea seeds were actually fossilized in the act of germination (Stockey and Crane, 1983; Crane and Stockey, 1985), attesting to their fertility. Joffrea seedlings have been found in growth position in lenses within the Channel-Fill Siltstone (Unit 3), often at densities of 20-40 plants per 10 cm^2, intermixed with about one percent platanaceous seedlings (Stockey and Crane, 1983). The seedlings are all of approximately similar ages (Figs. 57-79), suggesting more or less synchronous, rapid germination (Stockey and Crane, 1983). They were probably attempting to colonize temporarily emergent surfaces such as shorelines or sandbars when they were buried in place by an influx of sediment-laden water. These factors led Crane and Stockey (1985) to observe that "the combined evidence strongly suggests that Joffrea and perhaps similar Cercidiphyllum-like plants from the Upper Cretaceous and early Tertiary were opportunistic, "weedy" species capable of rapidly exploiting open ... floodplain habitats".

At Joffre Bridge Roadcut, Joffrea remains can be found from the Fluvial Channel Sandstone (Unit 2) to the Upper Lacustrine Sequence (Unit 6). This is not surprising, given that Joffrea appears have been capable of growing rapidly and producing copious amounts of leaves, inflorescences and seeds. Joffrea trees must have thrived along the banks of the river system, shedding large quantities of material into the surrounding depositional environments. The close association between cercidiphyllaceous and platanaceous remains at Joffre Bridge Roadcut and other Tertiary localities is not surprising, either. Both plants appear to have favored the same types of moist floodplain and riparian environments.

Family PLATANACEAE

Genus Platanus Linnaeus

Platanus nobilis Newberry (leaves)

Genus Macginicarpa Manchester

Macginicarpa manchesteri Pigg & Stockey (pistillate inflorescences and infructesceneces)

Genus Platananthus Manchester emend. Friis et al.

Platananthus speirsae Pigg & Stockey (staminate inflorescences)

(Plate [illegible] figs. 60-66)

Pigg and Stockey (1991) published descriptions of the platanaceous remains from Joffre Bridge Roadcut, and their work should be consulted for additional information and illustrations.

Description: The leaves, which were assigned to Platanus nobilis by Pigg and Stockey (1991), are simple and petiolate, with three palmate lobes, and sinuses about one-third as deep as the blade length (Fig. 60). Leaf apices are broadly acute, and the bases are rounded to truncate, becoming cuneate where the lamina joins the petiole. Leaf margins are serrate, with widely spaced teeth about 1.2 mm long. Leaf laminae range in size from about 42 mm wide and 34 mm long, to 210 mm wide and 280 mm long (Fig. 61). Primary venation is basally actinodromous. Moderately thick secondary veins diverge subopposite ly from the primaries at angles of 30-35° and terminate in the widely spaced teeth. Tertiary veins arise at approximately right angles to secondary veins.

Pistillate inflorescences and infructescences, which were assigned to Macginicarpa manchesteri by Pigg and Stockey (1991), are globose, and borne on peduncles 10-16 mm long (Fig. 62). Peduncles are spaced about 2-10 mm apart on long reproductive axes, in a subopposite to alternate arrangement. Individual inflorescences are 10-16 mm in diameter, and consist of numerous pistillate florets densely packed around a receptacular core. Individual carpels are 2.7-3.6 mm long and 0.7-1.2 mm wide, and sometimes appear to be clustered, possibly in groups of five. Mature infructescences reach diameters of 16-19 mm, and bear elliptical achenes 3.7-6.5 mm long and 1.2-2.1 mm wide, which sometimes retain curved styles (Fig. 63).

Staminate inflorescences, which were assigned to Platananthus speirsae by Pigg and Stockey (1991), are globose, and borne on peduncles 7-10 mm long. Peduncles are spaced about 2-10 mm apart on long reproductive axes, in a subopposite to alternate arrangement. Individual inflorescences are 8.5-9.0 mm in diameter, and consist of numerous stamens densely packed around a receptacular core (Fig. 65). Perianth parts are obscure. Stamens are 2.2-2.5 mm long, with short filaments about 0.8 mm long, elongate pollen sacs up to

2.2 mm long and 0.25 mm wide. They were dispersed in groups and have long connectives that form a conical, caplike extension at the apex (Fig. 66). The pollen grains are tricolpate, prolate, and 18-22 μm in diameter, with reticulate ornamentation, and a tectate/columellate wall.

Platanaceous seedlings from Joffre Bridge Roadcut have subopposite arranged, petiolate, ovate cotyledons. Laminae are about 5.2-7.5 mm long, with a maximum width of 5.4 mm. A few specimens show indications of actinodromous primary venation and reticulate higher-order venation. Young foliage leaves, where present, are helically arranged and exhibit characteristic platanaceous morphology, including serrate margins (Fig. 64). Venation is simple craspedodromous.

Occurrence: Several hundred specimens have been catalogued, including leaves; pistillate inflorescences; infructescences, some with mature achenes; staminate inflorescences and dispersed stamen groups, both with in situ pollen; and seedlings in several stages of development. Platanaceous remains are found primarily in the Channel-Fill Siltstone, Lower Lacustrine Sequence, and Mollusc Layer (Units 3 to 5). The seedlings are found in discrete lenses within the Channel-Fill Siltstone (Unit 3).

Discussion: The foliage and the globose, unisexual inflorescences from Joffre Bridge Roadcut resemble those of living Platanaceae (Boothroyd, 1930), but the inflorescences differ in size and mode of attachment (Pigg and Stockey, 1991). In living Platanus, the inflorescences are larger (around 20 mm in diameter), and there are one to several inflorescences per peduncle (Subgenus Platanus), or numerous inflorescence heads that are sessile on a reproductive axis (Subgenus Castaneophyllum). Extant Platanus carpels are clustered in groups of 5 to 9, and each bears a prominent ring of dispersal hairs that is lacking or not

preserved in the Joffre Bridge material. In the staminate flowers of extant Platanus, the connectives are shorter than those seen at Joffre Bridge, and the stamens are shed individually rather than in groups (Manchester, 1986). The pollen from Joffre Bridge is consistent in size, ornamentation and wall structure with that of modern Platanus species.

Pigg and Stockey (1991) reconstructed a platanaceous plant, informally designated the Joffre plane tree, from the platanaceous remains at Joffre Bridge Roadcut, on the basis of their exclusive co-occurrence at this well-documented locality. Because the various organs are disarticulated and have not been found in organic connection, they were assigned to separate generic names, rather than to a single taxon. Pigg and Stockey (1991) assigned the leaves to Platanus nobilis Newberry, sensu Wolfe and Wehr (1987). The pistillate inflorescences and infructescences were assigned to the fossil genus Macginicarpa (Manchester, 1986) based on the size of the inflorescence head, the grouping of the carpels, the carpel shape, and the lack of dispersal hairs. Because they are consistently borne on long peduncles, and because the perianth parts are poorly known, Pigg and Stockey established the new species M. manchesteri for them. Similarly, they assigned the staminate inflorescences to the fossil genus Platananthus (Manchester, 1986), and they established the new species P. speirsae for them because of their long peduncles and fairly large inflorescence heads.

Platanoid leaves and reproductive structures first appear in sediments of Lower Cretaceous (Albian) age, and the known platanoid and platanaceous material from Upper Cretaceous and Tertiary assemblages exhibits a wide range of diversity (Manchester, 1986; Crane et al., 1993; Pedersen et al., 1994). Platanus is the only extant genus within the family Platanaceae, and it includes six or seven living species, all of which are trees (Cronquist, 1981; Ernst,

1963). They are found from Central America to Ontario, and from the eastern Mediterranean region through the Himalaya mountains to Southeast Asia (Cronquist, 1981; Ernst, 1963). Although the living Platanus species show less diversity than is seen in fossil platanoids (Pedersen et al., 1994), they still enjoy a fairly wide distribution today, in contrast to the living species of Cercidiphyllum, Metasequoia, Glyptostrobus and Ginkgo.

Depositional settings indicate that the fossil Platanaceae favored riparian and floodplain environments, just as living Platanus species do today (Cronquist, 1981; Manchester, 1986). The Joffre plane trees clearly did as well, shedding vegetative and reproductive structures into the fluvial, lacustrine and backswamp environments represented by the Channel-Fill Siltstone, Lower Lacustrine Sequence and Mollusc Layer (Units 3 to 5). The platanaceous seedlings illustrate the ability of this plant to colonize open areas and disturbed soils. Found a more abundant seedlings of Joffrea (see discussion above) in lens the Channel-Fill Siltstone, the platanaceous seedlings appear to have been colonizing temporarily emergent shorelines or sandbars when they were buried in place.

Order URTICALES

Family ULMACEAE

Genus Chaetoptelea Liebmann

Chaetoptelea microphylla (Newberry) Hickey

(Plate 9 , Figs. 67-69)

Description: Leaf blades are narrow-ovate to lanceolate, and often slightly asymmetrical, 25-55 mm long and 7-15 mm wide, with a length-to-width ratio of 1.7-3.7 (Figs. 67, 69). Leaf apices are acute to long acuminate. Bases are

obtuse, rounded to cordate, and sometimes asymmetrical. Petioles are short, usually 0.7-1.5 mm long. Leaf margins are toothed, with acuminate serrations, mostly of type D-1 (Hickey, 1973), usually with 1 or 2 subsidiary teeth on the basal side (Fig. 68). Venation is pinnate, simple craspedodromous. The primary vein is moderately thick and straight to curved. Secondary veins curve smoothly from the primary to the margin, diverging from the primary at angles of about 50-60°, spaced 0.9-4.0 mm apart. Secondaries often dichotomize near the margin. Intersecondaries are rare. Tertiaries depart at steep to right angles.

Occurrence: About 60 leaves have been collected from the Channel-Fill Siltstone and Lower Lacustrine Sequence (Units 3-4).

Discussion: The family Ulmaceae is divided into two subfamilies, Celtoideae and Ulmoideae, the latter of which is usually considered to include six or seven extant genera (Sweitzer, 1971; Manchester, 1989). Some investigators, including Sweitzer (1971) and Manchester (1989), have considered the genus Chaetoptelea Liebmann to be congeneric with Ulmus L. However, leaves and fruits assignable to Chaetoptelea have been recognized in a number of Tertiary fossil assemblages (e.g., Burnham, 1986; Hickey, 1977; MacGinitie, 1941), which may strengthen the case for its retention as a distinct genus. There is only one living species, C. mexicana Leibmann, a large tree which is found in Central America south of 22° lattitude.

Burnham (1986) studied the foliar morphology of fossil leaves of Subfamily Ulmoideae from western North America, using discriminant analysis. She found that the early Tertiary specimens conformed to the morphological ranges of three extant genera: Zelkova Spach, Chaetoptelea and Ulmus. She recognized two morphotypes within Chaetoptelea, designated Chaetoptelea A and

Chaetoptelea B, which were distinguished on the basis of tooth/sinus types and higher-order venation.

The ulmaceous leaves from Joffre Bridge Roadcut are consistent with Burnham's Chaetoptelea A, as are those described as Chaetoptelea microphylla by Hickey (1977). In addition to Hickey's specimens from the late Paleocene Golden Valley Formation of North Dakota, leaves of the Chaetoptelea A type are known from a number of late Paleocene to late Eocene localities in California, Oregon, Washington, Wyoming and Alaska (Burnham, 1986).

At Joffre Bridge Roadcut, leaves of C. microphylla are found mainly in the Channel-Fill Siltstone and Lower Lacustrine Sequence (Units 3-4), along with remains of Joffrea and Platanus, and samaras of Deviacer, suggesting that Chaetoptelea may have shared the riparian environment with those taxa.

Subclass DILLENIIDAE

Order SALICALES

Family SALICACEAE

Genus ? Populus

Populus penhallowi Bell

(Plate 11, Fig. 84)

Description: The leaves are ovate, reaching lengths of 4.5 - 8.5 mm and widths of 3.5 - 4.5 mm (Fig. 84). The lamina is thin and membranaceous. The margin is entire, the apex is acute, and the base is obtuse and decurrent. Petioles are not preserved on these specimens. The venation is brochidodromous. The primary vein is straight. The secondaries arise at angles of about 40-50°,

curving to form loops near the margin. Higher order venation has not been preserved.

Occurrence: Eight specimens, most of which are fragmentary, have been recovered from the Concretion Zone (Unit 6a) of the Upper Lacustrine Sequence.

Discussion: These specimens are conspecific with a leaf from the Blindman River area that Penhallow (1902) referred to Populus ungeri Lesquereux. Bell (1949) noted that Penhallow's specimen differed from P. ungeri in both shape and venation, and he established the taxon P. penhallowi for it.

At both Joffre Bridge Roadcut and the mouth of the Blindman River, these leaves are preserved only as faint impressions in grey lacustrine mudstone. They appear to have been very delicate, with a membranaceous (Hickey, 1973, 1979) lamina, and must have been produced by a tree or shrub that grew near the margin of the lake.

Subclass ROSIDAE

Order SAPINDALES

Family SAPINDACEAE/ACERACEAE

Genus Deviacer Manchester

Deviacer sp.

(Plate 9 , Figs. 71, 72, 74)

Description: Fruits are schizocarpic samaras 1.5-2.4 mm long and 0.6-1.7 mm wide. None have been found in attachment, but scars indicate an attachment

angle of about 30° to the trend of the wing (Fig. 71). Nutlets are symmetrical and elliptic, 0.3-0.7 mm long and 0.2-0.4 mm wide (Fig. 74). The distal edge of the wing is straight to gently convex, and strongly veined. The proximal margin is occasionally convex immediately distal to the nutlet (Figs. 71, 72), but is more commonly gently concave throughout its length. The wing apex is rounded. Veins are numerous, and the majority are coalesced along the distal margin of the wing. They dichotomize and anastomose toward the proximal margin.

Occurrence: About 50 samaras have been collected from the Channel-Fill Siltstone and Lower Lacustrine Sequence (Units 3-4).

Discussion: Wolfe and Tanai (1987) observed that some Paleocene and Eocene samaras that had been assigned to the genus Acer differ significantly from those of younger and modern Acer species in the venation of the wing. These samaras "have an attachment scar that is on the same side of the samara as are the coalesced veins of the wing; the strongly veined "back" of the wing is thus distal in these fruits, rather than proximal as in Acer" (Wolfe and Tanai, 1987). They felt that these fruits, and associated leaves that had been assigned to "Acer" arcticum Heer and "Ampelopsis" acerifolia (Newberry) Brown, were not valid Acer, and postulated that they might represent an extinct genus of Aceraceae which they termed the "Acer" arcticum complex. Wolfe examined some of the samaras from Joffre Bridge Roadcut and felt that they might represent a new species of the "Acer" arcticum complex (Wolfe, pers. comm.).

Manchester (1994) erected the genus Deviacer for samaras bearing the attachment scar on the dorsal margin of the nutlet, like those of Wolfe and Tanai's "Acer" arcticum complex, rather than on the ventral margin, as in true

Acer. Deviacer samaras have not been found in attachment, and it is not known whether they were borne in pairs as in the Aceraceae, or in threes as is typical in the Sapindaceae (Manchester, 1994; Wolfe and Tanai, 1987). Noting that the attachment angle indicates that the proximal or dorsal margins of Deviacer samaras would have faced each other, as is typical in extant samaroid Sapindaceae, Manchester placed Deviacer in the family Sapindaceae "sensu lato". He observed that although the family name Aceraceae is well established, some authors have concluded that "there is no firm basis for treating it separately from the Sapindaceae" (Manchester, 1994).

Manchester (1994) named one species from the Eocene Clarno Formation of Oregon, Deviacer wolfei. The samaras from Joffre Bridge Roadcut differ from D. wolfei in size and shape, and thus represent a new species of Deviacer. They also lack the prominent proximal keel and recurved "rudder-like projection" (Manchester, 1994) seen adjacent to the attachment scar in D. wolfei.

The Deviacer samaras from Joffre Bridge Roadcut are found in the sediments of the Channel-Fill Siltstone and Lower Lacustrine Sequence (Units 3 and 4), associated with remains of Joffrea and the platanaceous tree described above, and a few leaves of "Acer" arcticum (see discussion below). Many of the Deviacer samaras show signs of abrasion, and may have carried for some distance by the river system before being washed into the abandoned channel setting and preserved.

Family SAPINDACEAE/ACERACEAE

Genus Acer Linnaeus

"Acer" arcticum Heer

(Plate 9, Figs. 70, 73)

Description: The leaves are petiolate and shallowly three-lobed, 60-80 mm wide and approximately 65 mm long, with a truncate base; the apices are not preserved (Figs. 70, 73). The margin has obtuse crenate teeth and rounded sinus. The venation is actinodromous. The two lateral primaries diverge from the medial primary at or near the base, at angles of 70-85°. Three or four secondaries diverge from the outer side of the lateral primaries. The teritaries are alternate, and those between the medial and lateral primaries tend to form a V-shaped pattern pointing apically.

Occurrence: Five fragmentary leaves (S9,607; S12,027; S12,029; S12,060; S16,181) have been recovered from the Channel-Fill Siltstone and Lower Lacustrine Sequence (Units 3-

Discussion: These leaves are not common or well preserved at Joffre Bridge Roadcut, but appear to be consistent with "Acer" arcticum as described by Wolfe and Wehr (1987) and Wolfe and Tanai (1987). The leaves resemble those of [illegible] in their overall shape and architecture. However, Wolfe and Wehr [illegible] Wolfe and Tanai (1987) noted that the rounded teeth and sinuses are not found in extant species of Acer, and suggested that these leaves may not represent true members of that genus. The leaves are commonly associated with samaras of the Deviacer type (see discussion above), which strongly supports the hypothesis that they are not leaves of true